Functional characterization of an essential mycobacterial protease

Functional characterization of an essential mycobacterial protease

A dissertation presented

by

Katherine J. Wu

to

The Division of Medical Sciences

in partial fulfillment of the requirements

for the degree of

Doctor of Philosophy

in the subject of

Microbiology and Immunobiology

Harvard University

Cambridge, Massachusetts

October 2018

Dissertation Advisor: Dr. Eric J. Rubin Katherine J. Wu

Functional characterization of an essential mycobacterial protease

Abstract

Mycobacterium tuberculosis (Mtb), the causative agent of tuberculosis, remains a global health threat due to its engimatic ability to withstand diverse environmental stresses in the host. The widespread phenomenon of antibiotic resistance can be at least partially attributed to *Mtb's* incredible adaptibility. As such, an increased understanding of how this bacterium grows and survives under different conditions is ncessary to continue developing tools to prevent the spread of disease.

In Chapter 1 of my dissertation, I present a brief overview of mycobacterial proteases. In Chapter 2, we explore the previously uncharacterized function of the predicted essential protease HtrA. We find that HtrA is essential and interacts with another essential protein of unknown function, LppZ. Loss of HtrA/LppZ leads to accumulation of the amidase Ami3, which is toxic when mannosylated. In the presence of HtrA/LppZ, Ami3 has a shorter half-life and accumulates to lower levels. These data suggest HtrA-LppZ blocks the toxicity of a cell wall enzyme. In Chapter 3, we explore another set of essential genes, FtsQLB, which we show to be critical for mediating proper mycobacterial cell division. We identify and characterize homologs of the conserved cell division regulators FtsL and FtsB, adding to a previous body of work characterizing their partner FtsQ, and show that, as a set, these enzymes appear to function similarly to their homologs in *E. coli*. We then identify a number of previously undescribed septally-localized factors which could be involved in cell wall regulation, including SepIVA. Finally, in Chapter 4, we present preliminary findings on another conserved mycobacterial protease, FtsH. We show that FtsH is not essential for viability in *Mycobacterium smegmatis* or *Mycobacterium tuberculosis.* However, FtsH may play a small role in the viability of

mycobacteria under conditions of oxidative stress. Additionally, we present candidate substrates for this protease.

Characterizing the critical proteins that allow mycobacteria to survive extreme environments is a crucial pursuit in the push for new tubericidal agents. This work forms the foundation for future work on the stress-responsive growth patterns of mycobacteria, particularly through the lens of regulated proteolysis.

Table of Contents

List of Figures and Tables

Chapter 2

Chapter 3

Chapter 4

Chapter 5

Appendices

Acknowledgments

This dissertation, and the whole of my graduate career, would not have been possible without the help of a veritable army of supportive peers, mentors, friends, and family. First and foremost, I thank my advisor, Eric Rubin, who has exceeded every expectation I have ever had of a mentor. Dr. Rubin's enthusiasm for science, quirky sense of creativity, ability to text and email at all hours of the day even while halfway around the world, and compassion for the mental and physical wellbeing of all his mentees—current and former—show in his every interaction. My PhD has been tumultuous to say the least, and Dr. Rubin has supported me at every step, prioritizing my happiness above my scientific output. I would not be the scientist or person I am today without him.

Additionally, I thank all the members of the Rubin and Fortune labs who have helped me along the way. The collaborative community I have found in these two labs has enabled me to learn countless new experimental methods, troubleshoot everything from bench work to writing, and learn from my (many) mistakes. In particular, Chidi Akusobi, Kasia Baranowski, Cara Boutte, Hesper Rego, and Junhao Zhu from the Rubin Lab and Sarah Fortune and Eli Gerrick from the Fortune Lab have provided me with invaluable knowledge and the push to trust my instincts (and acknowledge when they have failed me). Beyond this immediate network, I've been fortunate enough to be a part of two incredible departments—the Rubin Lab's original home in the Microbiology & Immunobiology Department at Harvard Medical School, and the Immunology & Infectious Diseases Department at the Harvard School of Public Health. The expertise of these two departments spans what entire *schools* could not, and I have never had to look far for help or advice. In particular, I am incredibly grateful for the contributions from Tom Bernhardt, Chris Sham, and many other members of the Bernhardt lab for their generosity and counsel, as well as Matt Waldor, Alyson Warr, Brandon Sit, Troy Hubbard, and many other members of the

Waldor Lab for their unprecedented kindness in letting me poach their equipment and resources at odd hours of the day.

Furthermore, I am incredibly grateful to the faculty mentors who have guided the course of my PhD. My original PQE committee, consisting of Dr. Simon Dove, Dr. Bob Husson, and Dr. David Rudner were the first to encourage me and catapult my project forward with clarity and direction. Dr. Dove then chaired my Dissertation Advisory Committee, serving alongside Dr. Marcia Goldberg and Dr. Matt Waldor. And of course, this dissertation would literally not come together without my dissertation examiners, Dr. Simon Dove, Dr. Thomas Bernhardt, Dr. Darren Higgins, and Dr. Christopher Sassetti. Together with Dr. Rubin, these scientists have given me role models to aspire to, and equipped me with the critical thinking skills to slowly acquire independence as I approach my own science.

My BBS class at Harvard, as well as the faculty leaders of the Division of Medical Sciences, have given me incredible support as I pursued extracurriculars that have enhanced my ability to communicate my own science. At Harvard, I've had the chance to express my love for health, innovation, and technology in many different ways, far beyond the bench. There is no other institution that could have given me the same opportunities. I am so grateful to have been a member of both Science in the News (SITN) and the Harvard Health Professions Recruitment and Exposure Program (HPREP) during my graduate career, and for all the peers who have helped me become a better science communicator and teacher along the way.

Last but not least, I thank my incredible friends and family both near and far. The execution and completion of my dissertation would not have been possible without the support of my mother and my extended family, or without the support of some of my closest friends, Brian Chhor, Jeremiah Cowen, Jonathan Lu, Stephanie Muscat, and Lauren Sweet. Finally, I thank my

partner, Kevin Wilson, who has stuck by me through the turmoil of career decisions, failed PCRs, and experiment-compromising blizzards. Thank you for keeping me laughing through these years and for challenging me to be the best scientist and person I can be, and for proving to me time and time again that no obstacle is insurmountable.

Chapter 1

Introduction

Chapter 1, Section 1.1: Mycobacterial proteases—an untapped resource

Tuberculosis is the leading cause of infectious disease deaths worldwide, contributing to approximately 1.7 million deaths each year (World Health Organization, 2017). Furthermore, the dramatic rise of drug-resistant strains, now including totally drug-resistant *Mycobacterium tuberculosis (Mtb)* (Parida *et al.* 2015), has prompted forecasts from both the Centers for Disease Control and Prevention (CDC) and World Health Organization (WHO) of a post-antibiotic era (Centers for Disease Control, 2013; World Health Organization, 2014), in which current antimicrobial regimens will become completely obsolete in the face of "superbugs." As such, there is an increasingly urgent need to develop new tubericidal agents.

To combat the extremes of the host environmental and its antimicrobial defenses, *Mtb* deploys a tightly controlled array of stress response systems. For instance, the *Mtb* genome encodes 12 alternative, stress-responsive sigma factors (Sharp *et al.* 2016), as well as both a proteasome and Clp protease, while most prokaryotes encode only one or the other. Mycobacterial proteases have emerged as particularly appealing therapeutic targets because several of the most conserved homologs, including Clp, FtsH, HtrA, and the proteasome, are essential for the growth or virulence of *Mtb* (Raju *et al.* 2012a).

Additionally, proteases are highly targetable for other reasons: first, their susceptibility to inhibition by various pharmacological compounds has already been established and clinically commercialized in humans (Poordad *et al.* 2011; Vermehren and Sarrazin 2011; Eriksson *et al.* 2008); second, they are widely conserved among bacteria, increasing the likelihood of broad-spectrum antibacterial activity; third, they are frequently found to be indispensible for virulence or normal growth; and fourth, their large, intricate structure and propensity to form complexes provides a large array of targetable surfaces (Zhang *et al.* 2012).

Despite their integral role in *Mtb* cell biology, mycobacterial proteases remain understudied. Here, I present a brief overview on what is understood so far of two key conserved proteases with high drug targeting potential in the genus *Mycobacterium*: HtrA and FtsH, both of which feature in my dissertation work.

HtrA, a stress-responsive periplasmic chaperone-protease

In other organisms, HtrA has been characterized as a non-essential, periplasmic protease with secondary chaperone function (Clausen *et al.* 2011). While often dispensable for normal growth, HtrA has been implicated in the virulence of several intracellular pathogens including *Campylobacter, Shigella, Helicobacter pylori, Yersinia enterocolitica, Listeria,* and *Salmonella* (Ingmer and Brøndsted 2009). In these organisms, HtrA appears to be crucial for tolerance of a common set of stressful conditions including high temperature, oxidative stress, and macrophage survival. Notably, homologs of HtrA have been identified in mitochondria, and seem to also contribute to protein quality control in eukaryotic cells. In fact, mutations in human homologs appear to be involved in cancer, arthritis, Parkinson's disease, and Alzheimer's disease (Zurawa-Janicka *et al.* 2010; Hansen and Hilgenfeld 2013). Thus, findings on bacterial HtrA may have applications beyond the prevention of infectious disease.

The well-characterized *E. coli* HtrA homolog DegP is induced in conditions of membrane stress (Ingmer and Brøndsted 2009), becoming essential during heat shock. DegP contains a protease domain with a conserved Ser-His-Asp catalytic triad and two PDZ domains that regulate substrate binding and access to the proteolytic chamber. Monomers oligomerize into hexamers via interactions between the protease and PDZ domains of neighboring subunits, and the complex becomes "switched" into an "on" state by the binding of substrates to the PDZ domains (Hansen and Hilgenfeld 2013). This allosteric activation triggers a rearrangement of the DegP

complex, reorienting the active site into an open structure to proteolyze substrates. The complex then operates via a hold-and-cut mechanism: the active site has similar binding specificity to the PDZ domain, such that each cleavage event generates a new C terminus to be recaptured by the PDZ domain (Clausen *et al.* 2011). As such, substrates are funneled through without the need for ATP hydrolysis (Frees *et al.* 2013). Although a handful of substrates have been identified in *E. coli* (Clausen *et al.* 2002), HtrA is mostly indiscriminate in its substrate specificity, preferring denatured, unfolded substrates with fairly hydrophobic C-termini. Folded substrates are sterically prevented from entering the proteolytic chamber, but remain enclosed by the PDZ domains and thus protected from degradation. This enables DegP's secondary function as a periplasmic chaperone in *E. coli*, ensnaring and guiding outer membrane proteins through the periplasm to their final destination (Hansen and Hilgenfeld 2013)—though more recent evidence shows that chaperone function plays a minor physiological role at best (Chang 2016).

A second *E. coli* HtrA homolog, DegS, is more structurally similar to mycobacterial HtrA: although its active site is in the periplasm, like its homolog DegP, DegS is anchored in the inner membrane and contains only one PDZ domain. In broad strokes, its pattern of oligomerization and activation is similar to that of DegP—disordered substrate binding to the PDZ domain catalyzes substrate funneling into the proteolytic chamber—though some specifics differ slightly between the two given their divergent structures. Strikingly, *E. coli* DegS is also unusually essential, solely due to its ability to cleave RseA, the anti-sigma factor for the alternative sigma factor SigE (Alba *et al.* 2001). However, three lines of evidence indicate that HtrA is not simply DegS in mycobacteria. First, while SigE is essential in *E. coli* and thus dependent on an essential protease for its release, SigE is nonessential in mycobacteria (Lew *et al.* 2011). Second, mycobacterial RseA is hypothesized to affect transcription in a non-canonical fashion unrelated to anti-sigma factor activity, and has been shown to be proteolyzed by the ClpC1P2 system (Rudra *et al.* 2015; Barik *et al.* 2010). Third, unlike DegS, mycobacterial HtrA contains a

long, N-terminal cytoplasmic domain that does not share sequence identity with any known non-mycobacterial protein; HtrA is essential in all well-studied mycobacteria, and the cytoplasmic domain is common to all iterations (Kapopoulou *et al.* 2011). Nevertheless, HtrA's synteny indicates that its transcription may be stress responsive, as it lies in an operon with SigE and RseA. Additionally, its high degree of structural conservation with homologs in other species indicates that HtrA is capable of recapitulating some of their functions. Thus, while HtrA's role in mediating the mycobacterial stress response may partially overlap with its homologs, it must deploy unconventional methods to cope with the changing environment, either repurposing conserved functions or utilizing entirely novel mechanisms to support mycobacterial growth and survival.

Mycobacteria harbor three homologs of HtrA (PepA, PepD, HtrA). A handful of studies have revealed that PepD (HtrA2) is a functional serine protease with chaperone activity that appears to participate in membrane stress response, making it a promising candidate for future study (MohamedMohaideen *et al.* 2008; White *et al.* 2010; White *et al.* 2011). In 2008, MohamedMohaideen *et al.* performed a biochemical analysis of PepD, showing that deletion of the gene, which encodes a functional serine protease, impairs the virulence of *Mtb.* Further work by White *et al.* in 2010 and 2011 revealed that PepD participates in a membrane stress response that involves the cleavage of a putative substrate to restore cell envelope homeostasis. These preliminary characterizations set precedent for the importance of HtrA in maintaining structural integrity in mycobacteria. However, while PepD appears to be crucial for mycobacterial virulence, it is not required for *in vitro* growth. In contrast, multiple transposon insertion sequencing datasets from the Rubin lab and other groups have implicated HtrA (HtrA1) as essential in both *Mtb* and its nonpathogenic relative *Mycobacterium smegmatis (Msm).*

The only other bacterial species in which an HtrA homolog appears to be crucial for survival under normal growth conditions is *Helicobacter pylori.* In *H. pylori,* HtrA is a secreted virulence factor that cleaves E-cadherin to disrupt intracellular adhesion, allowing *H. pylori* to breach host defenses along the gastrointestinal lining (Hoy *et al.* 2010). Strangely, this function doesn't appear to contribute strongly to *H. pylori* growth or survival *in vitro,* but rather dictates its interaction with the host; this may indicate that this HtrA serves another, yet undiscovered, purpose in *H. pylori*. However, biochemical techniques have already been deployed to neutralize HtrA homologs in *H. pylori* (Perna *et al.* 2014), effectively stymieing the growth of this pathogen—and the potential for HtrA targeting in other species has been the subject of much discussion (Raju *et al.* 2012; Skorko-Glonek *et al.* 2013; Wessler *et al.* 2017).

Thus, mycobacterial HtrA exists at the exciting intersection of essentiality and druggability. However, simply targeting HtrA without understanding its contributions to mycobacterial growth and survival would be impractical. Knowing HtrA's essential role in these organisms would clarify our ability to target this protease in the future. For instance, if HtrA's primary function serves to reinforce the integrity of the cell wall, using a protease inhibitor in conjunction with a peptidoglycan-targeting drug might create a synergy to drive the cell into a futile and ultimately lethal cycle of cell wall repair and disrepair. Furthermore, HtrA's crucial role in the virulence of many other pathogens demonstrates the urgency of developing broad-spectrum drugs against this protease, while being mindful of the homologs in human cells that might be caught in the crossfire.

FtsH, a widely conserved membrane protease with unusual roles

Similarly to HtrA, FtsH has been well characterized in other model organisms, where it has been observed to also have potential dual roles as a chaperone and protease (Schumann 1999). Mitochondria also harbor an FtsH homolog that has been implicated in several

neurodegenerative disorders (Janska *et al.* 2013, Okuno and Ogura 2013). However, generally, much less is known about FtsH homologs across species.

In contrast to HtrA, FtsH is a cytoplasmic AAA+ zinc metalloprotease with a conserved ATPase module. Unlike most other AAA+ proteases, FtsH is anchored in the inner membrane, and contains both its ATPase and proteolytic domains within the same peptide sequence; however, its sequence is well conserved with the rest of the AAA+ family (Licht and Lee 2008). When in active conformation, it assembles as a homohexamer and relies on ATP to drive substrate unfolding and spooling into the active chamber (Langklotz *et al.* 2012). However, compared to many other proteases, FtsH is not a particularly strong unfoldase, and thus proteins with partially or fully compromised folding status are most vulnerable to degradation (Dalbey *et al.* 2012).

Proteins are targeted for degradation by FtsH through a variety of mechanisms, typically involving recognition of some degradation sequence. Like Clp, FtsH can recognize ssrA-tagged proteins, but only performs a small subset of these degradations. Instead, as the primary proteolytic stronghold at the inner membrane, FtsH primarily degrades membrane proteins as a form of quality control, playing a prominent role in resolving misfolded or damaged proteins (Langklotz *et al.* 2012). For instance, when crucial components of the Sec translocase such as SecY become “jammed” with inefficiently exported proteins, FtsH quickly recognizes and proteolyzes the compromised machinery (Okuno and Ogura 2013).

Other known FtsH substrates in *E. coli* include the alternative sigma factor RpoH (Langklotz *et al.* 2012, Sauer and Baker 2011) as well as YfgM, a negative regulator of pathways responsive to extracytoplasmic and membrane stress (Bittner *et al.* 2017). However, while, like HtrA, FtsH

is also a typically nonessential protease, it plays an unusually crucial role in *E. coli* by degrading LpxC in its most well characterized function.

In *E. coli* and other Gram-negative bacteria, lipopolysaccharide (LPS) forms a crucial part of the outer membrane and its tightly regulated biosynthesis is essential for cell survival. The first committed step in synthesizing Lipid A, one of the core components of LPS, capitalizes upon a precursor that can be shuttled into either a pathway of LPS biosynthesis or phospholipid (PL) biosynthesis. LpxC funnels these resources into the LPS synthesis pathway, thus diverting precursors away from PL synthesis. Maintenance of balanced synthesis between these pathways is critical, and thus necessitates FtsH, which proteolyzes LpxC (Langklotz *et al.* 2012). Loss of *E. coli ftsH* is thus only possible in the presence of a gain-of-function suppressor mutation in *fabZ*, hastening the process of PL biosynthesis and thus restoring homeostasis to the LPS/PL ratio (notably, other suppressors have since been discovered, all of which repress LPS synthesis or push PL synthesis into overdrive) (Okuno and Ogura 2013).

Additionally, several FtsH adaptors and inhibitors have been identified in *E. coli*. Perhaps most notable are HflK and HflC—both single-pass inner membrane proteins that complex with FtsH and strongly inhibit its activity against certain membrane substrates (Dalbey *et al.* 2012).

While the substrates and molecular mechanisms of FtsH proteolysis remain areas of active research in *E. coli,* even less is known about mycobacterial FtsH. So far, no data of Δ*ftsH* mycobacterial strains have been published, leading some to speculate that this gene is essential in both *Mtb* and *Msm.* qPCR experiments have shown *ftsH* to be upregulated in conditions of oxidative stress and macrophage infection, but downregulated during stationary phase and starvation (Kiran *et al.* 2009). Additionally, while there appears to be a great deal of homology between mycobacterial FtsH and homologs in other bacterial species, no

mycobacterial substrates of this protease have yet been confirmed. Importantly, because of the many differences between *E. coli* and mycobacteria, including the absence of LPS in mycobacteria, these organisms are unlikely to share many of the best-characterized substrates. Specifically, if mycobacterial FtsH were to play any essential or conditionally essential roles in mycobacteria, they would likely be entirely novel. Thus, any findings on FtsH's function and substrates would illustrate new and important pathways in mycobacterial growth and survival.

The role of proteases in cell wall homeostasis

Conserved, essential proteases are the Swiss army knives of the cell, performing a variety of functions that involve many often-unrelated pathways. However, proteases at the inner membrane interface are particularly well poised to lend a hand to the construction and destruction of the cell wall—including both HtrA family proteases and FtsH.

Within the *E. coli* HtrA family, DegS is crucial to liberate the alternative sigma factor SigE under conditions of membrane stress; additionally, DegP both contributes to the activation of the Cpx protein-folding stress pathway and somewhat indiscriminately degrades misfolded proteins in the periplasmic space, many of which are destined for the cell wall and outer membrane. Somewhat analogously, from its position in the inner membrane, *E. coli* FtsH extracts its membrane protein substrates and degrades them, or targets substrates in the cytoplasm, also preferentially proteolyzing loosely or improperly folded proteins (Dalbey *et al.* 2012).

However, the scope of proteolytic regulation of the cell wall goes far beyond what has thus far been characterized in HtrA and FtsH homologs. Important lessons can be learned from the cell cycle itself, and the protein players that contribute to divisome formation (see **Chapter 3**). Many highly active cell wall enzymes, including hydrolases and penicillin binding proteins, must undergo cleavage to complete their activation or bring their brief tenure to a close. Many of

these systems have been identified in *E. coli, Pseudomonas aeruginosa,* and other commonly studied bacterial species. For instance, the *P. aeruginosa* protease CtpA, in conjunction with a lipoprotein partner, is responsible for degrading several putative cell wall hydrolases that would otherwise over-cleave peptide cross-links within peptidoglycan (Srivastava *et al.* 2018).

Additionally, several similar examples exist in mycobacteria: for one, mycobacterial PBPB is cleaved by the metalloprotease Rv2869 during oxidative stress (Mukherjee *et al*. 2009). Additionally, several factors involved in cell wall assembly are ultimately pupylated and subsequently degraded by the mycobacterial proteasome, including MurA, KasB, and MtrA (Festa *et al*. 2010). Notably, however, none of the aforementioned systems are essential for viability, and loss of CtpA, Rv2869, and the proteasome are possible under normal growth conditions. Given the tight regulation of cell wall integrity in all bacterial species, however, it seems that proteolysis is likely to play an essential role in at least some aspect of the construction of this layer of mycobacterial architecture. To test this hypothesis, I focused much of my dissertation on the roles of proteases in the construction and destruction of the cell wall.

Finally, the foci of my dissertation share a common theme: the characterization of conserved genes that have been retooled by the *Mycobacterium* genus for unusual and novel functions. Studies of proteases and the bacterial divisome are often informed by previous work in model organisms such as *E. coli*—but working in mycobacteria often forces research to take unexpected paths forward, illustrating the unusual ways these often pathogenic bacteria have evolved to survive the extremes of their unique environmental conditions.

Summary of Aims

The work described in this dissertation aims to broaden our understanding of mycobacterial proteases, particularly at the periplasmic interface. The implications are threefold: First, these

results can improve our understanding of the processes that help maintain mycobacterial physiology by investigating the unknown functions of essential genes. Second, findings in this area can add to the growing body of literature that studies conserved proteases across diverse families of bacteria, aiding drug discovery efforts and revealing how genes have evolved in divergent lineages. Third, understanding proteases that work at the inner membrane can reveal how cell wall architecture is regulated through post-translational mechanisms—a currently growing field of study.

In Chapter 2, we validate the unusual essentiality of HtrA and reveal, for the first time, a function for this protease in mycobacteria. With the help of a putative lipoprotein adaptor, LppZ, HtrA blocks the potential toxicity of Ami3, a putative cell wall amidase that is stabilized through mannosylation by Pmt. Loss of Ami3 or Pmt relieves the essentiality of both HtrA and LppZ.

In Chapter 3, we describe several conserved Fts proteins common to mycobacteria and several other families of bacteria in which these factors have been well described. In addition to drawing parallels between the mycobacterial divisome and the division machinery of other bacteria, we identify several novel divisome interactors, including SepIVA, which bears homology to several other DivIVA homologs.

Finally, in Chapter 4, we present preliminary findings on another mycobacterial protease, FtsH. For the first time, we present evidence that FtsH is essential in neither *Mtb* nor *Msm,* but reveal that this protease may play a role in guarding against the negative effects of oxidative stress in *Msm.* Additionally, we present preliminary findings on potential substrates of FtsH, generated through a protease trap-based immunoprecipitation. Together, these results present several routes through which mycobacteria have co-opted conserved proteins for functions uniquely tailored to their physiology and environmental stressors.

Chapter 1, Section 1.2: References

1. Alba BM, Zhong HJ, Pelayo JC, and Gross CA. degS (hhoB) is an essential Escherichia coli gene whose indispensible function is to provide _E activity. Mol Microbiol 40(6): 1323-1333, (2001).

2. Barik S, Sureka K, Mukherjee P, Basu J, and Kundu M. RseA, the SigE specific anti-sigma factor of Mycobacterium tuberculosis, is inactivated by phosphorylation-dependent ClpC1P2 proteolysis. Mol Microbiol 75(3): 592-606 (2010). doi: 10.1111/j.1365-2958.2009.07008.x.

3. Bittner LM, Arends J, and Narberhaus F. When, how and why? Regulated proteolysis by the essential FtsH protease in Escherichia coli. Biol Chem 398(5-6):625-635 (2017). doi: 10.1515/hsz-2016-0302.

4. Centers for Disease Control and Prevention. Antibiotic resistance threats in the United States, 2013 (2013).

5. Chang Z. The Function of the DegP (HtrA) Protein: Protease Versus Chaperone. IUBMB Life 68(11):904-907 (2016). doi: 10.1002/iub.1561.

6. Clausen, T et al. HTRA proteases: regulated proteolysis in protein quality control. Nat Rev Mol Cell Biol 12: 152-163 (2011).

7. Dalbey RE, Wang P and van Dijlb JM. Membrane Proteases in the Bacterial Protein Secretion and Quality Control Pathway. Microbiol Mol Biol Rev 76(2):311-330 (2012). doi: 10.1128/MMBR.05019-11.

8. Eriksson, BI et al. Dabigatran etexilate. Nat Rev Drug Discov 7: 557-558 (2008).

9. Festa RA, McAllister F, Pearce MJ, Mintseris J, Burns KE, Gygi SP, Darwin KH. Prokaryotic ubiquitin-like protein (Pup) proteome of Mycobacterium tuberculosis. PLoS One 5(1):e8589 (2010). doi:10.1371/journal.pone.0008589.

10. Frees D, Brøndsted L, and Ingmer H. Bacterial Proteases and Virulence. Regulated Proteolysis in Microorganisms, Chapter 7, Subcellular Biochemistry 66: 161-182 (2013). doi: 10.1007/978-94-007-5940-4_7.

11. Hansen G and Hilgenfeld R. Architecture and regulation of HtrA-family proteins involved in protein quality control and stress response. Cell Mol Life Sci 70:761-775 (2013). doi: 10.1007/s00018-012-1076-4.

12. Hoy B1, Löwer M, Weydig C, Carra G, Tegtmeyer N, Geppert T, Schröder P, Sewald N, Backert S, Schneider G, and Wessler S. Helicobacter pylori HtrA is a new secreted virulence factor that cleaves E-cadherin to disrupt intercellular adhesion. EMBO Rep 11(10):798-804 (2010). doi: 10.1038/embor.2010.114.

13. Ingmer H and Brøndsted L. Proteases in bacterial pathogenesis. Res Microbiol 160: 704-710 (2009). doi: 10.1016/j.resmic.2009.08.017.

14. Ingmer, H and Brondsted, L. Proteases in bacterial pathogenesis. Res Microbiol 160: 704-710 (2009).

15. Janska, H et al. Protein quality control in organelles - AAA/FtsH story. Biochim Biophys Acta 1833: 381-387 (2013).

16. Kapopoulou A, Lew JM, and Cole ST. The MycoBrowser portal: a comprehensive and manually annotated resource for mycobacterial genomes. Tuberculosis (Edinb). Jan 91(1): 8-13 (2011).

17. Kiran, M et al. Mycobacterium tuberculosis ftsH expression in response to stress and viability. Tuberculosis 89: S70-S73 (2009).

18. Langklotz, S et al. Structure and function of the bacterial AAA protease FtsH. Biochim Biophys Acta 1823: 40-48 (2012).

19. Lew JM, Kapopoulou A, Jones LM, and Cole ST. TubercuList - 10 years after. Tuberculosis (Edinb). Jan 91(1): 1-7 (2011).

20. Licht, S and Lee, I. Resolving Individual Steps in the Operation of ATP-Dependent Proteolytic Molecular Machines: From Conformational Changes to Substrate Translocation and Processivity. Biochemistry 47(12): 3595-3605 (2008).

21. MohamedMohaideen, NN et al. Structure and Function of the Virulence-Associated High Temperature Requirement A of Mycobacterium tuberculosis. Biochemistry 47: 6092-6102 (2008).

22. Mukherjee P, Sureka K, Datta P, Hossain T, Barik S, Das KP, Kundu M, Basu J. Novel role of Wag31 in protection of mycobacteria under oxidative stress. Mol Microbiol 73(1):103-19 (2009). doi:10.1111/j.1365-2958.2009.06750.x.

23. Okuno T and Ogura T. FtsH protease-mediated regulation of various cellular functions. Subcell Biochem 66:53-69 (2013). doi: 10.1007/978-94-007-5940-4_3.

24. Perna AM, Reisen F, Schmidt TP, Geppert T, Pillong M, Weisel M, Hoy B, Simister PC, Feller SM, Wessler S, and Schneider G. Inhibiting Helicobacter pylori HtrA protease by addressing a computationally predicted allosteric ligand binding site. Chem Sci 5:3583-3590 (2014).

25. Poordad F et al. Boceprevir for untreated chronic HCV genotype 1 infection. N Engl J Med 364: 1195-1206 (2011).

26. Raju RM, Goldberg AL, and Rubin EJ. Bacterial proteolytic complexes as therapeutic targets. Nat Rev Drug Discov 11: 777-789 (2012). doi: 10.1038/nrd3846.

27. Rudra P, Prajapati RK, Banerjee R, Sengupta S, and Mukhopadhyay J. Novel mechanism of gene regulation: the protein Rv1222 of Mycobacterium tuberculosis inhibits transcription by anchoring the RNA polymerase onto DNA. Nucleic Acids Res 43(12): 5855-5867 (2015). doi: 10.1093/nar/gkv516.

28. Sauer, RT and Baker, TA. AAA+ Proteases: ATP-Fueled Machines of Protein Destruction. Annu Rev Biochem 80: 587-612 (2011).

29. Schumann, W. FtsH - a single-chain charonin? FEMS Microbiol Rev 23: 1-11 (1999).

30. Sharp JD, Singh AK, Park ST, Lyubetskaya A, Peterson MW, Gomes AL, Potluri LP, Raman S, Galagan JE, and Husson RN. Comprehensive Definition of the SigH Regulon of Mycobacterium tuberculosis Reveals Transcriptional Control of Diverse Stress Responses. PLoS One 11(3): e0152145 (2016). doi: 10.1371/journal.pone.0152145.

31. Skorko-Glonek J, Zurawa-Janicka D, Koper T, Jarzab M, Figaj D, Glaza P, and Lipinska B. HtrA protease family as therapeutic targets. Curr Pharm Des 19(6):977-1009 (2013).

32. Srivastava D, Seo J, Rimal B, Kim SJ, Zhen S, and Darwin AJ. A Proteolytic Complex Targets Multiple Cell Wall Hydrolases in Pseudomonas aeruginosa. MBio 9(4). pii: e00972-18 (2018). doi: 10.1128/mBio.00972-18.

33. Vermehren, J and Sarrazin, C. New HCV therapies on the horizon. Clin MIcrobiol Infect 17: 122-134 (2011).

34. Wessler S, Schneider G, and Backert S. Bacterial serine protease HtrA as a promising new target for antimicrobial therapy? Cell Commun Signal 10;15(1):4 (2017). doi: 10.1186/s12964-017-0162-5.

35. White, MJ et al. PepD Participates in the Mycobacterial Stress Response Mediated through MprAB and SigE. J Bacteriol 192(6): 1498-1510 (2010).

36. White, MJ et al. The HtrA-Like Serine Protease PepD Interacts with and Modulates the Mycobacterium tuberculosis 35-kDa Antigen Outer Envelope Protein. PLoS ONE 6(3): e18175 (2011).

37. World Health Organization. Antimicrobial resistance: global report on surveillance 2014 (2014).

38. World Health Organization. Global Tuberculosis Report (2017).

39. Zhang, YJ et al. Global Assessment of Genomic Regions Require for Growth in Mycobacterium tuberculosis. PLoS Pathog 8(9): e1002946 (2012).

40. Zurawa-Janicka, D et al. HtrA proteins as targets in therapy of cancer and other diseases. Expert Opin Their Targets 14(7): 665-679 (2010).

Chapter 2

Characterization of mycobacterial HtrA

Chapter 2, Section 2.1: Mycobacterial HtrA is required to block the toxic activity of a putative cell wall amidase

Katherine J. Wu[1], Cara C. Boutte[2], Thomas R. Ioerger[3], Eric J. Rubin[1*]

1 - Department of Immunology and Infectious Diseases, Harvard T.H. Chan School of Public Health, Boston, MA 02115, USA

2 - Department of Biology, University of Texas at Arlington, Arlington, TX 76019, USA

3 - Department of Computer Science, Texas A&M University, College Station, TX 77843, USA

* - Correspondence: erubin@hsph.harvard.edu

Author contributions: K.J.W. and E.J.R. designed experiments and wrote the paper. K.J.W., C.C.B., and T.R.I. performed experiments and analyzed data. This work is currently under review at *Cell Reports* at the time of this writing.

SUMMARY

Mycobacterium tuberculosis, the causative agent of tuberculosis, withstands diverse environmental stresses in the host. The periplasmic protease HtrA is required to survive extreme conditions in most bacteria but is predicted to be essential for normal growth in mycobacteria. To elucidate its essential function, we tested HtrA essentiality in *Mycobacterium smegmatis*. We find that HtrA is, indeed, essential and interacts with another essential protein of unknown function, LppZ. However, the loss of any of three unlinked genes, including those encoding Ami3, a peptidoglycan muramidase, and Pmt, a mannosyltransferase, suppresses the essentiality of both HtrA and LppZ. Loss of HtrA/LppZ leads to accumulation of active Ami3, which is toxic when mannosylated. In the presence of HtrA/LppZ or absence of Pmt, Ami3 has a shorter half-life and accumulates to lower levels. These data suggest HtrA-LppZ blocks the toxicity of a cell wall enzyme in a novel mechanism of mycobacterial homeostasis.

INTRODUCTION

Mycobacterium tuberculosis (Mtb), the causative agent of tuberculosis, remains the greatest infectious killer in human history, claiming 1.5 million lives each year (WHO 2017). Despite this enormous public health burden, efforts to curb *Mtb's* spread and prevent rising rates of drug resistance have stagnated in recent decades. To combat the extremes of host defenses, *Mtb* deploys a tightly controlled array of stress response systems, including a large number of proteases. Recently mycobacterial proteases have emerged as appealing therapeutic targets because several of the most conserved homologs, including Clp, FtsH, HtrA, and the proteasome, are essential for the growth or virulence of *Mtb* (Raju *et al*. 2012a).

Despite their integral role in *Mtb* cell biology, mycobacterial proteases remain understudied. Recent work in our lab has implicated the mycobacterial Clp protease in the turnover of the essential transcriptional repressor WhiB1 (Raju *et al*. 2012b, Raju *et al*. 2014). Similarly, transposon insertion sequencing data have indicated that the periplasmic serine protease HtrA (MSMEG_5070, Rv1223) is essential in mycobacteria (Sassetti *et al*. 2001, Sassetti *et al*. 2003a, Sassetti *et al*. 2003b, Sassetti *et al*. 2011, Griffin *et al*. 2011, Zhang *et al*. 2012, DeJesus *et al*. 2013). Despite this, the reasons for HtrA's essentiality have remained unclear.

In *E. coli* and other organisms, HtrA is characterized as a non-essential, periplasmic protease with secondary chaperone function (Clausen *et al.* 2011). While dispensable for normal growth, HtrA is crucial for the virulence of several intracellular pathogens including *Campylobacter, Shigella, Helicobacter pylori, Yersinia enterocolitica, Listeria,* and *Salmonella* (Ingmer *et al*. 2009). In these species, HtrA is required to tolerate a common set of stressful conditions including high temperature, oxidative stress, and macrophage survival. The well-characterized *E. coli* HtrA homolog DegP is induced in conditions of membrane stress and becomes essential during heat shock (Ingmer *et al*. 2009). DegP contains a protease domain with a conserved Ser-

His-Asp catalytic triad and two PDZ domains (**Figure 2.1A**) that regulate substrate binding and access to the proteolytic chamber. Although a handful of substrates have been identified in *E. coli* (Clausen *et al*. 2002), DegP appears to be mostly indiscriminate in its specificity, preferring denatured, unfolded substrates with hydrophobic C-termini.

Like *E. coli* and many other organisms, virulent mycobacteria express three orthologs of HtrA. In *Mtb,* these are HtrA (MSMEG_5070, Rv1223), HtrA2/PepD (MSMEG_5486, Rv0983), and HtrA3/PepA (Rv0125, which apparently lacks a homolog in *Msm*); of these, only HtrA is predicted to be essential. However, this essentiality appears to be conserved across all mycobacteria, regardless of pathogenicity (Lew *et al.* 2011). Nevertheless, *htrA's* synteny indicates that its transcription may be stress responsive, as it lies in an operon with *sigE*, a stress-responsive alternative sigma factor (Manganelli *et al.* 2004). Additionally, its high degree of sequence conservation with homologs in other species indicate that HtrA may be capable of recapitulating some stress-responsive or virulence functions. While HtrA's role in mediating the mycobacterial stress response may partially overlap with its homologs in other species, its essentiality indicates it must be involved in a unique regulatory pathway that supports *Mtb* growth and survival.

Here, we present evidence that HtrA serves a previously undescribed and essential role in the regulation of mycobacterial growth by degrading a putative cell wall muramidase. HtrA engages in a periplasmic complex with another essential protein, LppZ, to control levels of the lethal hyperactivity of Ami3, an amidase stabilized by Pmt-mediated O-mannosylation. Loss of either *ami3* or *pmt* is sufficient to relieve the essentiality of both *htrA* and *lppZ*. These data expand upon a growing body of literature illustrating the complex ways in which bacteria regulate growth and division.

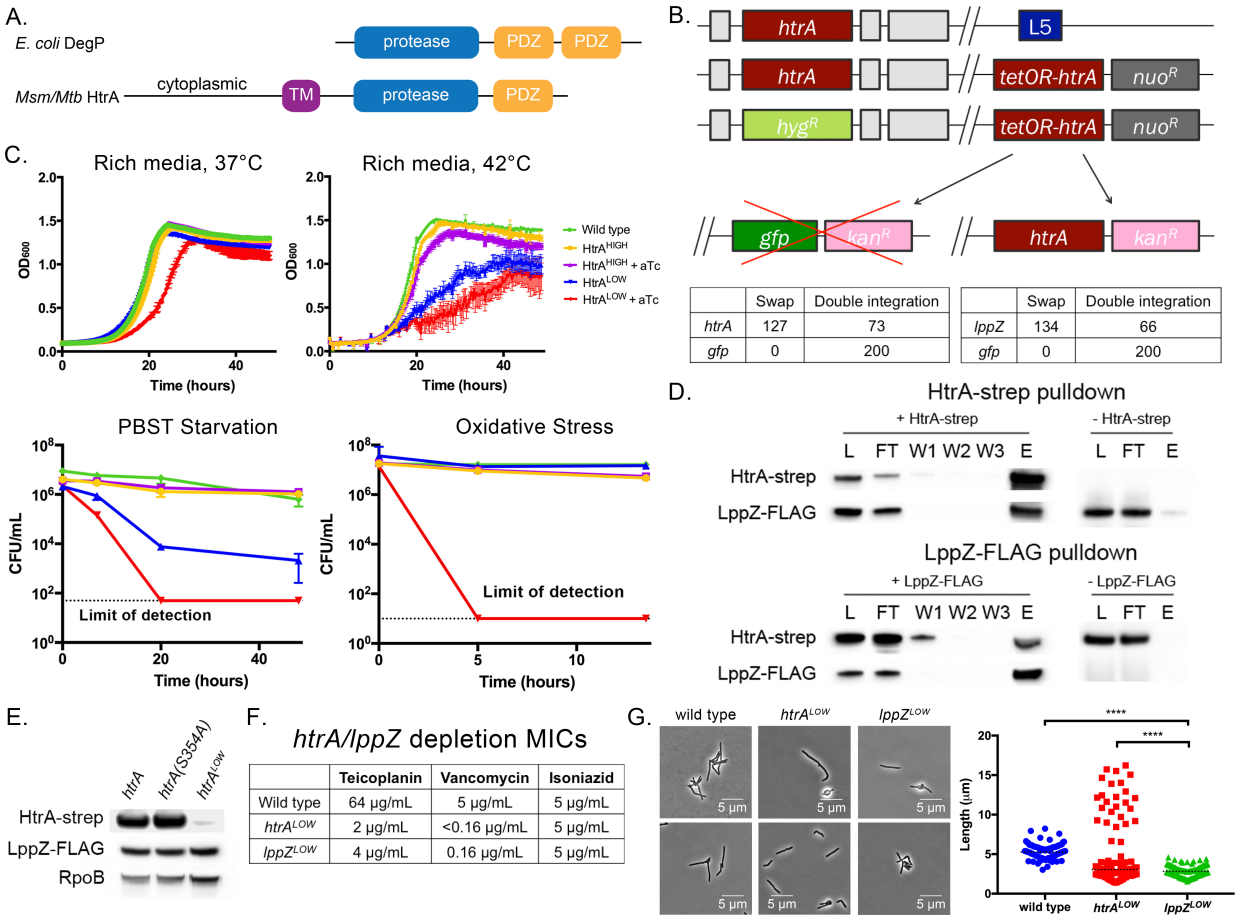

	Swap	Double integration
htrA	127	73
gfp	0	200

	Swap	Double integration
lppZ	134	66
gfp	0	200

	Teicoplanin	Vancomycin	Isoniazid
Wild type	64 µg/mL	5 µg/mL	5 µg/mL
htrA^{LOW}	2 µg/mL	<0.16 µg/mL	5 µg/mL
lppZ^{LOW}	4 µg/mL	0.16 µg/mL	5 µg/mL

Figure 2.1: HtrA-LppZ are essential interacting proteins in *Mycobacterium smegmatis.* A. DegP/HtrA homolog domain architecture. *E. coli* DegP contains a protease domain and two C-terminal PDZ domains. In contrast, mycobacterial HtrA is anchored in the inner membrane and contains a single PDZ domain. Additionally, mycobacterial HtrA has a cytoplasmic domain with no homology to any known protein. **B. HtrA and LppZ are essential by L5 swap.** Top: a schematic of the L5 essentiality swap. Placing a second copy of *htrA,* along with a nourseothricin resistance cassette, at the L5 phage integration site allows replacement of endogenous *htrA* with a hygromycin resistance cassette. This copy of *htrA* can be swapped for another copy of *htrA* with a different antibiotic resistance marker, but not for a functionally unrelated gene such as *gfp.* Bottom: quantification of *htrA* and *gfp* swaps. A total of 200 transformants were tested for antibiotic resistance. An equivalent swap was performed for *lppZ* and enumerated in the same manner. **C. Cells depleted of HtrA grow at a slower rate.** When regulated by an aTc-repressible promoter, *htrA* can be transcriptionally depleted from cells. Two strains were constructed: *htrA*^{HIGH}, which used a strong promoter susceptible to aTc-based repression, and *htrA*^{LOW}, a weak promoter susceptible to aTc-based repression. These strains were grown, with or without aTc, in each of four conditions: rich media at 37°C, high temperature (42°C), carbon-nitrogen starvation (PBS-Tween20), and oxidative stress (0.02% tert-butyl hydroperoxide). Error bars represent standard deviation of the mean. **D. HtrA and LppZ interact.** HtrA-Strep and LppZ-FLAG were individually immunoprecipitated using anti-

Strep and anti-FLAG magnetic beads, respectively, and the following fractions were analyzed by Western blotting: L = lysate, FT = flow through,
Figure 2.1 (Continued): W1 = wash 1, W2 = wash 2, W3 = wash 3, E = elution. Control immunoprecipitations lacking the respective bait were performed simultaneously and lysate, flow-through, and elution were analyzed. **E. LppZ is not a substrate of HtrA.** Strains expressing *htrA* under its native promoter or $htrA^{LOW}$ were grown to log phase and cell lysate was analyzed by Western blotting to detect levels of HtrA-Strep and LppZ-FLAG. **F. Cells lacking HtrA or LppZ are highly sensitive to cell wall-targeting antibiotics.** $htrA^{LOW}$ and $lppZ^{LOW}$, strains expressing the respective essential gene under a weak promoter, were grown in teicoplanin and vancomycin, antibiotics targeting D-ala-D-ala crosslinking in the mycobacterial cell wall, and isoniazid, an antibiotic that inhibits mycolic acid synthesis. **G. Depletion of HtrA or LppZ induces morphological defects.** $htrA^{LOW}$ and $lppZ^{LOW}$ were grown to log phase in aTc and observed under the microscope. Two representative images for each strain are shown. At least 100 cells were quantified in each condition. Dotted black lines indicate median values. ****p-value <0.0001.

RESULTS

HtrA-LppZ forms an essential complex in the mycobacterial periplasm

Previous transposon insertion-based (Tn-seq) screens have predicted the essentiality of *htrA* in both *Mycobacterium smegmatis (Msm)* and *Mycobacterium tuberculosis (Mtb)* (Sassetti *et al*. 2001, Sassetti *et al*. 2003a, Sassetti *et al*. 2003b, Sassetti *et al*. 2011, Griffin *et al*. 2011, Zhang *et al*. 2012, DeJesus *et al*. 2013). To confirm *htrA* essentiality, we attempted to delete these genes from the genome of *M. smegmatis* through mycobacterial recombineering and homologous recombination (**Figure 2.1B, top**). Briefly, a second copy of *htrA* was transformed into the L5 phage integration site with a nourseothricin resistance cassette, allowing the replacement of the endogenous copy of *htrA* with a hygromycin resistance cassette. We then attempted to transform *htrA* or an empty vector with a kanamycin resistance cassette into the L5 integration site (an "L5 swap"). Three outcomes can result from these experiments. First, integrations resulting in non-viable cells will prevent the growth of transformants on antibiotic selection. Second, successful "swaps" are those that acquire kanamycin resistance at the expense of nourseothricin resistance, indicating the replacement of the original integrated vector with the transformed vector. Third, the second vector may recombine in alongside the original vector, creating a double integrant that retains resistance to both antibiotics. In these experiments, *htrA* swapped in at a rate of 63.5%, while the empty vector yielded only double integrants (**Figure 2.1B, bottom**), indicating that HtrA is essential for survival.

To assess the phenotype of *htrA* hypomorphs, we constructed a depletion strain in which the only copy of *htrA* was under the control of an anhydrotetracycline (aTc)-repressible promoter. These cells clumped in liquid culture and exhibited a slower growth rate (**Figure 2.1C**), but remained viable, suggesting a minimal amount of HtrA is sufficient to sustain growth. As HtrA homologs in other bacterial species are associated with protection against environmental stress, we next tested the ability of *htrA*-depleted cells to survive extreme conditions, including high

Figure 2.2: Loss-of-function mutations in *ami3*, *pmt*, or *mprB* suppress *htrA* essentiality. A, B, and C. Double mutant phenotypes of *htrA* suppressor strains. Wild type *Msm*, single suppressor gene deletions, suppressor deletions with *htrA* deletions, and *htrA* complemented strains (see **Figure A1.1, A1.6**) were grown under conditions identical to those in **Figure 2.1,** including growth in rich media at 37°C, high temperature (42°C), carbon-nitrogen starvation (PBS-Tween20), and oxidative stress (0.02% tert-butyl hydroperoxide). Error bars represent standard deviation of the mean. **D. *htrA* suppressor mutants exhibit reduced cell length.** Single suppressor deletion strains (blue), *htrA* double deletion strains (red), and *htrA* complemented strains (green) were grown to log phase and analyzed for total cell length (see **Figure A1.2**). At least 70 cells were quantified in each condition. Dotted black lines indicate median values. **** = p-value <0.0001.

Figure 2.2 (Continued)

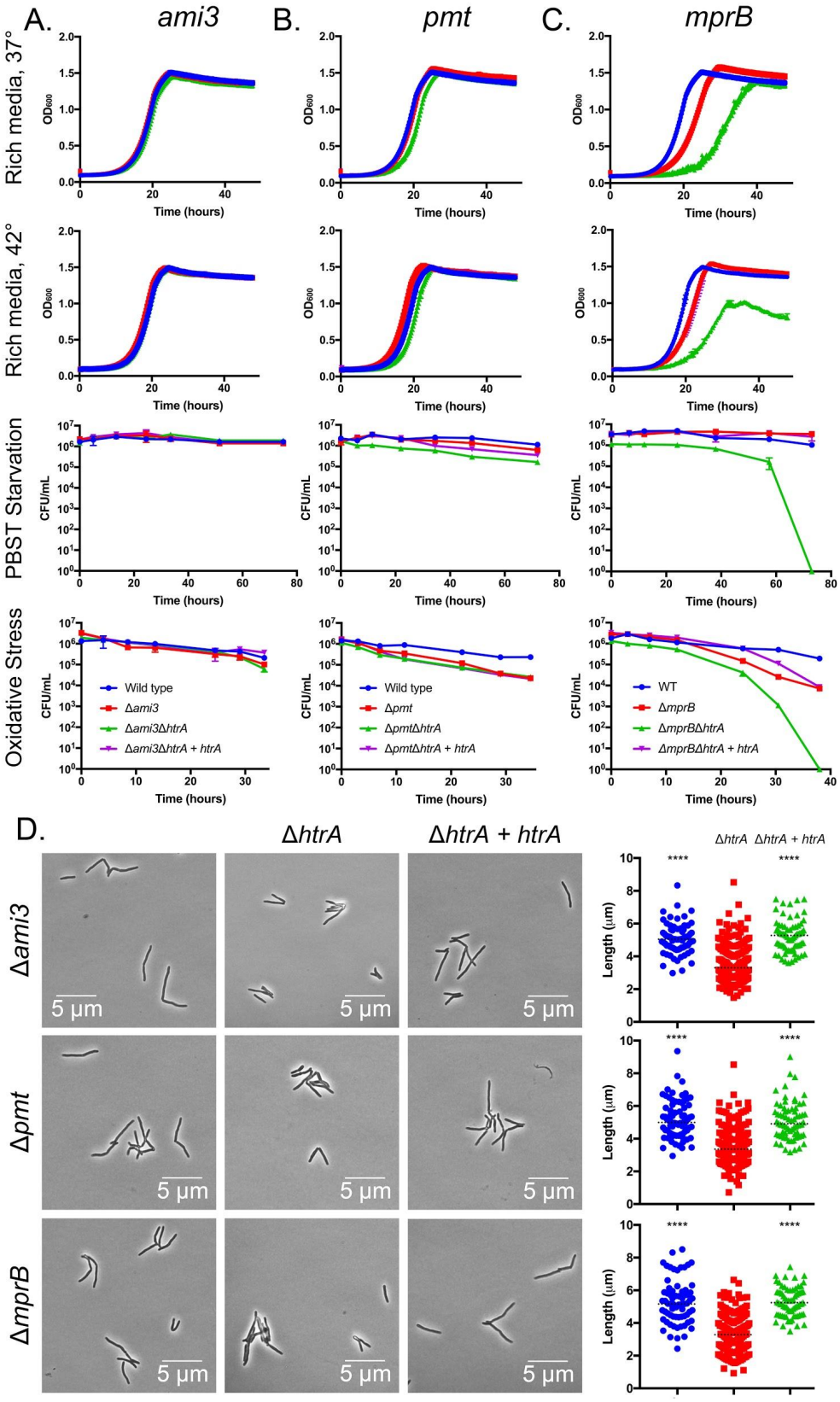

temperature, oxidative stress, and carbon-nitrogen starvation (**Figure 2.1C**). All tested conditions impaired the growth of or killed the most *htrA*-depleted cells, indicating that higher amounts of HtrA are required to sustain growth under environmental stress.

We reasoned that identifying binding partners could help define HtrA's function. To find interactors, we immunoprecipitated Strep-tagged HtrA and identified eluted proteins by mass spectrometry. The most abundant protein, LppZ (MSMEG_2369, Rv3006), had no known function. LppZ is also predicted to be essential in both *M. smegmatis* and *M. tuberculosis,* and is annotated as a putative secreted lipoprotein (Sassetti *et al*. 2001, Sassetti *et al*. 2003a, Sassetti *et al*. 2003b, Sassetti *et al*. 2011, Griffin *et al*. 2011, Zhang *et al*. 2012, DeJesus *et al*. 2013). We confirmed LppZ essentiality with an L5 swap (**Figure 2.1B**) and detected a stable interaction between HtrA and LppZ by co-immunoprecipitation of tagged proteins (**Figure 2.1D**).

Based on this interaction, LppZ could be a substrate or adaptor of HtrA activity. To distinguish between these possibilities, we tagged LppZ with a FLAG sequence and monitored its stability during depletion of *htrA*. LppZ levels were completely insensitive to alterations in HtrA (**Figure 2.1E**). This suggests that LppZ is a lipoprotein adaptor of HtrA's proteolytic activity, analagous to interactions described in *E. coli* between the periplasmic protease Prc and the lipoprotein NlpI (Singh *et al*. 2015, Tadokoro *et al*. 2004), and between DegP and recombinant mutants of the lipoprotein Lpp (Park *et al*. 2017).

If LppZ is an HtrA adaptor, LppZ mutants should phenocopy HtrA mutants. Indeed, both the *htrA* and *lppZ* depletion strains exhibited increased sensitivity to antibiotics targeting cell wall crosslinking (but not other antibiotics such as isoniazid) (**Figure 2.1F**), and severe morphological defects (**Figure 2.1G**). Cells bulged and shortened upon *htrA* or *lppZ* depletion; however, a small subpopulation branched in only the *htrA* depletion. Both these morphologies

are reminiscent of previously characterized strains in which dysregulation of cell wall machinery induces swelling and branching (Chao *et al*., 2013, Kieser *et al.* 2015). These data indicate that HtrA and LppZ likely act cooperatively as a complex in the same step of an essential genetic pathway that engages the cell wall.

Loss-of-function mutations in *ami3*, *pmt*, or *mprB* suppress *htrA* and *lppZ* essentiality

Unlike *E. coli* DegP, mycobacterial HtrA is membrane anchored and has only one PDZ domain. Furthermore, it has a unique cytoplasmic domain at its N-terminus that bears no homology to any know protein (Kapopoulu *et al*. 2011). To understand structure-function relationships in HtrA we made a series of domain deletions and tested their viability using L5 swaps. We found that both the cytoplasmic and PDZ domains are essential for function (**Figure A1.1A**) but do not affect HtrA's interaction with LppZ (**Figure A1.1B**). However, these experiments yielded a small number of survivors which grew despite loss of functional HtrA. We hypothesized that these might be due to mutations elsewhere in the chromosome and performed whole genome sequencing of these strains to identify potential extragenic suppressors of *htrA* essentiality.

We sequenced nine strains in total and compared their genomes to that of the parental strains. Each swapped strain carried at least one of the following mutations (**Figure A1.1C**): one of five different frameshift mutations in *ami3* (MSMEG_6406), a putative N-acetylmuramoyl-L-alanine amidase; a frameshift mutation in *pmt* (MSMEG_5447), a dolichyl-phosphate-mannose-protein mannosyltransferase; and two SNPs in *mprB* (MSMEG_5487), the sensor histidine kinase of a two-component regulatory system that also includes *mprA.* All of these genes are nonessential in *Mtb* (Sassetti *et al*. 2001, Zahrt *et al.* 2001, VanderVen *et al.* 2005). To verify these suppressors, we generated double deletion strains in fresh backgrounds. The Δ*ami3*Δ*htrA* and Δ*pmt*Δ*htrA* double deletion strains grew robustly under all growth conditions tested, including those in which the *htrA* depletion strain failed to grow or died (**Figure 2.2A, 2.2B**). However, the

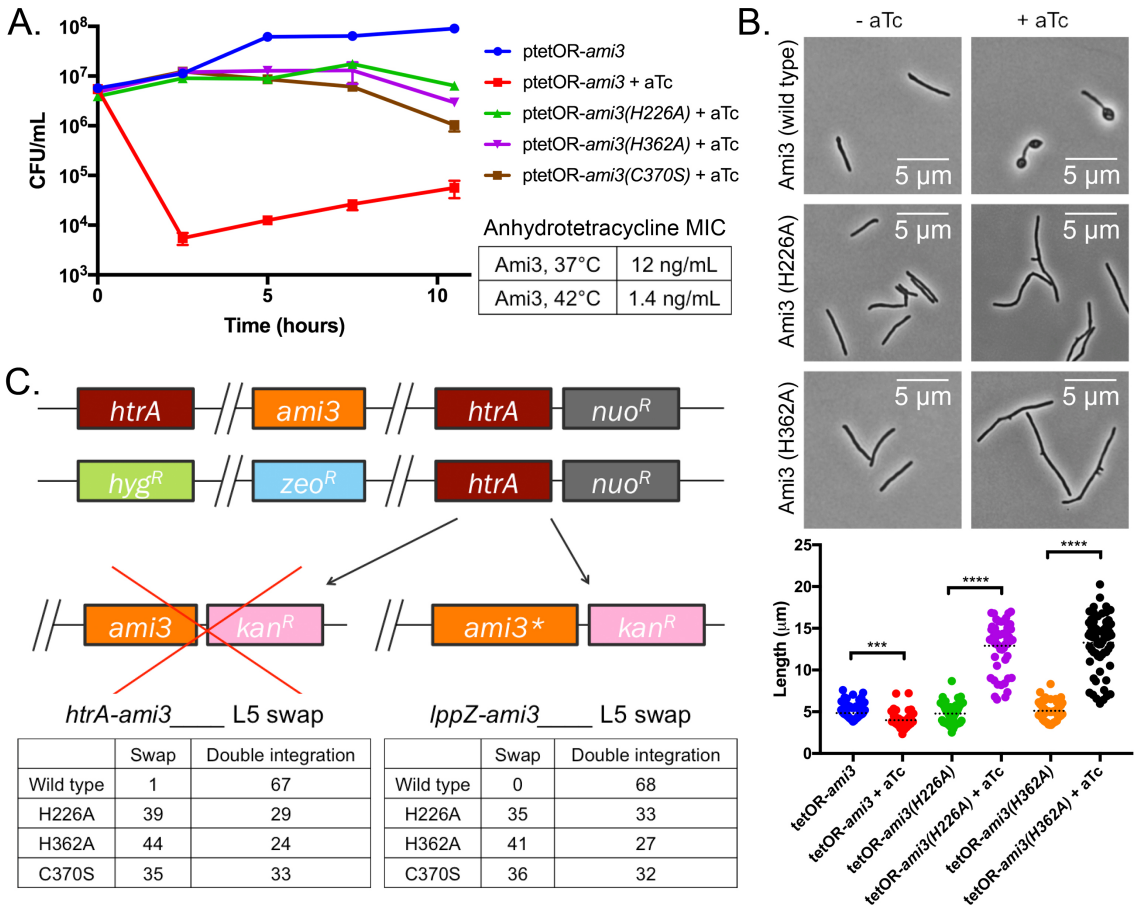

	Swap	Double integration
Wild type	1	67
H226A	39	29
H362A	44	24
C370S	35	33

	Swap	Double integration
Wild type	0	68
H226A	35	33
H362A	41	27
C370S	36	32

Figure 2.3: Ami3 hyperactivity is toxic. A. Overexpression of Ami3 is lethal. Left: strains expressing wild type *ami3* or its catalytic mutants regulated by an aTc-inducible promoter were grown in the presence or absence of 100 ng/mL aTc (see **Figure A1.3**). Aliquots were taken at the indicated time points and analyzed for colony forming units (CFUs). The uninduced wild-type Ami3 strain is representative of all uninduced strains. Error bars represent standard deviation of the mean. Right: aTc MIC of wild-type Ami3 overexpression at different temperatures. **B. Overexpressions of different variants of Ami3 yield divergent phenotypes.** Strains expressing wild-type *ami3* or its catalytic mutants regulated by an aTc-inducible promoter were grown in the presence or absence of 100 ng/mL aTc and observed under the microscope. At least 50 cells were quantified in each condition. Dotted black lines indicate data median. ***p<0.001, ****p<0.0001. **C. Ablation of Ami3 catalytic activity suppresses the essentiality of *htrA* and *lppZ*.** Top: the endogenous copies of *ami3* and *htrA* were replaced with zeocin and hygromycin resistance cassettes, respectively, and a copy of *htrA* was integrated at the L5 phage integration site. *ami3* or catatytically inactive variants of *ami3, ami3(H226A), ami3(H362A),* and *ami3(C370S),* were transformed into this background. *ami3** indicates the respective *ami3* allele. Full swaps that acquire kanamycin resistance at the expense of noursethricin resistance render strains devoid of *htrA* (or *lppZ*) and must thus carry a suppressor mutation. Bottom: quantification of *ami3* and *ami3** swaps. A total of 68 transformants were tested for antibiotic resistance. An equivalent swap was performed for *lppZ* and enumerated in the same manner.

Δ*mprB*Δ*htrA* double deletion strain, while viable, grew slowly even under optimal conditions, and remained moderately susceptible to environmental stress (**Figure 2.2C**). Importantly, loss of *ami3, pmt,* and *mprB* also allowed disruption of the otherwise essential *lppZ* (**Figure A1.2**). Given that *mprB* only partially suppresses the essentiality of *htrA* and the previously characterized, wide-reaching transcriptional effects of deleting *mprB* (He *et al.* 2006), we decided to focus our subsequent experiments on *ami3* and *pmt.*

These double deletion strains allowed us to study the growth and morphology of strains that lacked *htrA* and *lppZ.* The suppressed deletion strains grew at near normal rates (**Figure 2.2A, 2.2B, 2.2C, 2.2D**), unlike the *htrA* depletion strain. Additionally, Δ*ami3*Δ*htrA* and Δ*ami3*Δ*lppZ* were less sensitive to teicoplanin and vancomycin than the *htrA* and *lppZ* depletions (**Figure A1.2C**). However, double deletion strains in all backgrounds exhibited reduced cell length (**Figure 2.2D, Figure A1.2A, Figure A1.2B**), much like the *htrA* and *lppZ* depletions, indicating that the HtrA-LppZ complex may have an additional, non-essential function that affects cell division or elongation.

Ami3 is toxic when overexpressed

Because deletions of *ami3* and *pmt* could independently suppress the essentiality of both *htrA* and *lppZ,* we reasoned that these genes likely operate within the same pathway. In *E. coli*, the peptidoglycan endopeptidase MepS has been shown to be negatively regulated by the periplasmic protease Prc in conjunction with a lipoprotein adaptor, NlpI (Schwechheimer *et al.* 2015, Singh *et al*. 2015). Because the *htrA* and *lppZ* depletion phenotypes (**Figure 2.1F, 2.1G**) mimic cell wall dysregulation (Chao *et al*., 2013, Kieser *et al.* 2015), we hypothesized that the putative cell wall enzyme *ami3* might be a substrate of HtrA-LppZ. Indeed, when expressed under an aTc-inducible promoter (**Figure A1.3A**), *ami3* overexpression quickly led to cell death (**Figure 2.3A, top**). We found the aTc minimum inhibitory concentration (MIC) of this strain to be

about 12 ng/mL. This toxicity was exacerbated at high temperature (**Figure 2.3A, bottom**), mirroring the sensitivity of *htrA* depletion (**Figure 2.1C**). Furthermore, cells overexpressing *ami3* exhibited reduced cell length and large polar bulges (**Figure 2.3B**), phenocopying *htrA* and *lppZ* depletion (**Figure 2.1G**).

Ami3 exhibits some structural homology to *E. coli* AmiD, a zinc metalloprotease in the amidase_2 domain family of cell wall hydrolyzing amidases (Kelley *et al*. 2015, Senzani *et al*. 2017). Threading the Ami3 sequence into the AmiD structure using Phyre2 allowed us to identify a potential triad of zinc-coordinating residues in Ami3 consisting of two histidines (H226, H362) and a cysteine (C370). To test the contribution of Ami3 enzymatic activity to HtrA essentiality, we constructed mutants carrying amino acid substitutions in each of these residues and attempted to swap enzymatically inactive versions of *ami3* into a strain lacking the endogenous copies of both *ami3* and *htrA* and carrying a copy of *htrA* at the L5 integration site. We found that that the inactive alleles could exchange with *htrA* and, in an analogous experiment, *lppZ* (**Figure 2.3C**). Thus, HtrA and LppZ are only essential in the presence of Ami3 catalytic activity.

If Ami3 hyperactivity leads to cell death, mutating the catalytic residues of Ami3 might relieve toxicity. Indeed, overexpression of *ami3(H226A), ami3(H362A),* or *ami3(C370S)* was no longer lethal to cells (**Figure 2.3A**). However, full wild-type viability was not restored, indicating that even inactive *ami3* still retains some toxicity despite being expressed at levels broadly similar to the wild-type allele (**Figure 2.3C, A1.3B)**. Cells which overexpressed the mutant protein were still abnormal, albeit with a morphology distinct from that of wild-type Ami3 overexpression: overaccumulation of the catalytically inactive mutants of Ami3 resulted in long, branching cells (**Figure 2.3B**). These cells resemble a subpopulation of cells with increased length and branching observed upon *htrA* depletion (**Figure 2.1G**).

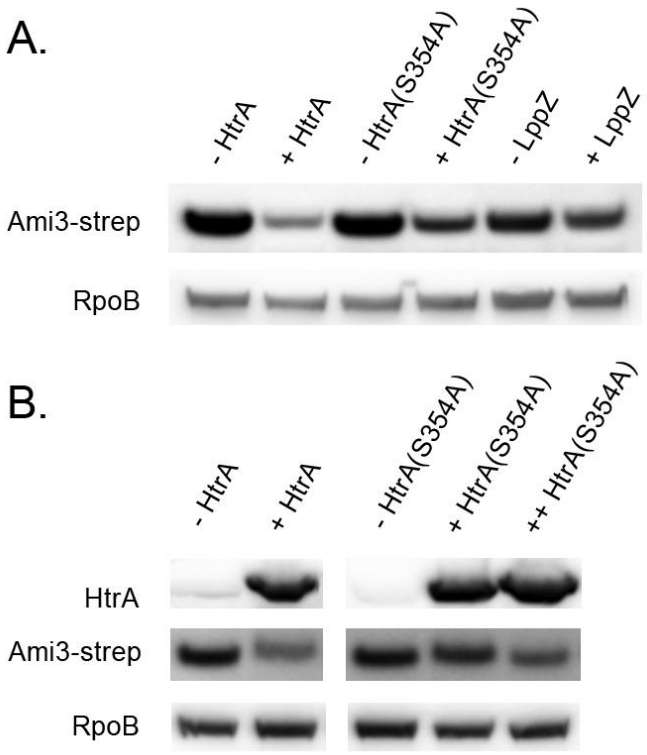

Figure 2.4: Induction of HtrA-LppZ decreases cellular Ami3 levels. A. HtrA and LppZ expression decrease Ami3 levels to varying degrees. Strains in which the only copy of *htrA* or *lppZ* was under an aTc-inducible promoter were constructed and grown with or without 100 ng/mL aTc for 12 hours. HtrA(S354A) is an allele of *htrA* shown to exhibit reduced catalytic activity in HtrA homologs due to a mutation in its catalytic serine (see **Figure A1.3**). Whole cell lysate was analyzed by Western blotting using anti-Strep and anti-RpoB as a loading control. **B. Higher expression of HtrA(S354A) further decreases Ami3.** A second copy of aTc-inducible *htrA(S354A)* was transformed into the mutant strain described in panel A, and all strains were grown with or without 100 ng/mL aTc for 8 hours. Whole cell lysate was analyzed by Western blotting using anti-Strep and anti-HtrA, and anti-RpoB as a loading control.

HtrA-LppZ detoxifies Ami3

Based on the correlation in phenotypes between *ami3* overexpression and *htrA* and *lppZ* depletion, we hypothesized that HtrA-LppZ negatively regulates Ami3. To test this, we constructed strains in which the only copies of *htrA* and *lppZ* were expressed only in the presence of inducer and monitored levels of Ami3.

As expected, Ami3 levels decreased with HtrA induction (**Figure 2.4A**). We next mutated the catalytic serine of HtrA, creating HtrA(S354A). In PepD, another mycobacterial HtrA homolog, this mutation ablates up to 90% of proteolytic activity (White *et al*. 2010, White *et al*. 2011). As expected, Ami3 levels were less affected by HtrA(S354A) induction despite similar levels of HtrA protein (**Figure 2.1E**). Increasing HtrA(S354A) expression further decreased Ami3 levels, but not to the levels achieved by wild-type HtrA (**Figure 2.4B**). Accordingly, strains expressing only HtrA(S354A) were more sensitive to Ami3 overexpression (**Figure A1.3C**). A similar but less robust decrease in Ami3 protein levels was observed upon LppZ induction (**Figure 2.4A**).

Finally, we tested the dependency of the HtrA-LppZ interaction on the presence of its potential substrate Ami3. We found that HtrA and LppZ interacted even in a Δ*ami3* background (**Figure A1.1D**). We conclude that the HtrA-LppZ complex negatively regulates Ami3, with HtrA likely serving as the limiting factor and catalytic agent. LppZ may act as an Ami3-specific adaptor or enhance HtrA activity.

Pmt stabilizes Ami3 through mannosylation

Because loss of *pmt* suppressed the essentiality of *htrA* and *lppZ* (**Figure 2.2B, 2.2D**), we hypothesized that it might be a positive regulator of Ami3 toxicity by driving its accumulation. Pmt has been previously characterized as a periplasmic mannosyltransferase with a catalytic aspartic acid at residue 68 (D68) (VanderVen *et al.* 2005; Liu *et al.* 2013); however, few of its

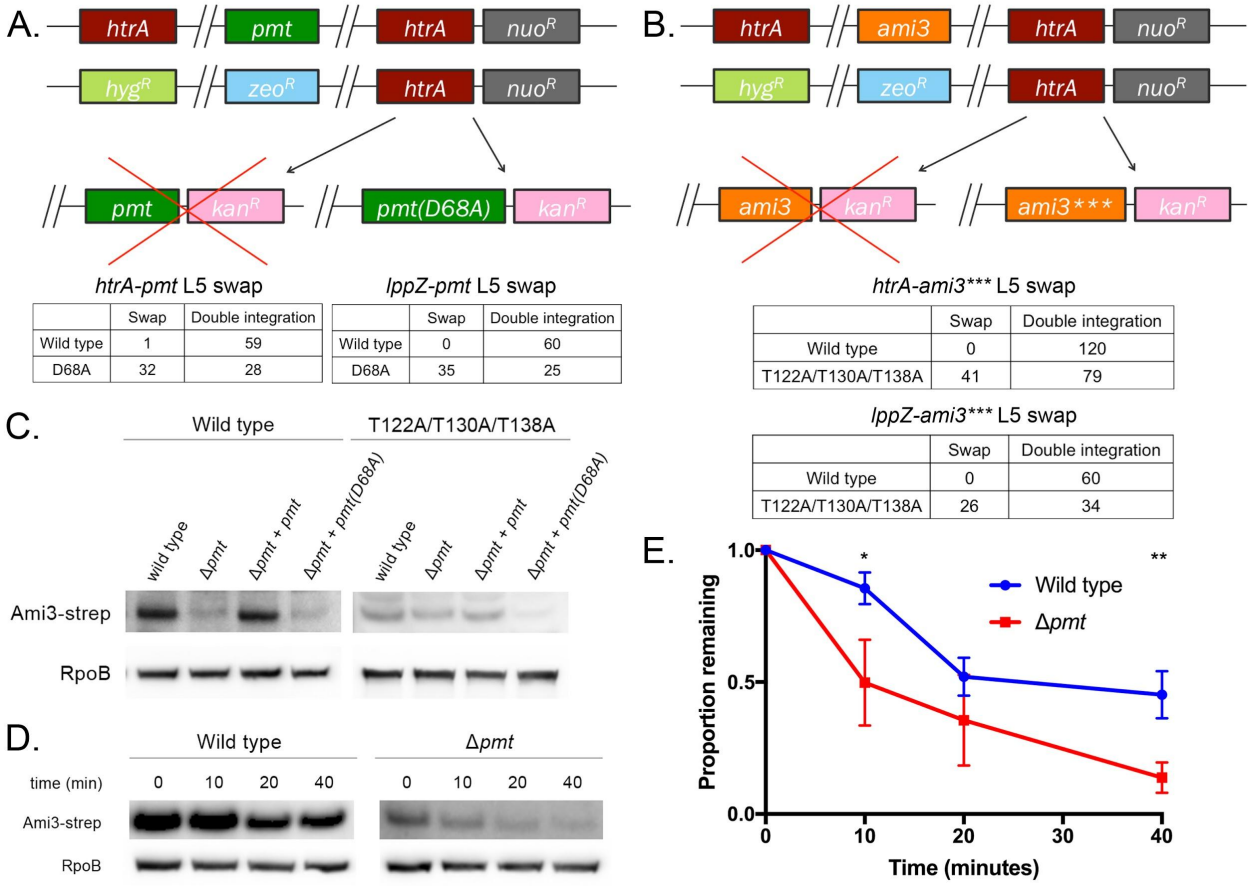

	Swap	Double integration
Wild type	1	59
D68A	32	28

	Swap	Double integration
Wild type	0	60
D68A	35	25

	Swap	Double integration
Wild type	0	120
T122A/T130A/T138A	41	79

	Swap	Double integration
Wild type	0	60
T122A/T130A/T138A	26	34

Figure 2.5: Pmt mannosylation stabilizes Ami3. A. Mutating the catalytic activity of Pmt suppresses the essentiality of *htrA* and *lppZ.* Top: the endogenous copies of *pmt* and *htrA* were replaced with zeocin and hygromycin resistance cassettes, respectively, and a copy of *htrA* was integrated at the L5 phage integration site. *pmt* or *pmt(D68A),* a catatytically inactive variant of *pmt,* were transformed into this background. Full swaps that acquire kanamycin resistance at the expense of noursethricin resistance render strains devoid of *htrA* (or *lppZ*) and must thus carry a suppressor mutation. Bottom: quantification of *pmt* and *pmt(D68A)* swaps. A total of 60 transformants were tested for antibiotic resistance. An equivalent swap was performed for *lppZ* and enumerated in the same manner. **B. Removing the mannosylation residues of Ami3 suppresses the essentiality of *htrA* and *lppZ.*** Top: the endogenous copies of *ami3* and *htrA* were replaced with zeocin and hygromycin resistance cassettes, respectively, and a copy of *htrA* was integrated at the L5 phage integration site. *ami3* or *ami3(T122A/T130A/T138A) (ami3***),* an allele of *ami3* in which all mannosylation sites have been mutated (see **Figure A1.4**), were transformed into this background. Full swaps that acquire kanamycin resistance at the expense of noursethricin resistance render strains devoid of *htrA* (or *lppZ*) and must thus carry a suppressor mutation. Bottom: quantification of *ami3* and *ami3**** swaps. A total of 120 transformants were tested for antibiotic resistance. An equivalent swap was performed for *lppZ* and enumerated in the same manner; a total of 60 transformants were tested for antibiotic resistance. **C. Ami3 levels decrease in cells missing Pmt.** Strains expressing Ami3-Strep or Ami3*** in a wild-type, Δ*pmt,* Δ*pmt+pmt,* or Δ*pmt+pmt(D68A)*

Figure 2.5 (Continued): background were grown to log phase. Whole cell lysate was analyzed by Western blotting using anti-Strep and anti-RpoB as a loading control. **D. Pmt mannosylation increases the stability of Ami3 protein.** At indicated time points after adding 250 µg/mL chloramphenicol, aliquots of cells were lysed and levels of Ami3-Strep were monitored by Western blot. Results are representative of three independent experiments. **E. Quantification of Ami3 stability.** Independent values of RpoB-normalized levels of Ami3 from Panel D quantified by densitrometry analysis. *$p<0.05$, **$p<0.01$. Error bars represent standard deviation of the mean.

targets have been identified. We tested the importance of this activity by mutating the catalytic aspartic acid D68 to an alanine, which decreases mannosyltransferase activity by over 50% (VanderVen *et al.* 2005). Using an L5 swap, we found that *pmt(D68A),* but not wild-type *pmt,* permitted growth of a strain missing either *htrA* or *lppZ* (**Figure 2.5A**).

To test if Ami3 is itself mannosylated by Pmt, we immunoprecipitated epitope-tagged Ami3, searched for modifications by mass spectrometry, and found mannosylation on three threonines: T122, T130, and T138 (**Figure A1.4A**). An allele substituting alanines for these residues (Ami3(T122A/T130A/T138A), or Ami3***) allowed growth of a strain lacking *htrA* (**Figure 2.5B**). We assessed the contribution of each mannosylated residue to Ami3 toxicity and found that T122 and T130 were critical while T138 did not affect Ami3 toxicity (**Figure A1.4B**). To test whether mannosylation contributed to Ami3 stability, we monitored Ami3 levels by Western blot in a Δ*pmt* strain (**Figure 2.5C, left**). Adding wild-type *pmt*, but not *pmt*(D68A), restored wild-type levels of Ami3. In contrast, Ami3*** was insensitive to the presence of Pmt (**Figure 2.5C, right**).

The simplest explanation for the effect of mannosylation on protein quantity is that the modification affects protein stability. To test this, we assayed the half-life of Ami3 in wild type and Δ*pmt* strains after inhibiting translation with chloramphenicol. Ami3 levels decreased significantly faster in the Δ*pmt* strain compared to wild-type cells (**Figure 2.5D, 2.5E**) demonstrating that mannosylation stabilizes Ami3 against degradation.

Because Pmt increases Ami3 stability, we reasoned that overexpression of Ami3 in cells lacking *pmt* may be less toxic. Indeed, the polar bulges characteristic of Ami3 overexpression were ameliorated when the protein was destabilized in both a ∆*pmt* background (**Figure 2.6A, 2.6B, A1.5**) and an Ami3*** overexpression (**Figure 2.6A, 2.6B**). Furthermore, Ami3 destabilization by

Figure 2.6: Removal of mannosylation partially rescues morphology and survival of Ami3 overexpressions. A. Loss of *pmt* relieves morphological defects in Ami3 overexpressions. Wild-type *ami3*, *ami3(H362A)*, or *ami3**** was overexpressed in either Δ*ami3* or Δ*ami3*Δ*pmt* cells (see **Figure A1.5**). **B. Quantification of cellular morphology of Ami3 overexpressions.** Cells were observed by microscopy and measured for total cell length, maximum cell width, and the proportion of the cell bulging (length of bulge over total cell length). At least 80 cells were quantified in each condition. Dotted black lines indicate median values. **C. Survival and morphological quantification of Ami3 overexpression.** Strains expressing wild-type *ami3*, *ami3(H362A)*, or *ami3**** under an aTc-inducible promoter were grown in the presence of absence or 100 ng/mL aTc. Aliquots were taken at the indicated time points for CFU analysis. The uninduced wild-type Ami3 strain is representative of all uninduced strains. The growth of various strains was compared, and demarcated by asterisks (*, comparing the overexpression of *ami3* in a wild-type or Δ*pmt* background), stars (★, comparing the overexpression of wild-type *ami3* or *ami3****), or X's (×, comparing the overexpression of *ami3(H362A)* in a wild-type or Δ*pmt* background). *p<0.05, **p<0.01, ***p<0.001, ****p<0.0001. Error bars represent standard deviation of the mean.

Figure 2.6 (Continued)

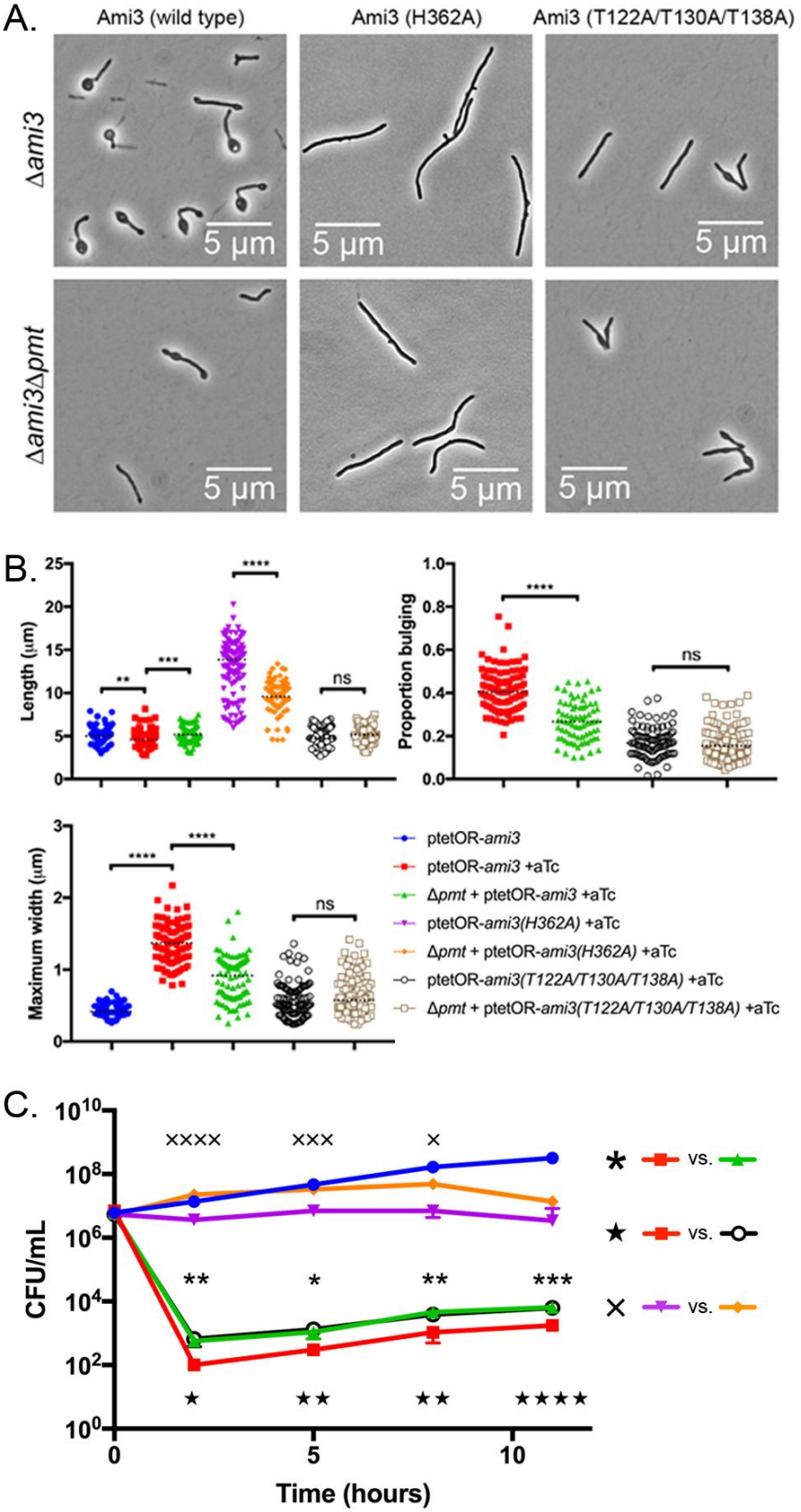

either genetic manipulation increased survival 5-fold (**Figure 2.6C**). To determine whether abundance and catalytic activity make independent contributions to toxicity, we monitored the growth of strains overexpressing Ami3(H362A), the catalytic mutant of Ami3 with protein levels most closely mimicking those of wild-type Ami3 (**Figure A1.3B**) in the Δ*pmt* background. As expected, growth of a strain overexpressing Ami3(H362A) was further rescued (**Figure 2.6C**) and its morphological defects were lessened (**Figure 2.6A, 2.6B**) by knocking out *pmt*. These results are consistent with a model where Ami3 activity and stability are independent, and altering both in combination has an additive effect on relieving the toxicity of overexpression.

Interestingly, we found that both HtrA and LppZ are also mannosylated (**Figure A1.4A**) in a Pmt-dependent manner (**Figure A1.4C**). However, because HtrA and LppZ still interact in a Δ*pmt* background (**Figure A1.1D**), mannosylation does not appear to affect their interaction. Indeed, strains expressing variants of *htrA* and *lppZ* in which the mannosylation sites were mutated grew as well as wild-type cells (**Figure A1.4D**). Additionally, HtrA still reduces Ami3 levels in a ∆*pmt* strain (**Figure A1.4E**), demonstrating that mannosylation of the members of this pathway is not required to elicit the activity of HtrA-LppZ against Ami3.

Amidases have redundant functions in *Msm*

While Ami3 has the potential to accumulate to toxicity, it is not an essential gene, and loss of *ami3* is not associated with any obvious phenotype (**Figure A1.6A, A1.6B**). However, Ami3 is not the only putative N-acetylmuramoyl-L-alanine amidase in *Msm*; Ami1 and Ami4 are also members of this family (Machowski *et al*. 2014), and several studies have presented evidence of Ami1's influence on normal cell division (Senzani *et al*. 2017, Li *et al*. 2018). In *E, coli*, amidases have redundant functions and none are individually essential for growth. To test for similar redundancy in *Msm,* we constructed strains lacking individual and multiple amidases. We found that all of these strains had normal growth kinetics and morphologies (**Figure A1.6A,**

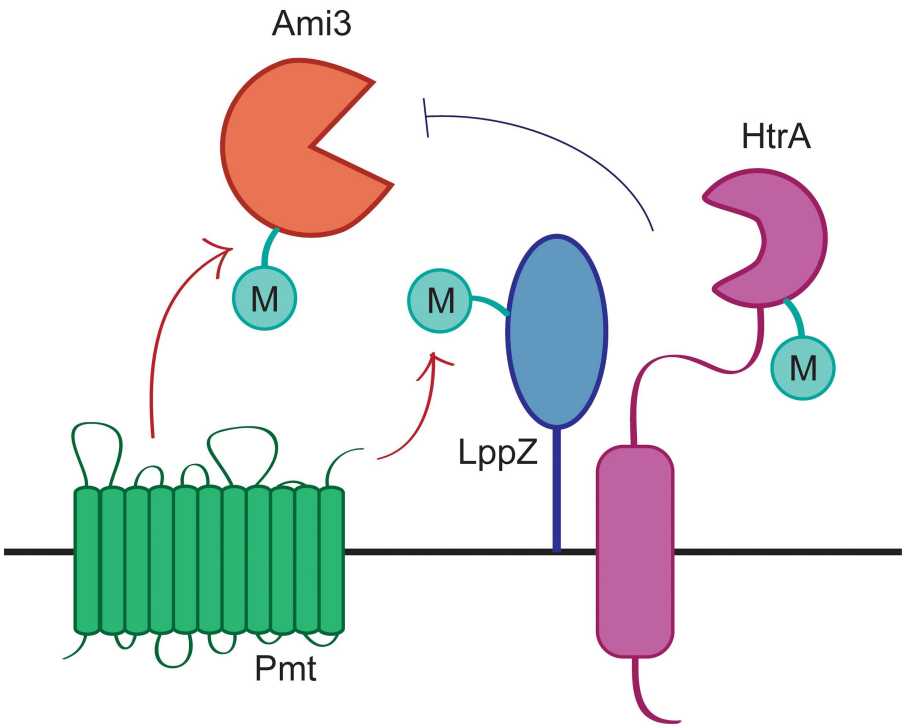

Figure 2.7: Model of HtrA-LppZ-mediated detoxification of Ami3. The muramidase Ami3, under the stabilizing influence of Pmt, potentially accumulates to toxic levels over the course of the cell cycle. The mannosylated HtrA-LppZ complex restores normal Ami3 levels to abrogate this lethality and is thus essential for viability.

A1.6B), but altered in their accumulation of the fluorescent molecule calcein (**Figure A1.6C**). In accordance with previous studies (Rego *et al.* 2017), we found rifampin susceptibility in these mutants in a manner that correlated with calcein permeability (**Figure A1.6D**). However, loss of either *ami1* or *ami4* was unable to suppress *htrA* essentiality (**Figure A1.6E**), highlighting Ami3's unique contribution to necessitating the activity of HtrA-LppZ.

DISCUSSION

Peptidoglycan hydrolases must be carefully regulated in a spatiotemporal manner to coordinate the complex processes of cell expansion and division. Dysregulation of cell wall enzymes has been shown to be toxic in species from *E. coli* to the various mycobacteria (Heidrich *et al*. 2001, Chao *et al.* 2013). The rapid turnover of cell wall requires an equally fast disposal of unwanted enzymes, and in the extracellular compartment, fewer mechanisms are available than in the cytoplasm. Proteolysis is one of the more rapid ways to effect change in the periplasm (Mukherjee *et al*. 2009, Festa *et al*. 2010). Protein processing and degradation have already been shown to play important roles in the fine-tuning of cell division proteins. For instance, the hydrolase RipA must be cleaved by the serine protease MarP to process peptidoglycan (Botella *et al*. 2017). Cleavage can also efficiently halt the activity of enzymes: PBPB is cleaved by the metalloprotease Rv2869 in *Mtb* during oxidative stress (Mukherjee *et al*. 2009). Finally, several factors involved in cell wall assembly have been shown to be targeted for pupylation and subsequent proteasomal degradation, including MurA, KasB, and MtrA (Festa *et al*. 2010). However, none of these proteolytic or processing systems are essential for viability and only take on critical roles under environmental stress.

We propose a model in which HtrA and LppZ are essential to degrade Ami3, thereby controlling its toxicity, (**Figure 2.7**). Over the course of the cell cycle, preexisting cell wall material must be cleaved to make room for newly synthesized precursors. Inherent in cell wall hydrolases such

as Ami3 is potential toxicity, as overactivity can destabilize the cell wall. Without spatiotemporal regulation, sustainable cellular growth cannot occur, thus necessitating the activity of periplasmic proteases that can detoxify highly active enzymes.

The finding that HtrA requires a second protein is consistent with other observations of periplasmic proteases that rely on partners for fine-tuned regulation. Lipoproteins have been shown to be allosteric modulators of proteases in a variety of contexts (Tadokoro *et al*. 2004, Singh *et al*. 2015, Park *et al*. 2017), and have also been shown to directly activate the activity of cell wall enzymes (Paradis-Bleau *et al.* 2010, Typas *et al.* 2010, Egan *et al.* 2014, Lupoli *et al.* 2014). It is possible that LppZ facilitates the interaction between HtrA and Ami3, enhances the activity of HtrA, primes Ami3 for detoxification by HtrA, or some combination of the above.

While we were unable to measure amidase activity directly, Ami3 is likely a *bona fide* amidase based on the phenotype of overexpression and requirement of catalytic residues for full toxicity, which mirror prior work in this field (Heidrich *et al*. 2001, Chao *et al*. 2013). In our work, all three mycobacterial N-acetylmuramoyl-L-alanine amidases are largely dispensable, though the importance of different amidases may vary in different *Msm* strains (Bavesh Kana, personal communication). Several alternative enzymes able to cleave peptidoglycan crosslinks likely operate in our strain under the growth conditions that we assayed, compensating for the loss of this family of amidases. Morever, we simply may not know the growth condition in which these amidases play a critical role.

If Ami3 is indeed an active amidase, it is perhaps surprising that even a catalytically inactive variant of Ami3 can arrest cell growth.There are several possibilities to explain our observations. First, these mutants might retain a small amount of activity that stunts growth when enough protein is produced. Second, amidase activity may account for only a portion of *ami3* toxicity,

which can still impair growth when expressed at high levels, perhaps by aggregating to levels the cell cannot tolerate. Third, Ami3 may engage with another cell wall enzyme that depends on Ami3 catalytic activity to execute its function. Enzymatically inactive Ami3 may thus lock its binding partner in a futile interaction that results in a failure to divide when the complex is sequestered or it fails to dissociate from peptidoglycan (**Figure 2.3B**). These models are not mutually exclusive.

In this context, mannosylation could alter protein folding or recognition by proteolytic enzymes. Post-translational modifications play an important role in the activation or stabilization of cell wall enzymes in mycobacteria. For instance, the peptidoglycan synthase PonA1 and MurA regulator CwlM must be phosphorylated to be active (Kieser *et al.* 2015, Boutte *et al.* 2016). Furthermore, Pmt might play a broad role in cell wall maintenance, as it contributes to the virulence, immunogenicity, permeability, and antibiotic susceptibility of *Mtb* and *M. abscessus* (Becker *et al*. 2017, Liu *et al*. 2013, Deng *et al*. 2016, Harriff *et al*. 2017). In fact, a ∆*pmt* mutant in *M. abscessus* is more susceptible to several antibiotics including rifampin (Becker *et al*. 2017).

Proteases are attractive drug candidates and, in fact, an inhibitor of mycobacterial MarP and HtrA has been described (Zhao *et al.*, 2015). However, at least for *Msm*, our results suggest that blocking HtrA could lead to high rates of resistance as there are multiple mechanisms to escape drug-mediated killing. This might be less true in *Mtb*, especially during infection, when it is possible that Ami3 plays a larger role to maintain cellular integrity or HtrA, LppZ, and Pmt contribute to the pathogen's virulence in additional ways (Liu *et al*. 2013, Deng *et al*. 2016, Harriff *et al*. 2017). Thus, targeting of the essential HtrA-LppZ pathway remains possible.

Materials and methods

Experimental model details: *Mycobacterium smegmatis* mc^2155 was grown in liquid media containing 7H9 salts (Becton-Dickinson) supplemented with 5 g/L albumin, 2 g/L dextrose, 0.85 g/L NaCl, 0.003 g/L catalase, 0.2% glycerol, and 0.05% Tween80, or plated on LB agar. For all oxidative stress experiments, strains were grown in Hartmans-de Bont (HdB) media, which was made as described (Hartmans and De Bont, 1992) with 0.05% Tween80. *E. coli* TOP10 was used for cloning. Antibiotic selection concentrations for *M. smegmatis* were as follows: 25 µg/mL kanamycin, 50 µg/mL hygromycin, 20 µg/mL zeocin, 20 µg/mL nourseothricin, and 5 µg/mL gentamicin. Antibiotic concentrations for *E. coli* were as follows: 50 µg/mL kanamycin, 100 µg/mL hygromycin, 50 µg/mL zeocin, and 40 µg/mL nourseothricin. Anhydrotetracyline was used at 100 ng/mL for gene induction or repression. All strains were grown at 37°C unless otherwise indicated.

Strain construction: Deletions of *htrA* and *lppZ* were generated by first transforming in a second copy of the gene at the L5 and Tweety phage integration sites (Lewis and Hatfull 2003; Pham *et al.* 2007), then using mycobacterial recombineering as previously described (van Kessel and Hatfull 2008) to delete the endogenous copy. Where indicated, *htrA* and *lppZ* were cloned into vectors with a tetON repressor to make their expression tetracycline inducible, or into vectors with a tetOFF repressor to make their expression tetracycline repressible.
All other deletions (*ami3, pmt,* and *mprB*) were generated by recombineering. To make the inducible overexpression strain, *ami3* was sub-cloned into a multi-copy episomal vector carrying both the tet operator and the tet repressor.
L5 swaps were performed as previously described (Pashley and Parish 2003); this technique was used to 1) test essentiality and suppression where indicated and/or 2) generate different allelic variants of *htrA* or *lppZ*. When testing essentiality or suppression, 60-200 colonies were patched for kanamycin and nourseothricin resistance.

A full list of strain details, including genotypes, plasmids, and primers, is available in **Table A1.1**.

Microscopy and image analysis: Still images were taken of cells immobilized on agar pads on a Nikon Ti inverted widefield epifluorescence microscope with a Photometrics coolSNAP CCD monochrome camera and a Plan Apo 100X objective with a numerical aperture of 1.4. Images were processed using NIS Elements version 4.3 and ImageJ. All aTc-repressible and -inducible strains were depleted or induced by the addition of 100 ng/mL anhydrotetracycline (aTc).

Growth rate determination and kill curves: For growth curves, strains were grown to mid-log phase, diluted to OD_{600} 0.005 in triplicate, and measured every 15 min in a Bioscreen growth curve machine (Growth Curves USA) at 37°C or 42°C, where indicated.

For environmental stress kill curves, strains were grown to mid-log phase, washed twice with PBS-Tween80, diluted to OD600 0.05, and rolled at 37°C in PBS-Tween80 or HdB + 0.02% tert-butyl hydroperoxide. At the indicated time points, 200 uL aliquots were removed, serially diluted in PBS-Tween80, and plated for CFUs.

For aTc-inducible overexpression kill curves, all steps were the same except cells were not washed before subculturing into 7H9 with kanamycin to maintain the episomal plasmid, with or without 100 ng/mL aTc.

Tert-butyl hydroperoxide and aTc were added once at the beginning of each experiment. Each kill curve was performed at least thrice, in triplicate, with similar results.

Immunoprecipitation and Western blotting: To identify potential interactors of HtrA, 200 mL mid-log phase cultures of a strain expressing HtrA-Strep and an untagged control were spun down and resuspended in 2 mL of Buffer W (100 mM Tris, 150 mM NaCl, 1 mM EDTA) with an EDTA-free protease inhibitor cocktail (Roche, Switzerland). The cells were lysed by bead

beating and SDS was added to the lysate to a final concentration of 1%. The lysate was pre-cleared of endogenously biotinylated proteins using Pierce Avidin Agarose for 1 hour at room temperature. The cleared supernatant was then added to MagStrep "type3" XT beads (IBA Lifesciences) and incubated overnight at 4°C. The beads were then washed three times with Buffer W and eluted using Buffer BX (IBA Lifesciences). The eluted samples were separated on a 4-12% NuPAGE Bis-Tris precast gel (Invitrogen Novex) and stained with Coomassie Blue. The entire lanes of eluted protein from the HtrA-Strep and untagged control immunoprecipitations were cut out and analyzed by the Harvard Taplin mass spectrometry facility. The unbiased immunoprecipitation was performed twice, both identifying LppZ as the top hit enriched in HtrA-Strep compared to the untagged control.

To search for mannosylation residues in HtrA-Strep, LppZ-FLAG, and Ami3-FLAG, all steps were performed as above except single bands were excised instead of entire lanes. Mass spectrometry was performed to specifically probe for hexose modifications. Scores above 19 were considered significant, and scores of 1000 were considered unequivocal. All analyses were performed twice.

For co-immunoprecipitations, 100 mL cultures were split in two and all steps were performed as above for samples incubated with MagStrep beads. For immunoprecipitations using α-FLAG M2 Magnetic Beads (Sigma Aldrich), SDS was not added, pre-clearing with avidin agarose was skipped, and elution was carried out with FLAG peptide. Co-immunoprecipitations were analyzed by Western blotting.

For Western blots, cultures were spun down, resuspended in IP buffer (10 mM Tris-HCl (pH 8), 100 mM NaCl, 1 mM EDTA), and lysed by bead beating. Supernatants were normalized by A280 protein concentration, diluted with 6X Laemmli buffer, and run on SDS-PAGE gels with 4-12% NuPAGE Bis Tris precast gels (Life Technologies). Membranes were blotted with rabbit α-FLAG (Sigma Aldrich) at 1:1000 in TBST + 5% milk, rabbit α-Strep (Genscript) at 1:1000 in TBST + 3% BSA, mouse α-RpoB (ThermoFisher Scientific) at 1:1000 in TBST + 5% milk, and

rabbit α-HtrA (a generous gift from Helene Botella and Sabine Ehrt) at 1:1000 in TBST + 5% milk.

MIC determination: The MIC of *M. smegmatis* and *M. tuberculosis* strains were performed using the Alamar Blue assay as previously described (Kieser *et al.* 2015).

Quantification and statistical analysis: All experiments were performed at least twice. Means were compared using a two-sided Student's *t*-test. $P < 0.05$ was considered significant. For most microscopy experiments, roughly 100-200 cells were analyzed and data medians are shown. No statistical methods were used to predetermine sample size, and the researchers were not blinded to sample identity.

Chapter 2, Section 2.2: References

1. Becker K, Haldimann K, Selchow P, Reinau LM, Dal Molin M, and Sander P. (2017). Lipoprotein Glycosylation by Protein-O-Mannosyltransferase (MAB_1122c) Contributes to Low Cell Envelope Permeability and Antibiotic Resistance of Mycobacterium abscessus. Front Microbiol 8:2123, doi:10.3389/fmicb.2017.02123.

2. Botella H, Vaubourgeix J, Lee MH, Song N, Xu W, Makinoshima H, Glickman MS, Ehrt S. (2017). Mycobacterium tuberculosis protease MarP activates a peptidoglycan hydrolase during acid stress. EMBO J 36(4):536-48, doi:10.15252/embj.201695028.

3. Boutte CC, Baer CE, Papavinasasundaram K, Liu W, Chase MR, Meniche X, Fortune SM, Sassetti CM, Ioerger TR, Rubin EJ. (2016). A cytoplasmic peptidoglycan amidase homologue controls mycobacterial cell wall synthesis. Elife 15;5. pii:e14590, doi:10.7554/eLife.14590.

4. Chao MC, Kieser KJ, Minami S, Mavrici D, Aldridge BB, Fortune SM, Alber T, and Rubin EJ. (2013). Protein Complexes and Proteolytic Activation of the Cell Wall Hydrolase RipA Regulate Septal Resolution in Mycobacteria. PLoS Pathog 9(2):e1003197, doi:10.1371/journal.ppat.1003197.

5. Clausen T, Kaiser M, Huber R, and Ehrmann M. (2011). HTRA proteases: regulated proteolysis in protein quality control. Nat Rev Mol Cell Biol 12:152-63, doi:10.1038/nrm3065.

6. Clausen T, Southan C, and Ehrmann M. (2002). The HtrA Family of Proteases: Implications for Protein Composition and Cell Fate. Mol Cell 10(3):443-55.

7. DeJesus MA and Ioerger TR. (2013). A Hidden Markov Model for identifying essential and growth-defect regions in bacterial genomes from transposon insertion sequencing data. BMC Bioinformatics 14: 303-314, doi: 10.1186/1471-2105-14-303.

8. Deng G, Zhang F, Yang S, Kang J, Sha S, and Ma Y. (2016). Mycobacterium tuberculosis Rv0431 expressed in Mycobacterium smegmatis, a potentially mannosylated protein, mediated the immune evasion of RAW 264.7 macrophages. Microb Pathog 100:285-92, doi:10.1016/j.micpath.2016.10.013.

9. Egan AJ, Jean NL, Koumoutsi A, Bougault CM, Biboy J, Sassine J, Solovyova AS, Breukink E, Typas A, Vollmer W et al. (2014). Outer-membrane lipoprotein LpoB spans the periplasm to stimulate the peptidoglycan synthase PBP1B. PNAS 111(22):8197-202, doi:10.1073/pnas.1400376111.

10. Festa RA, McAllister F, Pearce MJ, Mintseris J, Burns KE, Gygi SP, Darwin KH. (2010). Prokaryotic ubiquitin-like protein (Pup) proteome of Mycobacterium tuberculosis. PLoS One 5(1):e8589. doi:10.1371/journal.pone.0008589.

11. Griffin JE, Gawronski JD, Dejesus MA, Ioerger TR, Akerley BJ, and Sassetti CM. (2011). High-Resolution for Phenotypic Profiling Defines Genes Essential for Mycobacterial Growth and Cholesterol Catabolism. PLoS Pathog 7(9): e1002251, doi: 10.1371/journal.ppat.1002251.

12. Harriff MJ, Wolfe LM, Swarbrick G, Null M, Cansler ME, Canfield ET, Vogt T, Toren KG, Li W, Jackson M et al. (2017). HLA-E Presents Glycopeptides from the Mycobacterium tuberculosis Protein MPT32 to Human CD8+ T cells. Sci Rep 7(1):4622, doi:10.1038/s41598-017-04894-0.

13. Hartmans S and De Bont JAM. (1992). The genus Mycobacterium— nonmedical, Prokaryotes, 2nd:1214–37. New York, Springer-Verlag New York Inc.

14. He H, Hovey R, Kane J, Singh V, and Zahrt TC. (2006). MprAB is a stress-responsive two-component system that directly regulates expression of sigma factors SigB and SigE in Mycobacterium tuberculosis. J Bacteriol 188(6):2134-43.

15. Heidrich C, Templin MF, Ursinus A, Merdanovic M, Berger J, Schwarz H, de Pedro MA, and Höltje JV. (2001). Involvement of N-acetylmuramyl-L-alanine amidases in cell separation and antibiotic-induced autolysis of Escherichia coli. Mol Microbiol 41(1):167-78.

16. Ingmer H and Brøndsted L. (2009). Proteases in bacterial pathogenesis. Res Microbiol 160:704-10, doi:10.1016/j.resmic.2009.08.017.

17. Kapopoulou A, Lew JM, and Cole ST. (2011). The MycoBrowser portal: a comprehensive and manually annotated resource for mycobacterial genomes. Tuberculosis (Edinb). Jan 91(1):8-13.

18. Kelley LA, Mezulis S, Yates CM, Wass MN, Sternberg MJ. (2015). The Phyre2 web portal for protein modeling, prediction and analysis. Nat Protoc 10(6):845-58, doi:10.1038/nprot.2015.053.

19. Kieser KJ, Boutte CC, Kester JC, Baer CE, Barczak AK, Meniche X, Chao MC, Rego EH, Sassetti CM, Fortune SM et al. (2015). Phosphorylation of the Peptidoglycan Synthase PonA1 Governs the Rate of Polar Elongation in Mycobacteria. PLoS Pathog 11(6):e1005010, doi:10.1371/journal.ppat.1005010.

20. Lew JM, Kapopoulou A, Jones LM, and Cole ST. (2011). TubercuList - 10 years after. Tuberculosis (Edinb). Jan 91(1):1-7.

21. Lewis JA and Hatfull GF. (2003). Control of directionality in L5 integrase-mediated site-specific recombination. J Mol Biol 326:805-21, doi:10.1016/S0022-2836(02)01475-4.

22. Li X, He J, Fu W, Cao P, Zhang S, and Jiang T. (2018). Effect of Mycobacterium tuberculosis Rv3717 on cell division and cell adhesion. Microb Pathog 117:184-90, doi:10.1016/j.micpath.2018.02.034.

23. Liu CF, Tonini L, Malaga W, Beau M, Stella A, Bouyssié D, Jackson MC, Nigou J, Puzo G, Guilhot C et al. (2013). Bacterial protein-O-mannosylating enzyme is crucial for virulence of Mycobacterium tuberculosis. PNAS 110(16):6560-5, doi:10.1073/pnas.1219704110.

24. Lupoli TJ, Lebar MD, Markovski M, Bernhardt T, Kahne D, Walker S. (2014). Lipoprotein activators stimulate Escherichia coli penicillin-binding proteins by different mechanisms. J Am Chem Soc 136(1):52-5, doi:10.1021/ja410813j.

25. Machowski EE, Senzani S, Ealand C, and Kana BD. (2014). Comparative genomics for mycobacterial peptidoglycan remodelling enzymes reveals extensive genetic multiplicity. BMC Microbiol 14:75, doi:10.1186/1471-2180-14-75.

26. Manganelli R, Fattorini L, Tan D, Iona E, Orefici G, Altavilla G, Cusatelli P, and Smith I. (2004). The extra cytoplasmic function sigma factor sigma(E) is essential for Mycobacterium tuberculosis virulence in mice. Infect Immun 72(5):3038-41.

27. Misra R, CastilloKeller M, Deng M. (2000). Overexpression of protease-deficient DegP(S210A) rescues the lethal phenotype of Escherichia coli OmpF assembly mutants in a degP background. J Bacteriol 182(17):4882-888.

28. Mukherjee P, Sureka K, Datta P, Hossain T, Barik S, Das KP, Kundu M, Basu J. (2009). Novel role of Wag31 in protection of mycobacteria under oxidative stress. Mol Microbiol 73(1):103-19, doi:10.1111/j.1365-2958.2009.06750.x.

29. Paradis-Bleau C, Markovski M, Uehara T, Lupoli TJ, Walker S, Kahne DE, Bernhardt TG. (2010). Lipoprotein cofactors located in the outer membrane activate bacterial cell wall polymerases. Cell 143(7):1110-20, doi:10.1016/j.cell.2010.11.037.

30. Park H, Kim YT, Choi C, and Kim S. (2017). Tripodal Lipoprotein Variants with C-Terminal Hydrophobic Residues Allosterically Modulate Activity of the DegP Protease. J Mol Biol 429(20):3090-101, doi:10.1016/j.jmb.2017.09.011.

31. Pashley CA and Parish T. (2003). Efficient switching of mycobacteriophage L5-based integrating plasmids in Mycobacterium tuberculosis. FEMS Microbiol Lett 229:211-5, doi:10.1016/S0378-1097(03)00823-1.

32. Pham TT, Jacobs-Sera D, Pedulla ML, Hendrix RW, and Hatfull GF. (2007). Comparative genomic analysis of mycobacteriophage Tweety: evolutionary insights and construction of compatible site-specific integration vectors for mycobacteria. Microbiol 153:2711-23, doi:10.1099/mic.0.2007/008904-0.

33. Raju RM, Goldberg AL, and Rubin EJ. (2012). Bacterial proteolytic complexes as therapeutic targets. Nat Rev Drug Discov 11:777-89, doi:10.1038/nrd3846.

34. Raju RM, Jedrychowski MP, Wei JR, Pinkham JT, Park AS, O'Brien K, Rehren G, Schnappinger D, Gygi SP, and Rubin EJ. (2014). Post-Translation Regulation via Clp Protease Is Critical for Survival of Mycobacterium tuberculosis. PLoS Pathog 10(3):e1003994, doi:10.1371/journal.ppat.1003994.

35. Raju RM, Unnikrishnan M, Rubin DH, Krishnamoorthy V, Kandror O, Akopian TN, Goldberg AL, and Rubin EJ. (2012). Mycobacterium tuberculosis ClpP1 and ClpP2 Function Together in Protein Degradation and Are Required for Viability in vitro and During Infection. PLoS Pathog 8(2):e1002511, doi:10.1371/journal.ppat.1002511.

36. Rego EH, Audette RE, and Rubin EJ. (2017). Deletion of a mycobacterial divisome factor collapses single-cell phenotypic heterogeneity. Nature 546(7656):153-7, doi:10.1038/nature22361.

37. Sassetti CM and Rubin EJ. (2003). Genetic requirements for mycobacterial survival during infection. PNAS 100(22): 12989-12994, doi: 10.1073/pnas.2134250100.

38. Sassetti CM, Boyd DH, and Rubin EJ. (2001). Comprehensive identification of conditionally essential genes in mycobacteria. PNAS 98(22): 12712-12717, doi: 10.1073/pnas.231275498.

39. Sassetti CM, Boyd DH, and Rubin EJ. (2003). Genes required for mycobacterial growth defined by high density mutagenesis. Mol Microbiol 48(1): 77-84, PMID: 12657046.

40. Schwechheimer C, Rodriguez DL, and Kuehn MJ. (2015). NlpI-mediated modulation of outer membrane vesicle production through peptidoglycan dynamics in Escherichia coli. Microbiologyopen 4(3):375-89, doi:10.1002/mbo3.244.

41. Senzani S, Li D, Bhaskar A, Ealand C, Chang J, Rimal B, Liu C, Joon Kim S, Dhar N, and Kana B. (2017). An Amidase_3 domain-containing N-acetylmuramyl-L-alanine amidase is required for mycobacterial cell division. Sci Rep 7(1):1140, doi:10.1038/s41598-017-01184-7.

42. Singh SK, Parveen S, SaiSree L, and Reddy M. (2015). Regulated proteolysis of a cross-link-specific peptidoglycan hydrolase contributes to bacterial morphogenesis. PNAS 112(35):10956-61, doi:10.1073/pnas.1507760112.

43. Skórko-Glonek J, Wawrzynów A, Krzewski K, Kurpierz K, Lipińska B. (1995). Site-directed mutagenesis of the HtrA (DegP) serine protease, whose proteolytic activity is indispensable for Escherichia coli survival at elevated temperatures. Gene 163(1):47-52.

44. Tadokoro A, Hayashi H, Kishimoto T, Makino Y, Fujisaki S, and Nishimura Y. (2004). Interaction of the Escherichia coli lipoprotein NlpI with periplasmic Prc (Tsp) protease. J Biochem 135(2):185-91.

45. Typas A, Banzhaf M, van den Berg van Saparoea B, Verheul J, Biboy J, Nichols RJ, Zietek M, Beilharz K, Kannenberg K, von Rechenberg M et al. (2010). Regulation of peptidoglycan synthesis by outer-membrane proteins. Cell 143(7):1097-109, doi:10.1016/j.cell.2010.11.038.

46. van Kessel JC and Hatfull GF. (2008). Mycobacterial recombineering. Methods Mol Biol 435:203-15, doi:10.1007/978-1-59745-232-8_15.

47. VanderVen BC, Harder JD, Crick DC, and Belisle JT. (2005). Export-mediated assembly of mycobacterial glycoproteins parallels eukaryotic pathways. Science 309(5736):941-3.

48. White MJ, He H, Penoske RM, Twining SS, Zahrt TC. (2010). PepD participates in the mycobacterial stress response mediated through MprAB and SigE. J Bacteriol 192(6):1498-510, doi:10.1128/JB.01167-09.

49. White MJ, Savaryn JP, Bretl DJ, He H, Penoske RM, Terhune SS, Zahrt TC. (2011). The HtrA-like serine protease PepD interacts with and modulates the Mycobacterium tuberculosis 35-kDa antigen outer envelope protein. PLoS One 6(3):e18175, doi:10.1371/journal.pone.0018175.

50. World Health Organization. Global Tuberculosis Report (2017).

51. Zahrt TC and Deretic V. (2001). Mycobacterium tuberculosis signal transduction system required for persistent infections. PNAS 98(22):12706-11.

52. Zhang YJ, Ioerger TR, Huttenhower C, Long JE, Sassetti CM, Sacchettini JC, and Rubin EJ. (2012). Global Assessment of Genomic Regions Required for Growth in Mycobacterium tuberculosis. PLoS Pathog 8(9):e1002946, doi:10.1371/journal.ppat.1002946.

53. Zhao N, Darby CM, Small J, Bachovchin DA, Jiang X, Burns-Huang KE, Botella H, Ehrt S, Boger DL, Anderson ED et al. (2015). Target-based screen against a periplasmic serine protease that regulates intrabacterial pH homeostasis in Mycobacterium tuberculosis. ACS Chem Biol 10(2):364-71, doi:10.1021/cb500746z.

Chapter 3

Novel and conserved factors in mycobacterial septation

Chapter 3, Section 3.1: Characterization of conserved and novel septal factors in *Mycobacterium smegmatis*

Katherine J. Wu[1], Jenna Zhang[1], Catherine Baranowski[1], Vivian Leung[1], E. Hesper Rego[2], Yasu Morita[3], Eric J. Rubin[1,4] and Cara C. Boutte[1,5,*]

1 - Department of Immunology and Infectious Disease, Harvard TH Chan School of Public Health, Boston MA.

2 - Department of Microbial Pathogenesis, Yale University, New Haven, CT.

3 - Department of Microbiology, University of Massachusetts, Amherst, MA.

4 - Department of Microbiology and Immunobiology, Harvard Medical School, Boston, MA.

5 - Current address: Department of Biology, University of Texas at Arlington, Arlington, TX

*Corresponding author: cara.boutte@uta.edu

Author contributions: K.J.W., J.Z., C.C.B., and E.J.R. designed experiments. K.J.W. and C.C.B. wrote the paper. K.J.W., J.Z., C.B., V.L., H.R., Y.M., and C.C.B. performed experiments and analyzed data. This work has been published in the *Journal of Bacteriology*.

ABSTRACT

Septation in bacteria requires coordinated regulation of cell wall biosynthesis and hydrolysis enzymes so that new septal cross-wall can be appropriately constructed without compromising the integrity of the existing cell wall. Bacteria with different modes of growth and different types of cell wall require unique regulators to mediate cell growth and division processes. Mycobacteria have both a cell wall structure and mode of growth that are distinct from well-studied model organisms and use several different regulatory mechanisms. Here we identify and characterize homologs of the conserved cell division regulators FtsL and FtsB, and show that they appear to function similarly to their homologs in *E. coli*. We identify a number of

previously undescribed septally-localized factors which could be involved in cell wall regulation. One of these, SepIVA, has a DivIVA domain, is required for mycobacterial septation and is localized to the septum and the intracellular membrane domain. We propose that SepIVA is a regulator of cell wall precursor enzymes that contribute to construction of the septal cross-wall, similar to the putative elongation function of the other mycobacterial DivIVA homolog, Wag31.

The enzymes that build bacterial cell walls are essential for cell survival, but can cause cell lysis if misregulated. Thus, cell wall enzyme regulators serve a crucial function in cellular homeostasis. Periplasmic cell wall enzymes are regulated through interactions with transmembrane and cytoplasmic factors. The number and nature of these cell wall regulators is likely to vary in bacteria that grow in different ways. Mycobacteria comprise a genus that includes important pathogens such as *M. tuberculosis* and *M. leprae*; these species have a cell wall whose composition and construction varies greatly from that of well-studied model organisms. In this work we identify and preliminarily characterize some of the proteins that regulate the mycobacterial cell wall. We find that some of these regulators appear to be functionally conserved with their structural homologs in evolutionarily distant species such as *E. coli*, but other proteins have critical regulatory functions that may be unique to the actinomycetes.

INTRODUCTION

Division of rod-shaped bacteria is a tightly regulated process that requires new cell wall to be built in the middle of the cell orthogonal to the elongation axis. For decades, bacterial cell biologists have been occupied with questions about how periplasmic enzymes can be regulated in coordination with chromosome segregation (1) and how the cell wall can be bisected at each division event without compromising its integrity. Much of our understanding comes from the model organisms *Escherichia coli* and *Bacillus subtilis*, in which large protein complexes are

required to properly regulate septal enzymes (2), and information is passed from the cytoplasm to the periplasmic enzymes through conformational changes in the transmembrane factors in these complexes (3, 4).

E. coli and *B. subtilis* are both rod-shaped bacteria that extend along their lateral walls via intercalary growth; however, a number of rod-shaped species from far-flung phyla grow at the cell poles (5-14), including the mycobacteria, a genus which includes *Mycobacterium tuberculosis* and other pathogens. In *Mycobacterium smegmatis*, septation is thought to be broadly similar to the process in other rod-shaped bacteria. The mycobacterial septation apparatus contains homologs of many well-described septal factors from *E. coli* and *B. subtilis*, including FtsZ, PBP3, FtsW, and FtsQ. However, many essential septal factors are unaccounted for in the current annotations of mycobacterial genomes. These missing factors include FtsA and ZipA, which in *E. coli* are required for Z ring stabilization and recruitment of FtsK (15), and ZapA, which recruits and (16) stabilizes the Z ring. Some missing factors can be accounted for because a function can be filled through alternative mechanisms. For instance, mycobacteria have SepF (17), which is present in many bacterial species that lack FtsA and is thought to perform the function of FtsA and EzrA in anchoring FtsZ to the membrane and recruiting it to the midcell (18). Mycobacterial FtsZ may also be anchored to the membrane through a direct interaction with the intermembrane transglycosylase FtsW (19, 20) which, in turn, interacts with PBP3 (21), thus apparently cutting out some middlemen. Thus, in this context, FtsZ interacts with, and may directly regulate, several septal enzymes. Other missing canonical septal factors include FtsN, which is thought to initiate septation upon its late association with the divisome, and FtsB and FtsL, which are part of a trimer that includes FtsQ and are thought to be involved in regulating the initiation of septation (3, 22).

In addition to identifying the factors that perform the same septal functions that have been identified in *E. coli* and *B. subtilis*, we expect that mycobacteria will have septation factors that do not exist in these model species. These unidentified factors are likely to be involved in either: 1) coordination between septal and polar growth or 2) coordination of the insertion of the arabinogalactan and mycolic acid layers of the cell wall.

In lateral wall growers, the functions of cell elongation and cell septation are largely temporally and spatially separated and mediated by separate factors (23). In pole-growing species, septal and polar growth are temporally separate but spatially overlap: the conclusion of septation produces the cell poles, which then become critical for orienting the peripolar elongation complex (24). Thus, septation in these species must leave the newly formed cell poles in a state that allows elongation (25). This pole remodeling must require regulatory factors that do not exist in the lateral-wall growing model organisms.

Mycobacteria and other actinomycetes have an acid-fast cell wall, in which layers of arabinogalactan and mycolic acids are covalently affixed to the peptidoglycan layer. The enzymes that build these extra cell wall layers probably require septation-specific and elongation-specific regulatory factors to control their activity and coordinate it with the synthesis of the peptidoglycan. One of these elongation-specific regulators is likely to be the DivIVA homolog Wag31. Wag31 localizes to the cytoplasmic side of the inner membrane at the cell pole (26), is absolutely required for polar growth (24, 26) and interacts with (24, 27) and appears to regulate enzymes that make precursors for the mycolic acid layer of the cell wall at the growing poles (27). A similar system is likely to exist to help coordinate cell wall precursor production during septation.

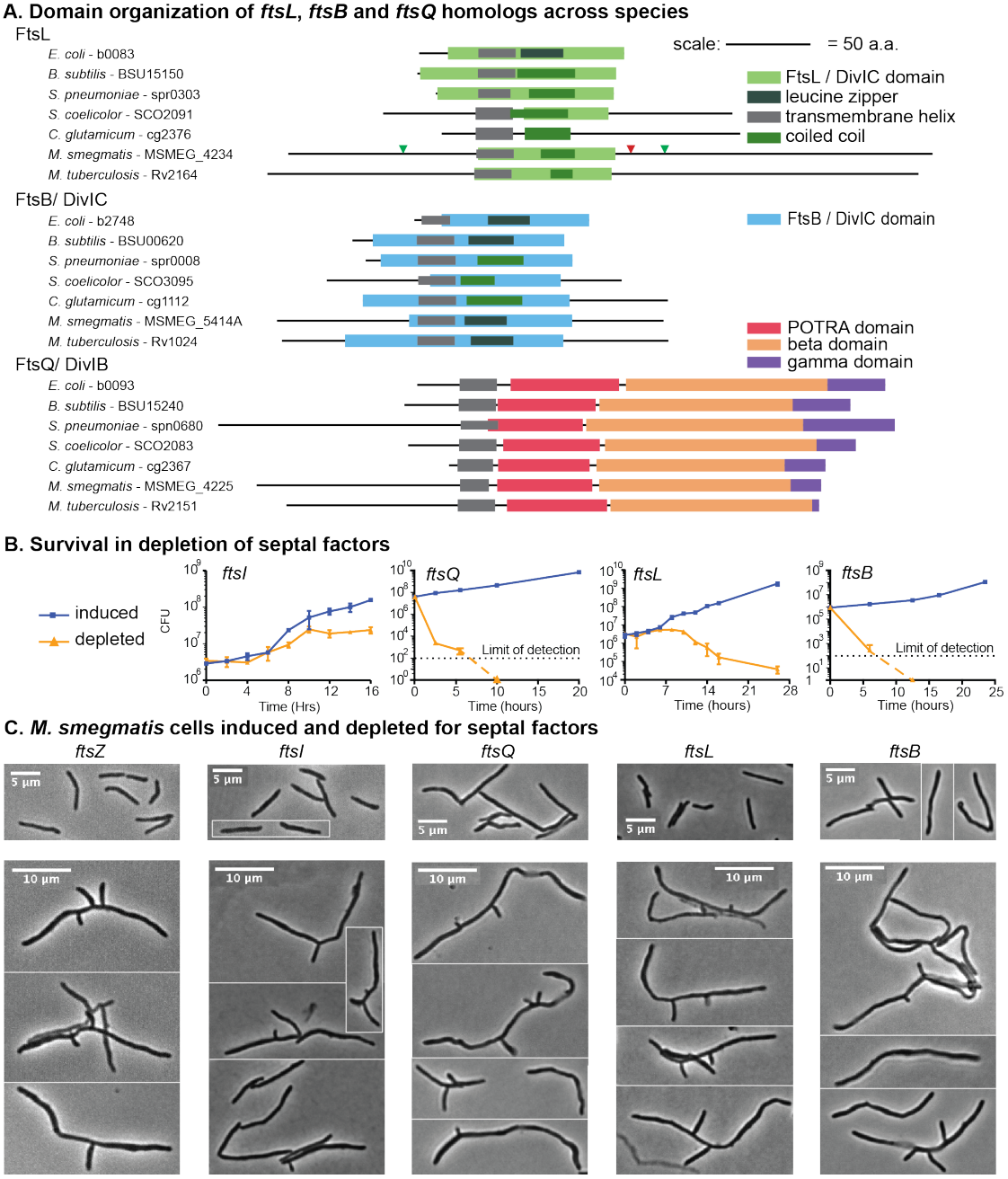

Figure 3.1: Essentiality and cell division function of septal factors. A. Domain structure diagrams of FtsQ, L and B from mycobacteria and other species in which these genes have been studied. Domains were defined through a number of secondary structure prediction programs. All gene and domain lengths are to scale. The *ftsL* truncation sites that supported growth are indicated with green arrows, the red arrow indicates a truncation site that did not support growth. **B.** Colony forming units of strains in which *ftsI, Q, L* is *B* are under the control of a tetracycline-controlled promoter, during depletion and induction of the indicated gene. **C.** Phase micrographs of *ftsZ, I, Q, L* and *B* depletion strains during induction of the gene (top) and depletion (bottom).

Here we sought to identify and characterize mycobacterial homologs for the known septal factors FtsB and FtsL, and to identify novel septal factors that could be involved in functions specific to pole-growing or acid-fast bacteria. We identify predicted structural homologs of FtsB and FtsL and show that they are septal proteins and appear to be recruited to the septum in a fashion similar to that observed in *E. coli*. We also find that FtsQ associates with novel factors that localize to the divisome. We further characterize one of these newly identified septal proteins, which we have named SepIVA. SepIVA has a conserved DivIVA domain, localizes to the division site and is required for cell division in *M. smegmatis*.

RESULTS

M. smegmatis (*Msmeg*) and *M. tuberculosis* (*Mtb*) encode homologs of *ftsI* and *ftsQ (divIB)*, but not annotated homologs for *ftsB* (*divIC)* or *ftsL*. Using HHPred, a Hidden Markov Model-based homology prediction tool (28), we identified putative homologs for both *ftsL* (MSMEG_4234, Rv2164) and *ftsB* (MSMEG_5414A, Rv1024). Although the sequences of the mycobacterial FtsL and FtsB proteins are not similar enough to the proteins from *E. coli* or *B. subtilis* to make a sequence alignment, these proteins share conserved domains that can be detected using a variety of secondary and tertiary structure prediction programs (28-33) (**Figure 3.1A**). The putative *ftsL* homolog is also highly syntenic: it is in an apparent operon with *ftsI* in evolutionarily distant species, including *Mtb*, *E. coli* and *B. subtilis.*

To determine whether these genes are essential for survival, we built *Msmeg* strains that allow us to repress transcription of putative septal factors. In these strains, the targeted gene was first complemented at the L5 phage attachment site with a tetracycline (tet)-inducible or tet-repressible promoter (34), then the endogenous copy of the gene was deleted using recombineering (35). We found that the depletion strains either died or failed to grow upon depletion of *ftsI*, *ftsQ*, *ftsL,* or *ftsB* (**Figure 3.1B**), confirming predictions from TnSeq

experiments in *Mtb* (36, 37) and *Msmeg* that these genes are all essential, as they are in *E. coli* and *B. subtilis*. To determine whether these genes are involved in septation, we compared the morphology of these depleted strains to that of the FtsZ-depleted strain, described previously (38). Our data show that depletion of *ftsZ, ftsI* (MSMEG_4233), *ftsQ, ftsL,* and *ftsB* all result in elongated, branched cells that are clearly defective for septation (**Figure 3.1C**).

The mycobacterial FtsL homologs have long, non-conserved N- and C-terminal extensions. To determine if these were important for function, we exchanged the wild-type *Msmeg ftsL* allele at the L5 site with alleles truncated at the N or C termini. We found that *ftsL* missing the first 67 codons or the last 158 codons could complement the wild-type *ftsL*, but an allele missing the last 178 codons did not support growth (**Figure 3.1A**).

In order to determine whether and when these cell division factors are associated with the divisome, we built strains expressing 1) a fusion between FtsZ and the mCherry2B protein (FtsZ-mcherry2B) and 2) either *ftsQ, ftsL, ftsB,* or *ftsK* fused to GFPmut3. This allowed us to simultaneously track the localization of these proteins during the course of the cell cycle using time-lapse microscopy. We found that all four Fts- proteins localize to the site of septation, as defined by co-localization with FtsZ (**Figure 3.2A**), and that FtsQ, L, B, and K are all recruited to the septal site after FtsZ (**Figure 3.2B**). We quantified the fluorescence signal at the cell center from one division event to the next and observed that the FtsZ signal always peaks ~70-80% of the way through the cell cycle, but that the peak has an earlier shoulder. The signal for FtsL and FtsB fully stabilizes by ~60% of the cell cycle, while the signal for FtsQ and FtsK fully stabilizes by ~70% of the cell cycle. The signal for all four proteins peaks between 70-80% of the cell cycle; these proteins did not exhibit localization during the shoulder period of the weaker localization of FtsZ (**Figure 3.2B**). Thus, the arrival of FtsZ precedes FtsL, FtsB, FtsQ, and FtsK localization to the septation site.

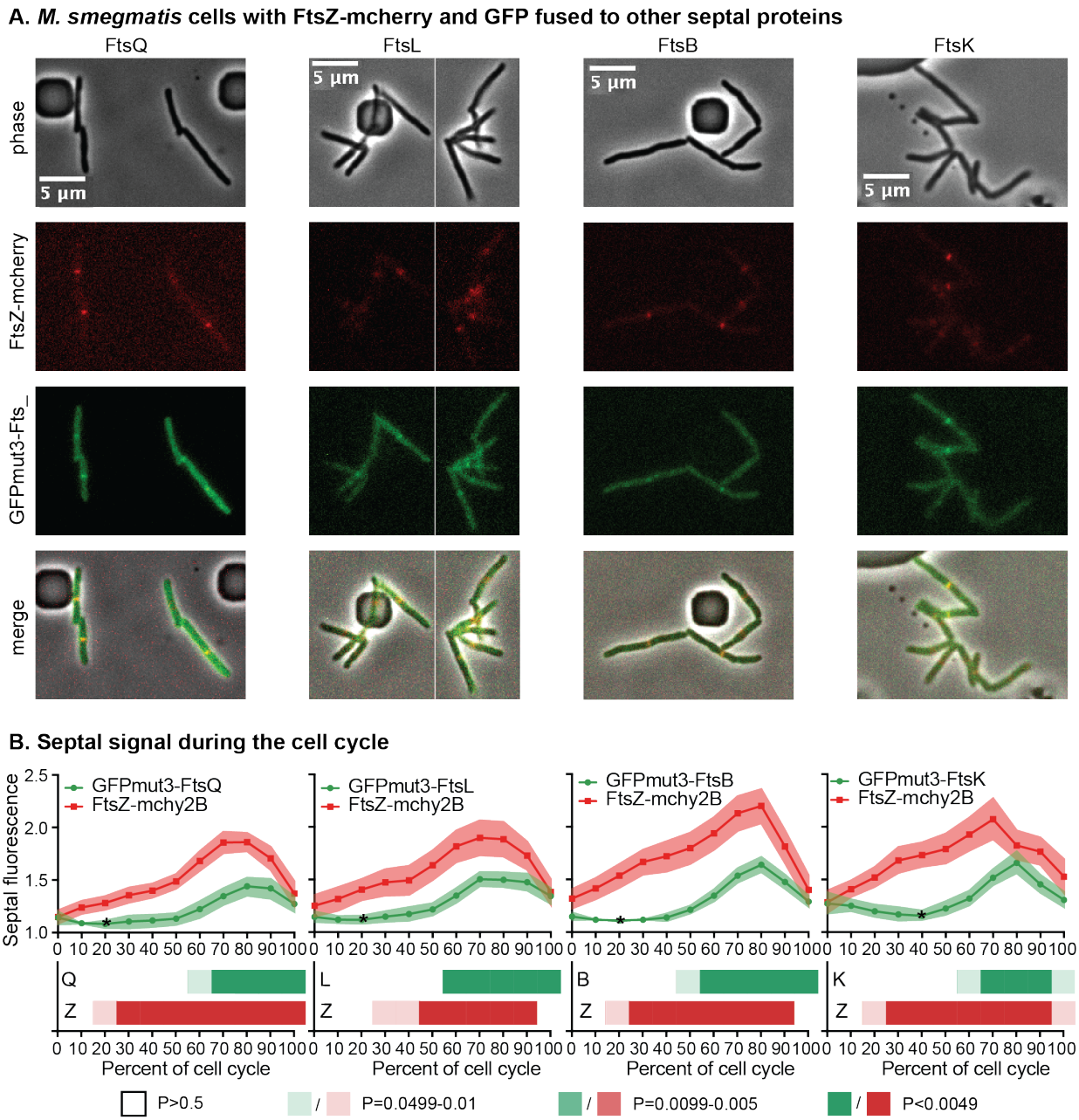

Figure 3.2: Localization of septal factors. A. Micrographs of strains which express FtsZ-mcherry2B and either GFPmut3-FtsQ, GFPmut3-FtsL, GFPmut3-FtsB, or FtsK-GFPmut3. **B.** Analysis of time-lapse movies taken of the strains described in A. Phase, red and green images were taken at 15 minute intervals, and the fluorescence intensity was quantified in each channel for between 40-60 cell division events from at least two independent biological replicate cultures. Top: fluorescence intensity at midcell over time, data is normalized to the signal at the dimmest time point for each cell. Error bars are 95% confidence intervals. Bottom: bar graph depicts the p-value of protein localization at the midcell, indicating whether the fluorescent signal at midcell at each time point is significantly different from the fluorescent signal at the time point with the least fluorescence. For FtsZ-mcherry2B, this is always the first time point. For the other fusions, the dimmest time point, to which the others are compared, is indicated

Figure 3.2 (Continued): with an asterisk. The comparisons in signal intensity were made using an ordinary one-way ANOVA with Dunnet correction for multiple comparisons. The darkly colored boxes indicate that there is high confidence that the protein localized to midcell at that time point.

We next sought to determine the dependency of localization of FtsZ, FtsK, FtsQ, FtsL, and FtsB to the mycobacterial septum. In *E. coli,* FtsZ localization to the septum and formation of the Z-ring complex directly precede FtsK recruitment. FtsK and FtsQ physically associate, recruiting FtsQ to the septum, where it brings together FtsL and FtsB to form the FtsQLB complex (39). To test if this model holds true in mycobacteria, we expressed the GFPmut3 fusions of *ftsK, ftsQ, ftsL,* and *ftsB* in the *ftsZ, ftsQ, ftsL,* and *ftsB* depletion strains and quantified their localization to the septum, as marked by FtsZ-mcherry2B (except in the *ftsZ* depletion strain). We found that all other tested Fts proteins were dependent on FtsZ. Furthermore, both FtsZ and FtsK could localize in the absence of FtsQ, L, or B, as in *E. coli.* However, while FtsL and FtsB failed to localize in the *ftsQ* depletion, FtsQ successfully localized in 40-70% of cells depleted of *ftsL* and *ftsB* (**Figure 3.3A,B and Table 3.1**).

To identify new proteins that interact with the mycobacterial divisome, we immunoprecipitated (IP) FtsQ-strep and identified interactors with mass spectrometry (40). We were able to IP several proteins with FtsQ-strep in two independent experiments (**Table 3.2**). Because we covalently cross-linked proteins in the cells before IP, we expect that many of the identified interaction partners may not directly interact with FtsQ, but are likely to be associated with the larger divisome complex. We found several proteins that are known to be associated with the divisome in other bacterial species, including FtsE, FtsH, and FtsK (41-44). We also found proteins that have previously been shown to localize to the mycobacterial divisome: FhaA (45) and PknA (46). Additionally, we found proteins involved in the secretion and co-translational insertion of membrane proteins, which is expected because FtsQ is a membrane protein. Finally, we found many proteins with unknown functions. Several of these are transmembrane and essential for survival in *Mtb* and *Msmeg* according to TnSeq screens (36). We hypothesize that these could be mediators of cell wall insertion during division or elongation.

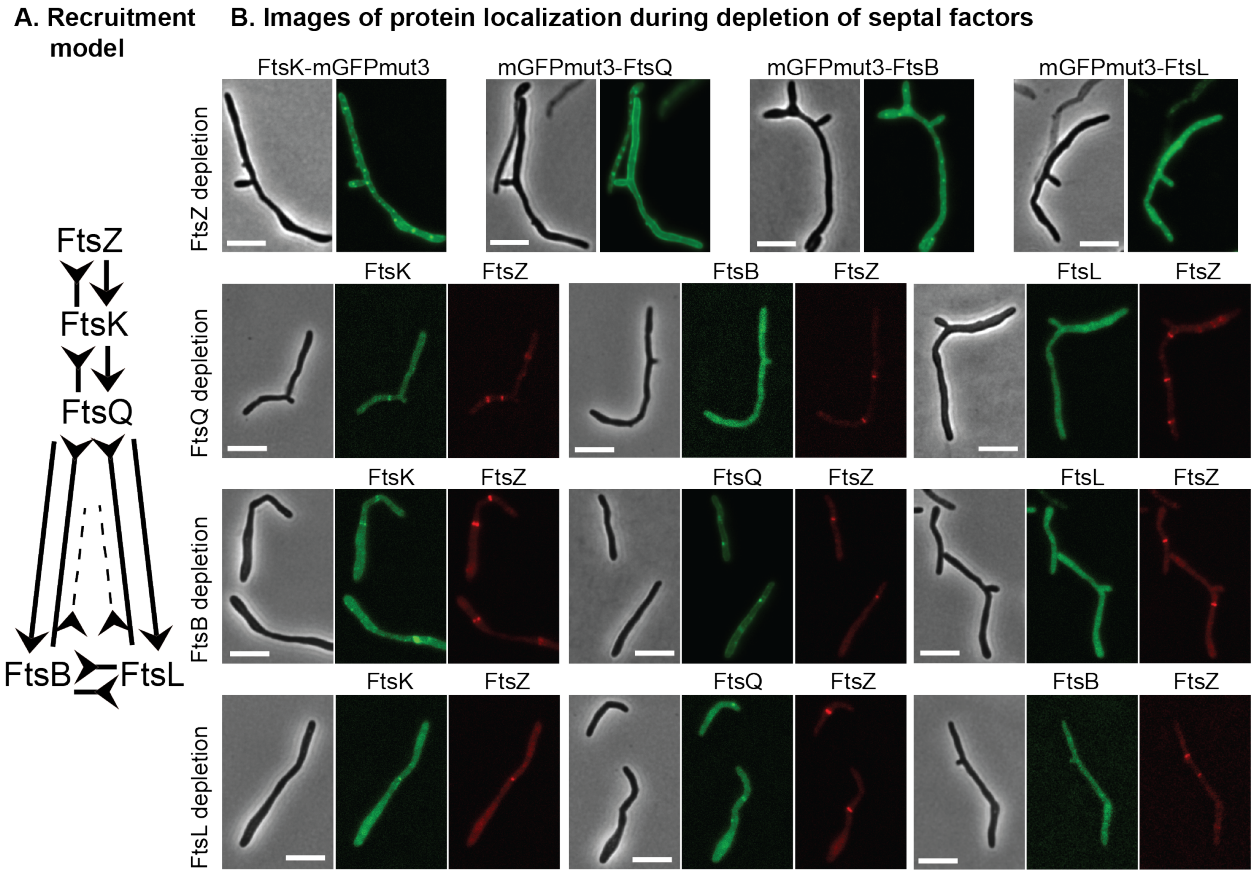

Figure 3.3: Dependency of localization between Fts septal factors. A. Model for the recruitment of septal factors to the midcell. Regular arrow heads indicate that the protein pointed to is recruited to midcell by the protein on the side of the arrow without a point. Arrows with inverted heads indicate that the protein pointed to is dependent on the other protein for localization to midcell. Dashed lines between FtsQ and FtsB and L indicate that FtsQ is partially dependent on FtsB and L for localization. **B.** Micrographs of strains depleted of FtsZ, FtsQ, FtsB, or FtsL, expressing FtsZ-mcherry2B (except in FtsZ depletion) and GFPmut3-FtsQ, GFPmut3-FtsL, GFPmut3-FtsB, or FtsK-GFPmut3. Multiple images from these experiments were used to produce the data in **Table 3.1**.

Table 3.1: Dependency of Localization. Ratios indicate the number of cells in which the fluorescent protein constructs listed in the left column localized to septa at midcell in strains in which the proteins across the top row were depleted, over the total number of such cells that were imaged. Only cells expressing an FtsZ signal, which served as a reference point for septal localization, were quantified.

Localization	Depletion			
FP-Fusion	FtsZ	FtsQ	FtsL	FtsB
FtsZ-mCherry	ND	75/75	75/75	75/75
GFPmut3-FtsQ	0/200	ND	30/75	54/75
GFPmut3-FtsL	0/200	2/75	ND	0/75
GFPmut3-FtsB	1/200	6/75	0/75	ND
FtsK-GFPmut3	0/200	62/75	65/75	66/75

To test whether these uncharacterized proteins could be involved in septation or elongation, we constructed *Msmeg* strains in which we expressed each gene tagged at either the C or N terminus with a fluorescent protein. We found that several of these factors appear to localize to the septum, poles, Intracellular Membrane Domain (IMD), or some combination of these sites (**Figure 3.4**). The IMD is a cytoplasmic polar membrane domain which seems to be the localization site of several cell wall precursor enzymes (47).

Of interest among the novel divisome factors was MSMEG_2416, henceforth called *sepIVA*, which is predicted to be essential in *Mtb* (36), has a conserved DivIVA domain, and shares 19.7% amino acid identity and 29.4% similarity with the well-studied mycobacterial DivIVA homolog Wag31 (MSMEG_4217). We attempted to construct a strain in which *sepIVA* could be transcriptionally depleted as in **Figure 3.1**; however, we were unable to obtain strains in which we could replace the endogenous *sepIVA* with a construct at the L5 phage integrase site with a non-native promoter. Instead, we used Oligo-mediated Recombineering with Bxb1 Integrase Targeting (ORBIT) (48) to integrate a vector with a DAS tag at the C-terminus of *sepIVA*. The DAS tag targets the attached protein for proteolysis by ClpXP upon expression of the adaptor protein SspB (49). We found that when SepIVA-DAS was degraded by expression of high levels of SspB, *Msmeg* cells continued to elongate but failed to divide, resulting in long, branched filaments (**Figure 3.5A**) like those seen in the transcriptional depletion of septal factors (**Figure 3.1**). These filamented cells were not viable (**Figure 3.5B**).

While the previously-studied DivIVA homologs in actinobacteria are all involved in cell elongation (24, 50-52), the DivIVA protein in *B. subtilis* is involved in septation site positioning and cell division (53, 54). DivIVA in *B. subtilis* works by recruiting the septation inhibitors MinC and MinD to the nascent poles at the end of each septation event and anchoring them there through the next cell cycle so that FtsZ rings do not form over the cell poles (55, 56). There are

Table 3.2: FtsQ pulldown data. Proteins whose peptides were pulled down with cross-linked FtsQ-strep. The “Ess TB?” and “Ess SM?” refer to predicted essentiality from TnSeq screens performed in *Mtb* (36) and *Msmeg*: Y=essential, N=non-essential, Y-D=domain essential. The “sum unique peptides” is the sum from the two independent IP experiments. Localization was determined by fusing GFPmut3 to the N (NT) or C (CT) termini of the indicated proteins – representative localization images are shown in **Figure 3.4**.

Gene	MSMEG #	TB #	annotation / conserved domains	ESS TB?	ESS Msm ?	localization	sum unique peptides
secA1	MSMEG_1881	Rv3240	SecA1 translocase	Y	Y		54
ffh	MSMEG_2430	Rv2916	signal recognition particle	Y	Y		50
	MSMEG_3748	Rv1697	thiamine pyrophosphokinase	Y	Y		32
choD	MSMEG_1604	Rv3409	cholesterol oxidase	N	N		32
	MSMEG_2416	Rv2927	DivIVA domain	Y	Y	NT fusion - septal and IMD	22
subI	MSMEG_4533	Rv2400	sulfate binding lipoprotein	Y	N		22
ftsK	MSMEG_2690	Rv2748	septation factor, DNA translocase	Y	Y		21
	MSMEG_6434	Rv3850	conserved hypothetical	N	N		20
ftsH	MSMEG_6105	Rv3610	membrane protease	Y	N		20
	MSMEG_4287	Rv2219	conserved membrane protein	Y	Y	NT fusion - septal	19
	MSMEG_2410	Rv2969	DsbA family, disulfide isomerase	Y	Y		19
secA2	MSMEG_3654	Rv1821	preprotein translocase ATPase	Y	N		19
	MSMEG_6051	N/A	ABC transporter		N		18
sugC	MSMEG_5058	Rv1238	ABC ATPase - sugar transport	N	N		18
	MSMEG_1642	Rv1747	ABC transporter	N	N		18
ftsY	MSMEG_2424	Rv2921	SRP receptor	Y	Y		16
	MSMEG_3027	Rv2553	MltG - endolytic transglycosylase	Y	Y - D	NT fusion - septal, poles, membrane	16
	MSMEG_5223	Rv1111	conserved membrane protein	Y	Y	CT fusion- septal and polar	15
	MSMEG_0690	Rv0338	iron sulfur reductase?	Y	Y		15

Table 3.2 (Continued)

	MSMEG_3655	Rv1819	ABC permease, drug exporter	N	N		15
ftsE	MSMEG_2089	Rv3102	ABC ATPase - cell division	N	N		14
pntA	MSMEG_0110	N/A	NAD(P) transhydrogenase alpha subunit		N		14
pstP	MSMEG_0033	Rv0018	protein phosphatase	Y	N		14
lppW	MSMEG_2439	Rv2905	alanine rich lipoprotein, PBP or beta-lactamase	N	N		14
	MSMEG_5419	N/A	cupredoxin, lipoprotein		N		13
	MSMEG_4254	Rv2187	Fad15 - long chain fatty acid coA ligase	N	N		13
	MSMEG_6394	Rv3802	conserved membrane protein, hydrolase/ esterase	Y	Y	NT fusion - septal and membrane	12
oxaA	MSMEG_6942	Rv3921	membrane protein insertase YidC	Y	Y	CT fusion - septal and membrane	11
pknA	MSMEG_0030	Rv0015	Serine Threonine protein kinase	Y	Y		11
	MSMEG_6725	N/A	ABC transporter, ATPase		N		11
	MSMEG_6282	Rv3718		N	N		9
	MSMEG_2727	N/A	periplasmic binding protein		N		9
	MSMEG_0736	Rv0383	conserved secreted protein	Y	Y - D	CT fusion - septal, poles, membrane	9
	MSMEG_1353	Rv0647	serine threonine protein kinase	Y	Y	NT fusion - IMD	9
rhlE	MSMEG_1930	Rv3211	RNA helicase rhlE (ribosome maturation)	Y	Y - D		9
ppk	MSMEG_2391	Rv2984	polyphosphate kinase	Y	N		9
deaD	MSMEG_5042	Rv1253	ATP dependent, DEAD box RNA helicase	N	N		9
	MSMEG_1252	N/A			N		9
	MSMEG_4484	Rv2345	conserved membrane protein	N	N		8
	MSMEG_1285	Rv0613	conserved hypothetical	N	N		8
purM	MSMEG_5798	Rv0809	phosphoribosylformylglycin amidine CYCLO-ligase	Y	N		8
ppiB	MSMEG_2974	Rv2582	prolyl cis-trans isomerase	Y	N		7
	MSMEG_0035	Rv0020	FhaA	Y	Y		7

Table 3.2 (Continued)

	MSMEG_0639	N/A	transporter		N		7
	MSMEG_4692	Rv2468	conserved hypothetical	N	N		7
fadD6	MSMEG_5086	Rv1206	very long chain acyl-coA synthetase	N	N		7
	MSMEG_1945	Rv3200	ion channel	N	Y - D		7
dnaJ	MSMEG_4504	Rv2373	co-chaperone	Y	N		6

Figure 3.4: Micrographs of merodiploid *Msmeg* cells expressing the indicated fluorescent protein fusions. Fluorescent images on top, phase images on bottom. The white arrows point to the polar localization, and grey arrows point to the patchy side-wall localization that is characteristic of proteins associated with the IMD (Intracellular Membrane Domain) (58).

Figure 3.4 (Continued)

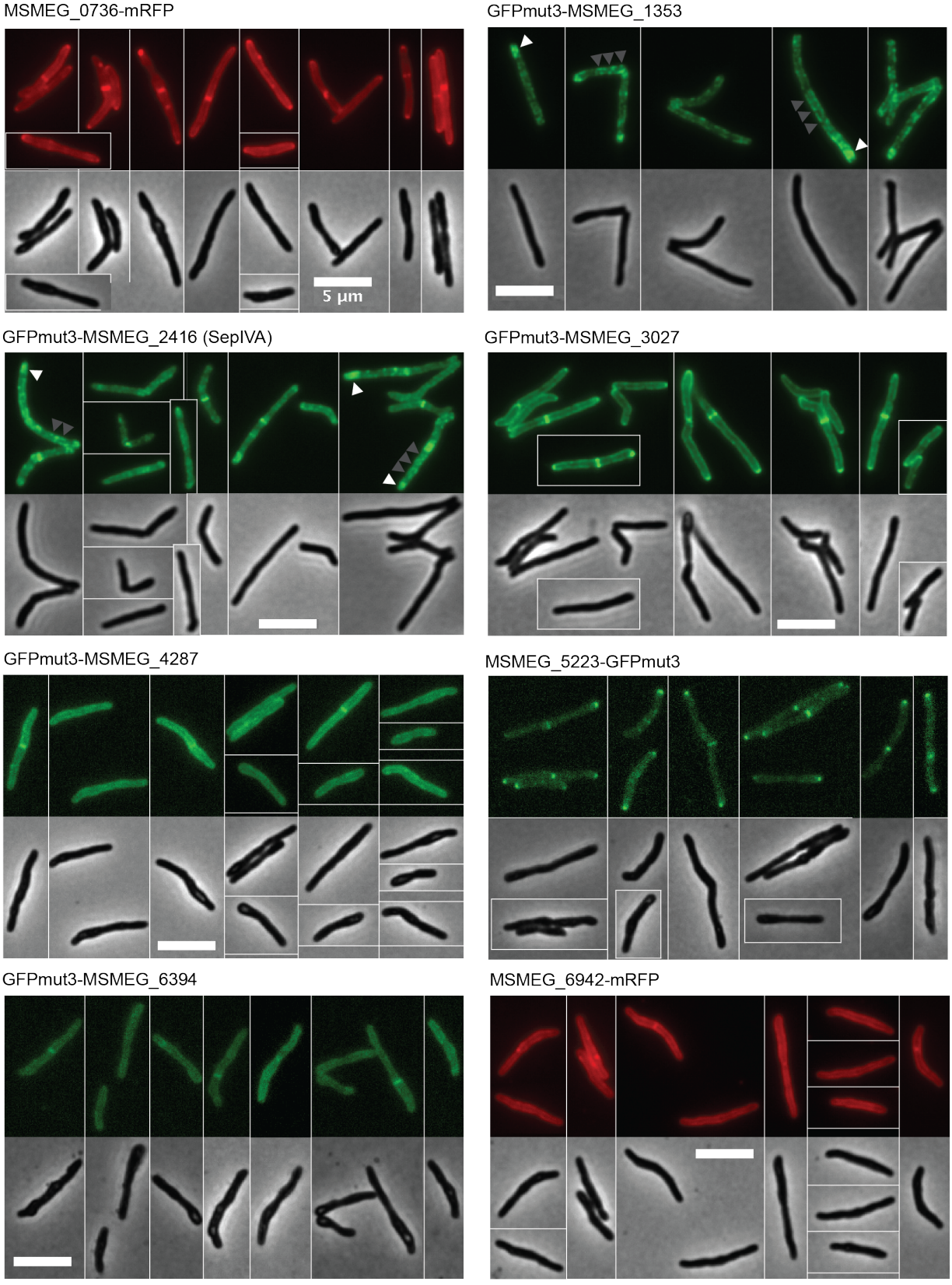

no apparent MinC homologues in *Msmeg*. Nevertheless, if SepIVA has a similar function in mycobacteria as DivIVA has in *B. subtilis*, then we would expect that it would localize to the cell division site after FtsZ, and that FtsZ would form extra Z-rings at the poles upon SepIVA depletion (54, 57).

We used time-lapse microscopy of a strain with merodiploid GFPmut3-SepIVA and FtsZ-mcherry2B constructs and found that the septal localization of SepIVA occurred late in septation (**Figure 3.5C**), well after the localization of FtsZ. However, we find that after depletion of SepIVA, FtsZ-mcherry2B still localizes, and does not form Z-rings near the pole (**Figure 3.5D**), as we would expect if SepIVA had the same function as the DivIVA homolog from *B. subtilis* (54, 57).

We did not observe consistent polar localization of SepIVA, but did often see a localization pattern that was similar to the IMD localization pattern observed previously (58): the proteins dynamically populate a region near the pole in some cells and are patchily present along the membrane (**Figure 3.5E**). To assess whether the localization of SepIVA coincides with the IMD, we conducted co-localization analysis on a strain expressing both GFPmut3-SepIVA and mCherry-GlfT2, which has previously been shown to be associated with the IMD (58). We find that these two protein fusions significantly co-localize, with a Pearson's R coefficient of 0.87± 0.03 (**Figure 3.5F**). Although the co-localization was significant, it was not perfect. We observed that GFPmut3-SepIVA localized more brightly to the septum and mCherry-GlfT2 localized more brightly at the subpolar region. We conclude that SepIVA could be associated with the IMD, but that its association with the septation site could be independent of the IMD.

Figure 3.5: Cellular role and localization of SepIVA. A. Micrographs of SepIVA-DAS depletion strains with very low levels (left) and high levels (right) of the degradation-mediation factor SspB which corresponds to normal levels of SepIVA (left) and low levels of SepIVA (right). **B.** Colony forming units of SepIVA-DAS depletion strains with SspB expressed at various levels. High levels of SspB expression correspond to low levels of SepIVA (dark orange). **C.** Analysis of septal localization from time-lapse movies of the strain with GFPmut3-SepIVA and FtsZ-mcherry2B constructs. Phase, red and green images were taken at 15 minute intervals, and the fluorescence intensity was quantified in each channel for 40-60 cell cycles from at least two independent biological replicate cultures. Top- fluorescence intensity at midcell over time, data is normalized to the signal at the dimmest time point for each cell. Error bars are 95% confidence intervals. Bottom – p-value, indicating whether the fluorescent signal at each time point is significantly different from the fluorescent signal at the dimmest time point (t=0 for FtsZ and t=30 for SepIVA). The darkly colored boxes indicate that there is high confidence that the protein localized to midcell at that time point, see p-value color scale on top panel. **D.** Images of the SepIVA-DAS tweety::FtsZ-mcherry2B strain depleted of SepIVA by SspB expression. Left – phase, right – FtsZ-mcherry2B. **E.** Selected time-lapse images from one of the movies used in **(C)**, one and a half cell cycles. The dark gray arrows with white outlines indicate the oldest pole, the white arrows indicate the newest pole and the medium gray arrows indicate an intermediate-age pole. Top - phase; middle - GFPmut3-SepIVA; bottom – FtsZ-mcherry2B. **F.** Representative images of the mc^2155 *glftT2*::mCherry-*glfT2* L5::GFPmut3-*sepIVA* strain. The Pearson's correlation coefficient between these two protein fusions, calculated from 16 images representing 200-400 cells, is R=0.87±0.03.

Figure 3.5 (Continued)

A. Cell morphology during induced degradation of SepIVA

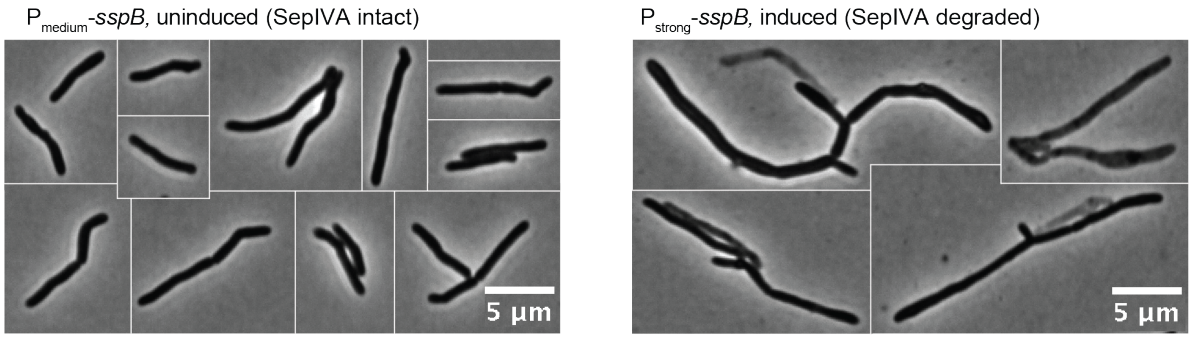

B. Survival in degradation of SepIVA

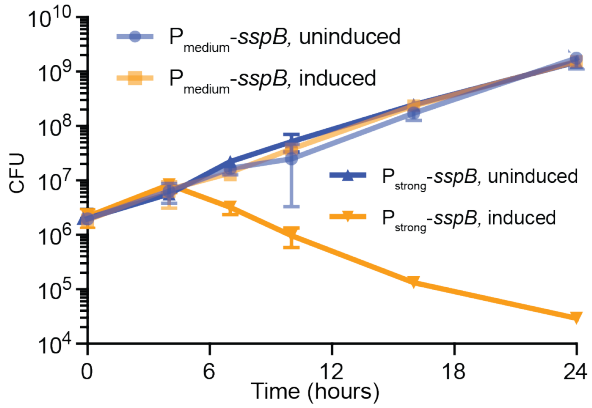

C. Septal signal during the cell cycle

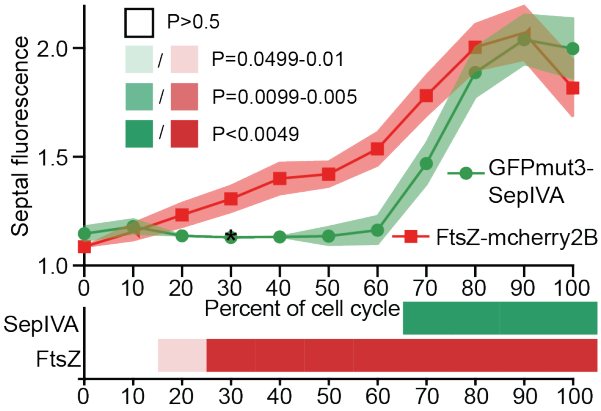

D. Localization of FtsZ-mCherry in SepIVA depletion

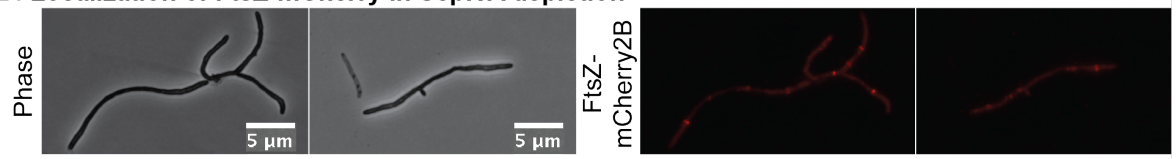

E. Micrographs of GFPmut3-SepIVA and FtsZ-mcherry2B across the cell cycle

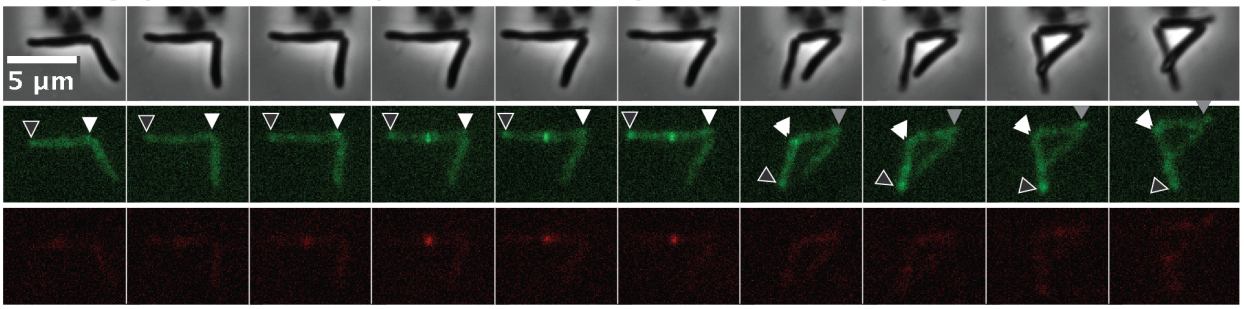

F. Co-localization of GFPmut3-SepIVA and mCherry-GlfT2

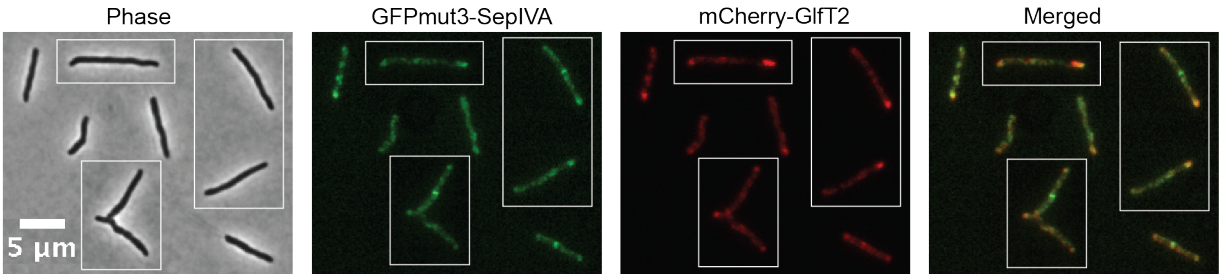

Discussion

Cell septation in mycobacteria has been shown to involve many factors which are conserved in species as evolutionarily distant as the model organisms *E. coli* and *B. subtilis* (17, 21, 59). However, mycobacterial septation is still poorly understood, both because not all the homologs of conserved septal factors have been studied and identified, and because septation in pole-growing actinomycetes likely requires additional functionalities that are not required in the lateral wall-growing Gram-positive and Gram-negative species. In this work, we identify and characterize structural homologs of broadly conserved septal factors in *Msmeg*, and describe a new septation factor that appears to have a previously undescribed function.

FtsQ, FtsL, and FtsB are septal factors in *E. coli* that do not have enzymatic activity but are involved in cueing the initiation of septation, probably through conformational changes that are propagated to their interaction partners (60). Our work confirms that these proteins are likely to have a similar function in mycobacteria (**Figure 3.1, 3.2**). We find that FtsQ, L, B, and K all localize to the septation site after FtsZ, as has been observed in other species (39, 61); thus, none of them are likely to be involved in early divisome assembly. FtsQ, L, B, and K all start to localize significantly to the midcell co-incident with the strengthening of the FtsZ-mcherry2B signal. We observe that FtsL and FtsB seem to brighten at midcell slightly before FtsQ and FtsK. This result is confusing in light of the dependency of localization data, which shows that FtsK localization is independent of the presence of Q, L, and B, and that FtsL and FtsB require FtsQ for localization (**Figure 3.3, Table 3.1**); one naturally assumes that FtsQ would localize before L and B. While our dependency of localization results mirror those seen in *E. coli* (39, 61), comparable timing of localization experiments have not been done in that organism, to our knowledge. There are several factors that make these data difficult to interpret. Firstly, the signal to noise ratio varies between the GFPmut3 fusion constructs, possibly because of partial mislocalization or proteolysis of some of the fusion proteins. Secondly, the brighter signal could

be due to an increase in the number of proteins being recruited to the septal site or to a compaction of the Z ring such that more of those proteins emit their light into a smaller number of pixels in the detector. We suspect that these septal factors may be accumulating near the septal site for a while before we can see them above the noise in the images. The earlier timing of FtsL and FtsB localization, the partial dependency of FtsQ localization on FtsB and FtsL and the interdependency of FtsB and FtsL localization (62)(63) implies that these proteins may all slowly accumulate at midcell and help stabilize each other there.

We find that FtsQ associates with known septal factors, and several other factors that are expected to interact with membrane proteins (**Table 3.2**). The localization patterns of the novel divisome-associated factors (**Figure 3.4**) corroborates the idea that septal and polar elongative factors are likely to be in close contact during certain times of the mycobacterial cell cycle. We did not find FtsL or FtsB in this IP experiment, however. These negative results are difficult to interpret: FtsQ, L, and B are expected to be present in very low copy numbers (64), and so they are not likely to be identified in the mass spectrometry experiment.

One new septal factor, which we have named SepIVA, is essential for cell division and localizes to the midcell late in the cell cycle (**Figure 3.5C**). The FtsZ-mcherry2B signal in the GFPmut3-SepIVA, FtsZ-mcherry2B strain peaked later in the cell cycle than the FtsZ-mcherry2B signal in the experiments in **Figure 3.2**, implying that the two fluorescent protein constructs in this strain may interfere slightly with the timing of divisome assembly. SepIVA appears to dynamically move from the septum to the Intracellular Membrane Domain (IMD) over the course of the cell cycle (**Figure 3.5EF**). While the exact function of the IMD is still being explored, the available data suggest that it is a site for organizing the enzymes involved in the biosynthesis of cell surface precursor molecules (58). The presence of SepIVA at both the septum and IMD implies that these functional zones have coordinated functions. Alternatively, SepIVA may have multiple

independent functions, as has been seen in the DivIVA homolog from *Listeria monocytogenes* (65).

Interestingly, SepIVA has a DivIVA domain and shares considerable similarity with Wag31, the well-studied DivIVA homolog in mycobacteria. Wag31 localizes to the poles and is essential for elongation, but how it mediates its role in elongation is not clear. It seems likely that Wag31 is an enzymatic activator of some of the cell wall precursor enzymes with which it interacts (24, 27, 66). SepIVA, like Wag31, does not have apparent enzymatic domains of its own, so it seems likely that it is also a regulator. However, it does not appear to have a function similar to the DivIVA homolog in *B. subtilis*, which regulates inhibitors of Z-ring formation at the cell poles (55, 56): depletion of SepIVA does not lead to misplacement of Z rings to the pole in *Msmeg* (**Figure 3.5D**). The GpsB proteins from *B. subtilis* and *Streptococcus pneumoniae* are shortened DivIVA homologs that are important in regulating septation (67, 68); SepIVA may be more similar to these in function than it is to *B. subtilis* DivIVA proper. In *B. subtilis*, GpsB and EzrA work together to move PBP1 to the septum and then away from the poles after septation (67). In *S. pneumoniae*, GpsB and DivIVA coordinate peptidoglycan synthesis between the septum and periphery, partly by interactions with the septal factor EzrA (68). DivIVA homologs in general seem to be involved in recruiting other proteins to their sites of activity and regulating them (26, 65, 69). Thus, we surmise that SepIVA may recruit and activate cell wall precursor enzymes or transmembrane cell wall enzymes that are required for the construction of the septal cross-wall, similarly to how Wag31 apparently regulates such enzymes during elongation (24, 27, 66).

It is worth noting that all of the experiments presented here were done in *Msmeg.* All the genes and proteins studied have close homologs in *M. tuberculosis*. However, close homologs have been shown to have slightly different functions between these two species (70-72), so we cannot be sure that these proteins all behave identically in *M. tuberculosis.*

Although various rod-shaped bacteria may look indistinguishable in the light microscope, there are several different ways to build a rod-shaped cell (10, 73). These different modes of cell morphogenesis have conserved and distinct mechanisms of assembling and arranging the cell wall. Here, we show that the actinomyecete *Msmeg* expresses the conserved septation proteins FtsQ, FtsL, and FtsB. We also find that *Msmeg* has a previously undescribed septal factor, SepIVA, which may have a function that is restricted to pole-growing actinomycetes.

Materials and Methods

Bacterial strains and culture conditions

M. smegmatis mc^2155 was cultured in 7H9 (Becton-Dickinson, Franklin Lakes, NJ) media with 5 g/L albumin, 2 g/L glucose, 0.85 g/L NaCl, 0.003 g/L catalase, 0.2% glycerol and 0.05% Tween80 added, or plated on LG agar. *E. coli* DH5α, TOP10 or XL1 Blue were used for cloning. For *Msmeg*, antibiotic concentrations were: 25 μg/ml kanamycin, 50 μg/ml hygromycin, 20 μg/ml nourseothricin, 20 μg/ml zeocin. For *E. coli*, antibiotic concentrations were: 50 μg/ml kanamycin, 100 μg/ml hygromycin, 50 μg/ml zeocin, 40 μg/ml nourseothricin. Anhydrotetracyline was used at between 50 and 250 ng/ml for gene induction or repression. Acetamide was used at 0.2% for *ftsZ* induction.

Strain construction

Gene knockouts of essential genes were made by first integrating a copy of the gene at the L5 site (74) under the control of a promoter with the tet operator. *ftsI* and *ftsL* were cloned into vectors with the tetON repressor, so their expression was tetracycline dependent. *ftsB* and *ftsQ* were cloned into vectors with the tetOFF repressor, so their expression was tetracycline-repressible (34). Once these essential genes were complemented at the L5, the endogenous

copies were knocked out using recombineering (35) as described (75). Mutants, epitope-tagged and fluorescent-protein tagged versions of genes were made by swapping L5 integrating vectors with different antibiotic markers (76). We were unable to knock out MSMEG_2416 in any background in which it was complemented with a non-native promoter, so we used ORBIT (Kenan Murphy – manuscript in revision) to introduce a vector that inserts a FLAG-DAS tag at the C-terminus of MSMEG_2416, and induced sspB to cause the MSMEG_2416 protein to be proteolyzed (77). The ORBIT primer had a Bxb1 phage integration site flanked by 70 base pairs of homology before and after the stop codon of MSMEG_2416. Merodiploid expression constructs were integrated at the L5 site, except FtsZ-mcherry2B, which was integrated at the Tweety integrase site (78). All strains used are listed in **Table A2.1**. All plasmids used are listed in **Table A2.2**. All primers used are listed in **Table A2.3**.

Bioinformatic protein analysis.

The FtsL/ DivIC and the FtsB/ DivIC domains were defined using the NCBI's Conserved Domain Database (33) or HHPred (28). The transmembrane helices were predicted using the TMHMM server (29). Coiled coils were predicted using the Coils/Pcoils tool in the MPI Bioinformatics Toolkit (30). Leucine zippers are coiled coils that contain four leucines that are each seven residues apart. The *ftsQ* homologs were analyzed in order to find the POTRA, β, and γ structural domains defined in (31). Because the sequence homology between *ftsQ* homologs was low, the PredictProtein secondary structure prediction tool (32) was used to define the domains according to secondary structure.

Microscopy and image analysis

Still images were taken of cells immobilized on agar pads on a Nikon Ti inverted widefield epifluorescence microscope with a Photometrics coolSNAP CCD monochrome camera, a 49002 green filter cube, a 49008 red filter cube and a Plan Apo 100X objective with a numerical

aperture of 1.4. Images were processed using NIS Elements version 4.3 and ImageJ. Time lapse movies were taken at 15 minute intervals of cells growing in CellASIC microfluidic plates (Millipore Sigma) on a Nikon Eclipse Ti inverted widefield epifluorescence microscope with a Spectra X LED light source and an Andor Zyla sCMOS camera and a Plan Apo 100X objective with a numerical aperture of 1.4. The microscope was equipped with a Prior stage controlled with Nikon Perfect Focus and an In vivo Scientific environmental chamber set at 37. The green images were taken with a 465-495 excitation filter and a 515-555 emission filter. The red fluorescent images were taken with a 528-553 excitation filter and a 590-650 emission filter. Images were processed using NIS Elements version 4.5 and ImageJ. The videos were analyzed by custom semi-automated ImageJ and MATLAB scripts. Briefly, in ImageJ, fluorescence line profiles were measured consistently from new pole to old pole for a single cell at every time point in the cell cycle. These line profiles were then imported into MATLAB, and analyzed by a custom script. The maximum fluorescence intensity from the middle third of the cell was determined at every time point. Then for every cell, each time-point was interpolated to 1/10 of the cell cycle for that cell so as to be able to average many cells consistently. The midcell fluorescent signal values for each cell cycle were divided by the value at the time point with the lowest signal for that cell. These normalized values were averaged to make the tops graphs in **Figures 3.2B** and **3.5C**. The time point with the lowest average signal was then compared to the other time points using an ordinary one-way ANOVA with Dunnet correction for multiple comparisons in order to build the p-value graphs at the bottom of **Figures 3.2B** and **3.5C**. These midcell fluorescent values were calculated for between 50 and 70 cells for each strain measured, and the data are presented with error bars representing 95% confidence intervals.

All aTc-dependent depletion strains were depleted by either 1) the addition of 50-250 ng/mL anhydrotetracycline (aTc) or 2) washing of cells in 7H9 lacking aTc and depleted as such for 9

hours. The FtsZ depletions were conducted by washing cells grown in 7H9 + 0.2% acetamide with 7H9 and growing without acetamide for 7 hours before imaging.

The co-localization analysis was performed by taking red (mCherry-GlfT2) and green (GFPmut3-SepIVA) fluorescent and phase images of mc^2155 L5::CB910-*sepIVA glfT2::*mCherry-*glfT2* from two independent cultures. The background was subtracted from the fluorescent images. The phase images were used to create a mask, outside of which all pixel data was deleted in the fluorescent images. The coloc2 program in ImageJ was used to calculate the Pearson's correlation coefficient for all the pixels within the cell masks from 16 individual images, representing 100-200 cells from each biological replicate. The Pearson's R values were converted to Fisher's z-values, and the mean and 95% confidence interval of the z-values was calculated, then the average R value was calculated from the Fisher's z-values.

Immunoprecipitations

To identify potential interactors of FtsQ, a 1 L cultures of the *ftsQ-strep* strain and a wild-type control were spun down and resuspended in PBS tween 80 + 0.13% paraformaldehyde. The cultures were incubated with the paraformaldehyde for an hour at 37°, then resuspended in a wash buffer of 100 mM Tris, 150 mM NaCl, 1 mM EDTA, protease inhibitor and 0.1% n-Dodecyl-β-D-maltose (DDM) (Cayman Chemical). The cells were lysed twice using a French press and lysate was pelleted at 15000 rpm for 15 minutes at 4°. The supernatant was incubated with Streptactin-covered beads (Iba). The beads were washed with the wash buffer, and the protein was eluted with Buffer BX (IBA). The eluted samples were separated on 4-12% NuPAGE Bis-Tris precast gel (Invitrogen Novex) and then stained with Coomassie blue. The entire lane of eluted protein from the FtsQ-strep and control pulldowns were cut out and sent to Harvard Taplin facility for mass spectrometry analysis. The pulldown was performed twice and

results were sorted first for hits that appeared in both runs and then for enrichment in the FtsQ pulldown as compared to the wild type control pulldown.

This research received no specific grant from any funding agency in the public, commercial, or not-for-profit sectors.

Chapter 3, Section 3.2: References

1. Wu LJ, Errington J. 2011. Nucleoid occlusion and bacterial cell division. Nat Rev Microbiol 10:8–12.

2. Blaauwen den T, de Pedro MA, Nguyen-Disteche M, Ayala JA. 2008. Morphogenesis of rod-shaped sacculi. FEMS Microbiology Reviews 32:321–344.

3. Tsang M-J, Bernhardt TG. 2015. A role for the FtsQLB complex in cytokinetic ring activation revealed by an ftsL allele that accelerates division. Mol Microbiol 95:925–944.

4. Yang DC, Tan K, Joachimiak A, Bernhardt TG. 2012. A conformational switch controls cell wall-remodelling enzymes required for bacterial cell division. Mol Microbiol 85:768–781.

5. Daniel RA, Errington J. 2003. Control of Cell Morphogenesis in Bacteria. Cell 113:767–776.

6. Randich AM, Brun YV. 2015. Molecular mechanisms for the evolution of bacterial morphologies and growth modes. Front Microbiol 6: 580.

7. Brown PJB, de Pedro MA, Kysela DT, Van der Henst C, Kim J, De Bolle X, Fuqua C, Brun YV. 2012. Polar growth in the Alphaproteobacterial order Rhizobiales. Proc Natl Acad Sci USA 109:1697–1701.

8. Thanky NR, Young DB, Robertson BD. 2007. Unusual features of the cell cycle in mycobacteria: Polar-restricted growth and the snapping-model of cell division. Tuberculosis 87:231–236.

9. Aldridge BB, Fernandez-Suarez M, Heller D, Ambravaneswaran V, Irimia D, Toner M, Fortune SM. 2012. Asymmetry and aging of mycobacterial cells lead to variable growth and antibiotic susceptibility. Science 335:100–104.

10. Howell M, Brown PJ. 2016. Building the bacterial cell wall at the pole. Current Opinion in Microbiology 34:53–59.

11. Kalakoutskii LV, Agre NS. 1976. Comparative aspects of development and differentiation in actinomycetes. Bacteriol Rev 40:469–524.

12. Braña A. 1982. Mode of cell wall growth of Streptomyces antibioticus. FEMS Microbiology Letters 13:231–235.

13. Lohnis F. 1921. Studies upon the life cycles of the bacteria. National Academy of Sciences Vol XVI.

14. Gottlieb D. 1953. The physiology of the actinomycetes. The Sixth International Congress for Microbiology, Rome 122–136.

15. Pichoff S, Lutkenhaus J. 2002. Unique and overlapping roles for ZipA and FtsA in septal ring assembly in Escherichia coli. The EMBO Journal 21:685–693.

16. Buss JA, Peters NT, Xiao J, Bernhardt TG. 2017. ZapA and ZapB form an FtsZ-independent structure at midcell. Mol Microbiol 2:2006.0008–12.

17. Sharma AK, Chatterjee A, Basu J, Kundu M, Gupta S, Banerjee SK. 2015. Essential protein SepF of mycobacteria interacts with FtsZ and MurG to regulate cell growth and division. Microbiology (Reading, Engl) 161:1627–1638.

18. Duman R, Ishikawa S, Celik I, the HS, 2013. Structural and genetic analyses reveal the protein SepF as a new membrane anchor for the Z ring. Proceedings of National Academy of Sciences 110:E4601-10.

19. Datta P. 2002. Interaction between FtsZ and FtsW of Mycobacterium tuberculosis. Journal of Biological Chemistry 277:24983–24987.

20. Rajagopalan M, Maloney E, Dziadek J, Poplawska M, Lofton H, Chauhan A, Madiraju M. 2005. Genetic evidence that mycobacterial FtsZ and FtsW proteins interact, and colocalize to the division site in Mycobacterium smegmatis. FEMS Microbiology Letters 250:9–17.

21. Datta P, Dasgupta A, Singh AK, Mukherjee P, Kundu M, Basu J. 2006. Interaction between FtsW and penicillin-binding protein 3 (PBP3) directs PBP3 to mid-cell, controls cell septation and mediates the formation of a trimeric complex involving FtsZ, FtsW and PBP3 in mycobacteria. Mol Microbiol 62:1655–1673.

22. Liu B, Persons L, Lee L, De Boer PAJ. 2015. Roles for both FtsA and the FtsBLQ subcomplex in FtsN-stimulated cell constriction in Escherichia coli. Mol Microbiol 95:945–970.

23. Blaauwen den T, de Pedro MA, Nguyen-Distèche M, Ayala JA. 2008. Morphogenesis of rod-shaped sacculi. FEMS Microbiology Reviews 32:321–344.

24. Meniche X, Otten R, Siegrist MS, Baer CE, Murphy KC, Bertozzi CR, Sassetti CM. 2014. Subpolar addition of new cell wall is directed by DivIVA in mycobacteria. Proc Natl Acad Sci USA 111:E3243–51.

25. Howell M, Aliashkevich A, Salisbury AK, Cava F, Bowman GR, Brown PJB. 2017. Absence of the Polar Organizing Protein PopZ Results in Reduced and Asymmetric Cell Division in Agrobacterium tumefaciens. J Bacteriol 199:e00101–17–16.

26. Kang CM, Nyayapathy S, Lee JY, Suh JW, Husson RN. 2008. Wag31, a homologue of the cell division protein DivIVA, regulates growth, morphology and polar cell wall synthesis in mycobacteria. Microbiology 154:725–735.

27. Xu W-X, Zhang L, Mai J-T, Peng R-C, Yang E-Z, Peng C, Wang H-H. 2014. The Wag31 protein interacts with AccA3 and coordinates cell wall lipid permeability and lipophilic drug resistance in Mycobacterium smegmatis. Biochemical and Biophysical Research Communications 448:255–260.

28. Soding J, Biegert A, Lupas AN. 2005. The HHpred interactive server for protein homology detection and structure prediction. Nucleic Acids Research 33:W244–W248.

29. Krogh A, Larsson B, Heijne von G, Sonnhammer ELL. 2001. Predicting transmembrane protein topology with a hidden markov model: application to complete genomes11Edited by F. Cohen. Journal of Molecular Biology 305:567–580.

30. Alva V, Nam S-Z, Söding J, Lupas AN. 2016. The MPI bioinformatics Toolkit as an integrative platform for advanced protein sequence and structure analysis. Nucleic Acids Research 44:W410–W415.

31. Robson SA, King GF. 2006. Domain architecture and structure of the bacterial cell division protein DivIB. Proceedings of the National Academy of Sciences 103:6700–6705.

32. Rost B, Yachdav G, Liu J. 2004. The PredictProtein server. Nucleic Acids Research 32:W321–W326.

33. Marchler-Bauer A, Derbyshire MK, Gonzales NR, Lu S, Chitsaz F, Geer LY, Geer RC, He J, Gwadz M, Hurwitz DI, Lanczycki CJ, Lu F, Marchler GH, Song JS, Thanki N, Wang Z, Yamashita RA, Zhang D, Zheng C, Bryant SH. 2015. CDD: NCBI's conserved domain database. Nucleic Acids Research 43:D222–D226.

34. Klotzsche M, Ehrt S, Schnappinger D. 2009. Improved tetracycline repressors for gene silencing in mycobacteria. Nucleic Acids Research 37:1778–1788.

35. van Kessel JC, Hatfull GF. 2008. Mycobacterial recombineering. Methods Mol Biol 435:203–215.

36. Griffin JE, Gawronski JD, DeJesus MA, Ioerger TR, Akerley BJ, Sassetti CM. 2011. High-Resolution Phenotypic Profiling Defines Genes Essential for Mycobacterial Growth and Cholesterol Catabolism. PLoS Pathog 7:e1002251.

37. Zhang YJ, Ioerger TR, Huttenhower C, Long JE, Sassetti CM, Sacchettini JC, Rubin EJ. 2012. Global Assessment of Genomic Regions Required for Growth in Mycobacterium tuberculosis. PLoS Pathog 8:e1002946.

38. Dziadek J. 2003. Conditional expression of Mycobacterium smegmatis ftsZ, an essential cell division gene. Microbiology 149:1593–1603.

39. Goehring NW, Gonzalez MD, Beckwith J. 2006. Premature targeting of cell division proteins to midcell reveals hierarchies of protein interactions involved in divisome assembly. Mol Microbiol 61:33–45.

40. Schmidt TG, Skerra A. 2007. The Strep-tag system for one-step purification and high-affinity detection or capturing of proteins. Nat Protoc 2:1528–1535.

41. Yang DC, Peters NT, Parzych KR, Uehara T, Markovski M, Bernhardt TG. 2011. An ATP-binding cassette transporter-like complex governs cell-wall hydrolysis at the bacterial cytokinetic ring. Proc Natl Acad Sci USA 108:E1052–60.

42. Meisner J, Montero Llopis P, Sham L-T, Garner E, Bernhardt TG, Rudner DZ. 2013. FtsEX is required for CwlO peptidoglycan hydrolase activity during cell wall elongation in Bacillus subtilis. Mol Microbiol 89:1069–1083.

43. Vicente M, Rico AI, Martinez-Arteaga R, Mingorance J. 2005. Septum Enlightenment: Assembly of Bacterial Division Proteins. J Bacteriol 188:19–27.

44. Wang L, Lutkenhaus J. 1998. FtsK is an essential cell division protein that is localized to the septum and induced as part of the SOS response. Mol Microbiol 29:731–740.

45. Gee CL, Papavinasasundaram KG, Blair SR, Baer CE, Falick AM, King DS, Griffin JE, Venghatakrishnan H, Zukauskas A, Wei JR, Dhiman RK, Crick DC, Rubin EJ, Sassetti CM, Alber T. 2012. A Phosphorylated Pseudokinase Complex Controls Cell Wall Synthesis in Mycobacteria. Science Signaling 5:ra7.

46. Nagarajan SN, Upadhyay S, Chawla Y, Khan S, Naz S, Subramanian J, Gandotra S, Nandicoori VK. 2015. Protein Kinase A (PknA) of Mycobacterium tuberculosis Independently Activated and Is Critical for Growth in Vitroand Survival of the Pathogen in the Host. J Biol Chem 290:9626–9645.

47. Hayashi JM, Luo C-Y, Mayfield JA, Hsu T, Fukuda T, Walfield AL, Giffen SR, Leszyk JD, Baer CE, Bennion OT, Madduri A, Shaffer SA, Aldridge BB, Sassetti CM, Sandler SJ, Kinoshita T, Moody DB, Morita YS. 2016. Spatially distinct and metabolically active membrane domain in mycobacteria. Proc Natl Acad Sci USA 113:5400-5405.

48. Murphy KC, Nelson S, Nambi S, Papavinasasundaram K, Baer CE, Sassetti CM. ORBIT: a new paradigm for genetic engineering of mycobacterial chromosomes.

49. Kim J-H, Wei J-R, Wallach JB, Robbins RS, Rubin EJ, Schnappinger D. 2010. Protein inactivation in mycobacteria by controlled proteolysis and its application to deplete the beta subunit of RNA polymerase. Nucleic Acids Research 39:2210–2220.

50. Letek M, Ordonez E, Vaquera J, Margolin W, Flardh K, Mateos LM, Gil JA. 2008. DivIVA Is Required for Polar Growth in the MreB-Lacking Rod-Shaped Actinomycete Corynebacterium glutamicum. J Bacteriol 190:3283–3292.

51. Hempel AM, Wang SB, Letek M, Gil JA, Flardh K. 2008. Assemblies of DivIVA Mark Sites for Hyphal Branching and Can Establish New Zones of Cell Wall Growth in Streptomyces coelicolor. J Bacteriol 190:7579–7583.

52. Flärdh K. 2003. Essential role of DivIVA in polar growth and morphogenesis in Streptomyces coelicolor A3(2). Mol Microbiol 49:1523–1536.

53. Cha JH, Stewart GC. 1997. The divIVA minicell locus of Bacillus subtilis. J Bacteriol 179:1671–1683.

54. Edwards DH, Errington J. 1997. The Bacillus subtilis DivIVA protein targets to the division septum and controls the site specificity of cell division. Mol Microbiol 24:905–915.

55. Marston AL, Thomaides HB, Edwards DH, Sharpe ME, Errington J. 1998. Polar localization of the MinD protein of Bacillus subtilis and its role in selection of the mid-cell division site. Genes & Development 12:3419–3430.

56. Marston AL, Errington J. 1999. Selection of the midcell division site in Bacillus subtilis

through MinD-dependent polar localization and activation of MinC. Mol Microbiol 33:84–96.

57. Eswaramoorthy P, Winter PW, Wawrzusin P, York AG, Shroff H, Ramamurthi KS. 2014. Asymmetric division and differential gene expression during a bacterial developmental program requires DivIVA. PLoS Genet 10:e1004526.

58. Hayashi JM, Luo C-Y, Mayfield JA, Hsu T, Fukuda T, Walfield AL, Giffen SR, Leszyk JD, Baer CE, Bennion OT, Madduri A, Shaffer SA, Aldridge BB, Sassetti CM, Sandler SJ, Kinoshita T, Moody DB, Morita YS. 2016. Spatially distinct and metabolically active membrane domain in mycobacteria. Proceedings of the National Academy of Sciences 113:5400–5405.

59. Kieser KJ, Rubin EJ. 2014. How sisters grow apart: mycobacterial growth and division. Nat Rev Microbiol 12:550–562.

60. Tsang M-J, Bernhardt TG. 2015. A role for the FtsQLB complex in cytokinetic ring activation revealed by an ftsL allele that accelerates division. Mol Microbiol 95:925–944.

61. Goehring NW, Beckwith J. 2005. Diverse Paths to Midcell: Assembly of the Bacterial Cell Division Machinery. Current Biology 15:R514–R526.

62. Buddelmeijer N, Judson N, Boyd D, Mekalanos JJ, Beckwith J. 2002. YgbQ, a cell division protein in Escherichia coli and Vibrio cholerae, localizes in codependent fashion with FtsL to the division site. Proceedings of the National Academy of Sciences 99:6316–6321.

63. Wadenpohl I, Bramkamp M. 2010. DivIC Stabilizes FtsL against RasP Cleavage. J Bacteriol 192:5260–5263.

64. Guzman L-M, Barondess JJ, Beckwith J. 1992. FtsL, an Essential Cytoplasmic Membrane Protein Involved in Cell Division in Escherichia coli. J Bacteriol 174:7717–7728.

65. Kaval KG, Hauf S, Rismondo J, Hahn B, Halbedel S. 2017. Genetic Dissection of DivIVA Functions in Listeria monocytogenes. J Bacteriol 199:e00421–17–16.

66. Jani C, Eoh H, Lee JJ, Hamasha K, Sahana MB, Han J-S, Nyayapathy S, Lee J-Y, Suh J-W, Lee SH, Rehse SJ, Crick DC, Kang C-M. 2010. Regulation of Polar Peptidoglycan Biosynthesis by Wag31 Phosphorylation in Mycobacteria. BMC Microbiology 10:327.

67. Claessen D, Emmins R, Hamoen LW, Daniel RA, Errington J, Edwards DH. 2008. Control of the cell elongation–division cycle by shuttling of PBP1 protein in Bacillus subtilis. Mol Microbiol 68:1029–1046.

68. Fleurie A, Manuse S, Zhao C, Campo N, Cluzel C, Lavergne J-P, Freton C, Combet C, Guiral S, Soufi B, Macek B, Kuru E, VanNieuwenhze MS, Brun YV, Di Guilmi A-M, Claverys J-P, Galinier A, Grangeasse C. 2014. Interplay of the Serine/Threonine-Kinase StkP and the Paralogs DivIVA and GpsB in Pneumococcal Cell Elongation

and Division. PLoS Genet 10:e1004275.

69. Hamoen LW, Errington J. 2003. Polar Targeting of DivIVA in Bacillus subtilis Is Not Directly Dependent on FtsZ or PBP 2B. J Bacteriol 185:693–697.

70. Hett EC, Chao MC, Deng LL, Rubin EJ. 2008. A Mycobacterial Enzyme Essential for Cell Division Synergizes with Resuscitation-Promoting Factor. PLoS Pathog 4:e1000001.

71. Kieser KJ, Baranowski C, Chao MC, Long JE, Sassetti CM, Waldor MK, Sacchettini JC, Ioerger TR, Rubin EJ. 2015. Peptidoglycan synthesis in Mycobacterium tuberculosis is organized into networks with varying drug susceptibility. Proc Natl Acad Sci USA 112:13087–13092.

72. Chao MC, Kieser KJ, Minami S, Mavrici D, Aldridge BB, Fortune SM, Alber T, Rubin EJ. 2013. Protein Complexes and Proteolytic Activation of the Cell Wall Hydrolase RipA Regulate Septal Resolution in Mycobacteria. PLoS Pathog 9:e1003197–16.

73. Randich AM, Brun YV. 2015. Molecular mechanisms for the evolution of bacterial morphologies and growth modes. Front Microbiol 6:938–13.

74. Lewis JA, Hatfull GF. 2003. Control of Directionality in L5 Integrase-mediated Site-specific Recombination. Journal of Molecular Biology 326:805–821.

75. Boutte CC, Baer CE, Papavinasasundaram K, Liu W, Chase MR, Meniche X, Fortune SM, Sassetti CM, Ioerger TR, Rubin EJ, Laub M. 2016. A cytoplasmic peptidoglycan amidase homologue controls mycobacterial cell wall synthesis. eLife 5:e14590.

76. Pashley CA, Parish T. 2003. Efficient switching of mycobacteriophage L5-based integrating plasmids in Mycobacterium tuberculosis. FEMS Microbiology Letters 229:211–215.

77. Kim J-H, Wei J-R, Wallach JB, Robbins RS, Rubin EJ, Schnappinger D. 2010. Protein inactivation in mycobacteria by controlled proteolysis and its application to deplete the beta subunit of RNA polymerase. Nucleic Acids Research 39:2210–2220.

78. Pham TT, Jacobs-Sera D, Pedulla ML, Hendrix RW, Hatfull GF. 2007. Comparative genomic analysis of mycobacteriophage Tweety: evolutionary insights and construction of compatible site-specific integration vectors for mycobacteria. Microbiology 153:2711–2723.

Chapter 4

Preliminary characterization of mycobacterial FtsH

Chapter 4, Section 4.1: Mycobacterial FtsH is a non-essential protease involved in the response to oxidative stress

Katherine J. Wu[1,2], Lauren Elson[1,3], Eric J. Rubin[1,2]

1 - Department of Immunology and Infectious Disease, Harvard TH Chan School of Public Health, Boston MA.

2 - Department of Microbiology and Immunobiology, Harvard Medical School, Boston, MA.

3 - Department of Chemistry, Harvard College, Cambridge, MA.

Author contributions: K.J.W. and E.J.R. designed experiments. K.J.W. and L.E. performed experiments and analyzed data. This work is ongoing in the Rubin Lab.

INTRODUCTION

FtsH has been best characterized in *E. coli,* an organism in which it is uniquely essential. In *E. coli,* this homohexameric AAA+ protease serves a quality control function, recognizing diverse substrates that range from LPS biosynthesis machines to alternative sigma factors. Its essentiality is dependent on its ability to degrade LpxC, maintaining the delicate balance between LPS and PL biosynthesis. Loss of FtsH results in overproduction of LPS at the expense of PL, and only a concurrent suppressor mutation that either suppresses LPS biosynthesis or increases PL biosynthesis can suppress *ftsH* essentiality (Katz *et al.* 2008; Langklotz *et al.* 2011; Bittner *et al.* 2017).

However, despite being typically nonessential for viability under normal growth conditions, in some other bacteria, including *Salmonella,* FtsH has been characterized for its roles in virulence. For instance, FtsH has been shown to degrade the conserved virulence factor MgtC, which promotes *Salmonella* survival in macrophages and magnesium-depleted media, with the assistance of MgtR, which shuttles MgtC into the FtsH degradation chamber (Alix *et al.* 2008).

Notably, pathogenic mycobacteria also encode MgtC, which appears to serve a similar role in maintaining bacterial viability within macrophages (Alix *et al.* 2008). However, no studies have yet tied MgtC to FtsH.

Preliminary characterizations of FtsH in mycobacteria are sparse; in fact, the most recent characterization of this protease in the *Mycobacterium* genus was in 2010. What's more, the data have produced somewhat incongruous results. In 2009, Kiran *et al.* attempted a knockout of the gene, but were unsuccessful, and instead generated knockdowns using an antisense RNA and an overexpression strain of *ftsH* in *Mtb.* Their results showed *ftsH* to be upregulated in conditions of oxidative stress and macrophage infection, but downregulated during stationary phase and starvation (Kiran *et al.* 2009). While ectopic expression of *Msm ftsH* appears to be lethal in *E. coli, Mtb ftsH* can complement an *E. coli ftsH* knockout, and both mycobacterial variants appear to degrade known *E. coli* FtsH substrates (Anilkumar *et al.* 2004, Srinivasan *et al.* 2006). These studies indicate at least some degree of conservation between mycobacterial FtsH and homologs in other species, though any physiological relevance of these studies is entirely speculative. Additionally, no studies so far have verified a mycobacterial FtsH substrate, though indirect evidence indicates that FtsZ levels may drop in an *ftsH* overexpression (Kiran *et al.* 2009).

Even the essentiality of *ftsH* has previously been in question. Tn-seq studies in *Mtb* have generated conflicting results about the essentiality of *ftsH*; however, one study from our lab predicted conditional essentiality for *ftsH* in a mouse infection model (Zhang *et al.* 2013). As such, *ftsH* remains almost entirely unexplored in mycobacteria, despite its potential importance to the virulence of this pathogenic genus.

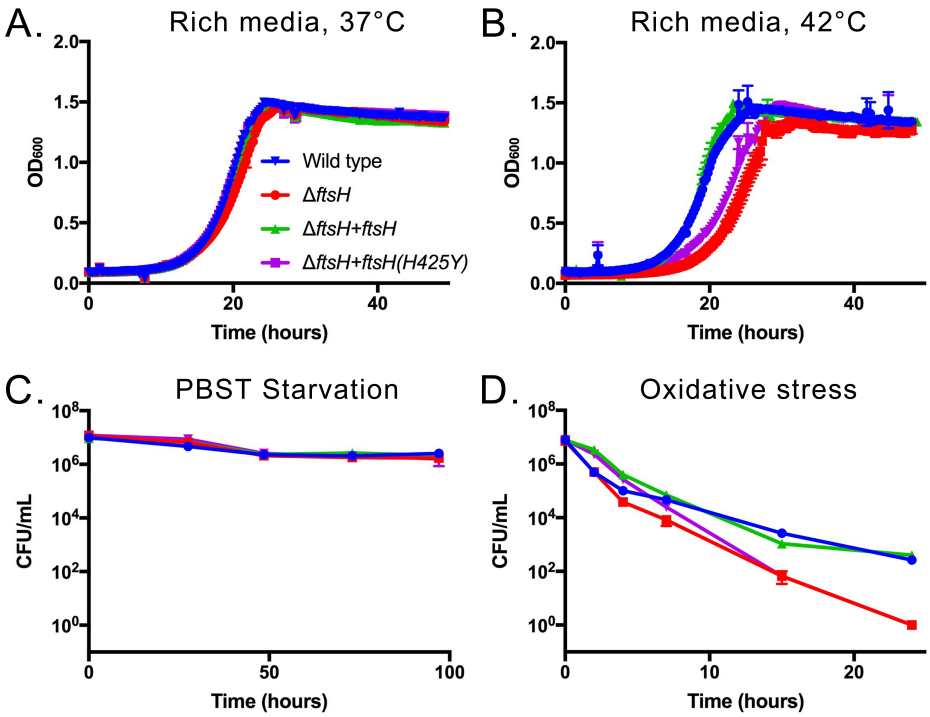

Figure 4.1: Cells that lack FtsH proteolytic activity are more sensitive to oxidative stress. The indicated strains of *Mycobacterium smegmatis* (wild type, an *ftsH* knockout [Δ*ftsH*], an *ftsH* knockout with *ftsH* complemented at the L5 integration site under its native promoter [Δ*ftsH+ftsH*], and an *ftsH* knockout with *ftsH(H425Y)* complemented at the L5 integration site under its native promoter [Δ*ftsH+ftsH(H425Y)*]) were subjected to the following conditions: normal growth in rich media at 37°C (**panel A**), high temperature at 42°C (**panel B**), carbon-nitrogen starvation in PBS-Tween80 (**panel C**), or oxidative stress in 0.02% tert-butyl hydroperoxide (**panel D**).

RESULTS

To elucidate the functional relevance of *ftsH,* we constructed Δ*ftsH* mutants in both *Msm* and *Mtb* using mycobacterial recombineering, confirming that *ftsH* is indeed dispensable in these mycobacteria under normal growth conditions (**Figure 4.1A**), mirroring its nonessentiality in most other bacterial species. Further testing in *Msm* revealed that *ftsH* was additionally dispensable in carbon-nitrogen depleted media (**Figure 4.1C**). Mild to moderate growth defects were observed when the strain was exposed to high temperature and oxidative stress (**Figure 4.1B,D**); however, because there is no defect in doubling time at high temperature, this defect may be of little significance. These data are in keeping with previous findings on the transcriptional regulation of *ftsH* during starvation and oxidative stress (Kiran *et al.* 2009).

To expand upon these findings, we complemented back a wild-type copy of *ftsH* or a copy in which the putative zinc-binding motif was ablated (*ftsH(H425Y)*). This mutation has been utilized in *E. coli* studies of FtsH and reliably destroys proteolytic activity while retaining ATPase activity, allowing substrates to be funneled into the catalytic site but not degraded, creating a protease "trap." We found that while wild-type *ftsH* restored normal growth phenotypes, *ftsH(H425Y)* did not, indicating that *ftsH* proteolytic activity appears to be crucial for mediating its stress survival function. These same results held true when we performed the same genetic complementations with *Mtb ftsH* or *ftsH(H425Y)* (data not shown)—an unsurprising finding given that *Msm* and *Mtb ftsH* exhibit nearly 90% sequence homology. Additionally, microscopy showed that Δ*ftsH* cells exhibit no obvious morphological defects (data not shown).

We next focused our efforts on the *ftsH(H425Y)* strain, a variant of which has previously been used in *E. coli* as a proteolytic trap to identify potential substrates (**Figure 4.2**) (Westphal *et al.* 2012). We Strep-tagged both *ftsH* and *ftsH(H425Y)* and expressed these constructs in Δ*ftsH* strains. We

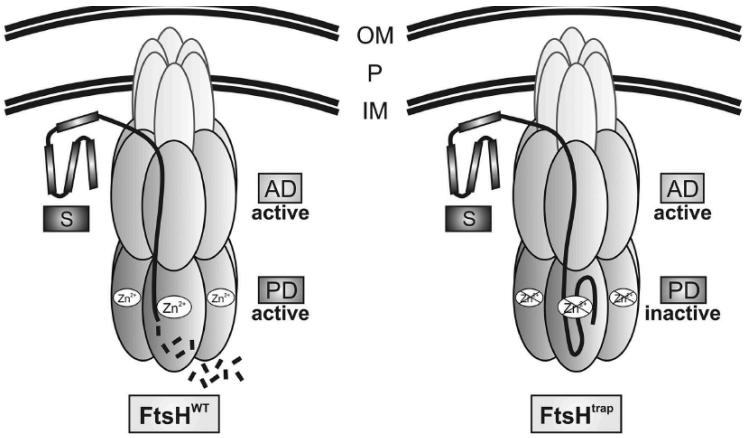

Figure 4.2: A schematic of an FtsH proteolytic trap. A mutation in the conserved zinc-binding motif renders FtsH proteolytically inactive. However, the ATPase domain remains active, allowing substrates to be unfolded and spooled into the dead-end chamber. This creates a "trap" that can be expressed in a tagged form and used in co-immunoprecipitation. *Figure adapted from (Westphal* et al. *2012).*

Table 4.1: FtsH pulldown data. Proteins whose peptides were pulled down with cross-linked FtsH-strep.

Gene name	MSMEG #	TB #	Annotations/descriptions
alaS	MSMEG_3025	Rv2555c	alanyl-tRNA synthetase, catalyzes attachment of alanine to tRNA, protein biosynthesis
polA	MSMEG_3839	Rv1629	DNA polymerase I
ppc	MSMEG_3097		phosphoenolpyruvate carboxylase, forms oxaloacetate for TCA cycle
rpsD	MSMEG_1523	Rv3458c	produces ribosomal protein S4, one of primary rRNA binding proteins. In *E. coli*: important for translational accuracy, maintaining protein homeostasis, translational repressor protein.
	MSMEG_4533	Rv2400c	sulfate-binding protein, ATPase-coupled sulfate transmembrane transporter activity
fadA3	MSMEG_5273	Rv1074c	acetyl-CoA acetyltransferase
trxB	MSMEG_6933	Rv3913	thioredoxin-disulfide reductase, catalytic
pgk	MSMEG_3085	Rv1437	phosphoglycerate kinase, catalytic, involved in step 2 of subpathway (of glycolysis) that synthesizes pyruvate from G3P
mihF	MSMEG_3050	Rv1388	integration host factor, important for RNA binding & translation, heat stable polypeptide, essential for viability
	MSMEG_6512		acyl-CoA dehydrogenase domain protein
	MSMEG_3058		lipoprotein, NlpA family protein
	MSMEG_4709	Rv2486	enoyl-CoA hydratase, catalytic, metabolic
	MSMEG_0690	Rv0338c	iron-sulfur cluster-binding protein
dapD	MSMEG_5104	Rv1201c	catalytic activity, L-lysine biosynthesis via DAP pathway
	MSMEG_6193	Rv3679	anion-transporting ATPase, ATPase activity/ATP binding

next grew the strains, exposed them to paraformaldehyde as a crosslinking agent, and performed Streptactin pulldowns. The proteins identified in the elution are listed in **Table 4.1**.

Notably, **Table 4.1** lists only those proteins that appeared in the elution of mutant pulldown, but not in the wild-type pulldown, indicating that these are likely substrates of proteolysis rather than adaptors or other binding partners. No common interactors were identified from both data sets, and thus we did not include candidates for adaptors.

DISCUSSION AND FUTURE DIRECTIONS

The results produced so far are extremely preliminary, and have only been conducted in *Msm.* Several more experiments must be done to draw any conclusions about FtsH function in mycobacteria. However, our data thus far prove that *ftsH* is indeed dispensable under normal growth conditions; furthermore, *ftsH* knockouts survived fairly well under all stress conditions tested. Even the most extreme phenotype observed in the oxidative stress condition (**Figure 4.1D**) did not completely kill the strain, and the effects were progressive, while other, better-characterized mutants that fail to be stress responsive have shown much more rapid death in similar conditions (see **Chapter 2**). If FtsH contributes to survival under oxidative stress, it is a partial contribution that acts in concert with many other factors and would be an unlikely drug candidate on its own.

However, because all of these results have been conducted *in vitro,* while Tn-seq has identified the host environment as perhaps the most physiologically relevant conditions under which FtsH is active (Zhang *et al.* 2012), there is a pressing need for follow-up experiments in *Mtb*. The knockouts generated in *Mtb* do not exhibit obvious growth defects under normal growth conditions, but should be exposed to *in vitro* oxidative stress and high temperature, and, more importantly, be tested for viability in macrophages and in mice. Additionally, because an FtsH

proof-of-concept pulldown has been successfully performed in *Msm,* there is a high likelihood that the equivalent experiment in *Mtb* will yield promising candidates. Notably, *Msm* is not pathogenic, and thus may not encode many of the most important FtsH substrates, especially if this gene plays its most critical roles in the host. Targeted testing of substrate candidates such as MgtC (which is in the *Mtb* genome but not the *Msm* genome) or FtsZ (proposed in Kiran *et al.* 2009) may be warranted. In the meantime, more biochemical data is needed to confirm the pulldown candidates identified in *Msm.*

MATERIALS AND METHODS

Experimental model details: *Mycobacterium smegmatis* mc^2155 was grown in liquid media containing 7H9 salts (Becton-Dickinson) supplemented with 5 g/L albumin, 2 g/L dextrose, 0.85 g/L NaCl, 0.003 g/L catalase, 0.2% glycerol, and 0.05% Tween80, or plated on LB agar. *Mycobacterium tuberculosis* H37Rv was cultured in Middlebrook 7H9 salts supplemented with OADC (oleic acid, albumin, dextrose, catalase [BD Biosciences, Franklin Lakes, NJ]), 0.25% glycerol, and 0.05% Tween-80 or plated on 7H10 agar. For all oxidative stress experiments, strains were grown in Hartmans-de Bont (HdB) media, which was made as described (Hartmans and De Bont, 1992) with 0.05% Tween80. *E. coli* TOP10 was used for cloning. Antibiotic selection concentrations for *M. smegmatis* and *M. tuberculosis* were as follows: 25 µg/mL kanamycin, 50 µg/mL hygromycin, 20 µg/mL zeocin, and 5 µg/mL gentamicin. Antibiotic concentrations for *E. coli* were as follows: 50 µg/mL kanamycin, 100 µg/mL hygromycin, and 50 µg/mL zeocin. Anhydrotetracyline was used at 100 ng/mL for gene induction or repression. All strains were grown at 37°C unless otherwise indicated.

Strain construction: Deletions of *ftsH* were generated by mycobacterial recombineering as previously described (van Kessel and Hatfull 2008). Complementations were generated by transforming integrating vectors into *M. smegmatis* at the L5 site (Lewis and Hatfull, 2003).

Growth rate determination and kill curves: For growth curves, strains were grown to mid-log phase, diluted to OD_{600} 0.005 in triplicate, and measured every 15 min in a Bioscreen growth curve machine (Growth Curves USA) at 37°C or 42°C, where indicated.

For environmental stress kill curves, strains were grown to mid-log phase, washed twice with PBS-Tween80, diluted to OD600 0.05, and rolled at 37°C in PBS-Tween80 or HdB + 0.02% tert-butyl hydroperoxide. At the indicated time points, 200 uL aliquots were removed, serially diluted in PBS-Tween80, and plated for CFUs.

Tert-butyl hydroperoxide was added once at the beginning of each experiment. Each kill curve was performed at least thrice, in triplicate, with similar results.

Immunoprecipitation: To identify potential interactors of FtsH, 200 mL mid-log phase cultures of a strain expressing FtsH-Strep or FtsH(H425Y)-Strep were spun down and resuspended in 2 mL of Buffer W (100 mM Tris, 150 mM NaCl, 1 mM EDTA) with an EDTA-free protease inhibitor cocktail (Roche, Switzerland). The cells were lysed by bead beating and SDS was added to the lysate to a final concentration of 1%. The lysate was pre-cleared of endogenously biotinylated proteins using Pierce Avidin Agarose for 1 hour at room temperature. The cleared supernatant was then added to MagStrep "type3" XT beads (IBA Lifesciences) and incubated overnight at 4°C. The beads were then washed three times with Buffer W and eluted using Buffer BX (IBA Lifesciences). The eluted samples were separated on a 4-12% NuPAGE Bis-Tris precast gel (Invitrogen Novex) and stained with Coomassie Blue. The entire lanes of eluted protein from the FtsH-Strep or FtsH(H425Y)-Strep and untagged control immunoprecipitations were cut out and analyzed by the Harvard Taplin mass spectrometry facility. The unbiased immunoprecipitation was performed twice.

Chapter 4, Section 4.2: References

1. Alix, E and Blanc-Potard, AB. Peptide-assisted degradation of the *Salmonella* MgtC virulence factor. *EMBO J* 27: 546-557 (2008). doi: 10.1038/sj.emboj.7601983.

2. Anilkumar, G *et al.* Genomic organization and *in vivo* characterization of proteolytic activity of FtsH of *Mycobacterium smegmatis. Microbiology* 150: 2629-2639 (2004).

3. Bittner LM, Arends J, and Narberhaus F. When, how and why? Regulated proteolysis by the essential FtsH protease in *Escherichia coli*. *Biol Chem* 398(5-6):625-635 (2017). doi: 10.1515/hsz-2016-0302.

4. Hartmans S and De Bont JAM. (1992). The genus Mycobacterium— nonmedical, Prokaryotes, 2nd:1214–37. New York, Springer-Verlag New York Inc.

5. Katz, C *et al.* Dual Role of FtsH in Regulating Lipopolysaccharide Biosynthesis in *Escherichia coli. J Bacteriol* 190(21): 7117-7122 (2008).

6. Kiran, M *et al. Mycobacterium tuberculosis ftsH* expression in response to stress and viability. *Tuberculosis* 89: S70-S73 (2009).

7. Langklotz, S *et al.* Structure and function of the bacterial AAA protease FtsH. *Biochim Biophys Acta* 1823: 40-48 (2012).

8. Lewis JA and Hatfull GF. (2003). Control of directionality in L5 integrase-mediated site-specific recombination. J Mol Biol 326:805-21, doi:10.1016/S0022-2836(02)01475-4.

9. Srinivasan, RS *et al.* Functional characterization of AAA family FtsH protease of *Mycobacterium tuberculosis. FEMS Microbiol Lett* 259: 97-105 (2006).

10. van Kessel JC and Hatfull GF. (2008). Mycobacterial recombineering. Methods Mol Biol 435:203-15, doi:10.1007/978-1-59745-232-8_15.

11. Westphal, K *et al.* A Trapping Approach Reveals Novel Substrates and Physiological Functions of the Essential Protease FtsH in *Escherichia coli. J Biol Chem* 287(51): 42962-42971 (2012).

12. Zhang YJ, Ioerger TR, Huttenhower C, Long JE, Sassetti CM, Sacchettini JC, and Rubin EJ. (2012). Global Assessment of Genomic Regions Required for Growth in Mycobacterium tuberculosis. PLoS Pathog 8(9):e1002946, doi:10.1371/journal.ppat.1002946.

13. Zhang, YJ *et al.* Tryptophan Biosynthesis Protects Mycobacteria from CD4 T-Cell-Mediated Killing. *Cell* 155(6): 1296-1308 (2013).

Chapter 5

Discussion

Chapter 5, Section 5.1: Summary of results and potential implications

As the causative agent of tuberculosis, the pathogenic bacterium *Mycobacterium tuberculosis* remains the greatest infectious killer in history. It is estimated to infect at least a fourth of the global population (Centers for Disease Control, 2018; World Health Organization, 2018), and has maintained this steady hold on the human population for decades long after the advent of antibiotic therapy. An estimated 600,000 new cases of multi-drug-resistant or rifampicin-resistant tuberculosis emerged in the year 2016 (World Health Organization, 2017).

Due to ever-rising rates of drug resistance, current treatment regimens grow increasingly less effective against *Mtb*; as such, there is a dire need for new tubericidal drugs and compounds. Much of the attention in this line of research has turned to processes essential to bacterial physiology—namely, genes essential for growth or virulence.

A particularly appealing group of genes for drug targeting is proteases. Proteases are extraordinarily diverse: Commonly united by only the vague task of degrading other proteins, they are poised to act in every cellular compartment in every function imaginable. Even with this immense diversity, mycobacteria have managed to co-opt several highly conserved proteases for unique functions (Raju *et al.* 2012a). For instance, unlike a lot of other bacteria, which normally encode *either* Clp *or* a proteasome, mycobacteria have both. What's more, they express multiple proteases that are highly conserved but typically nonessential in other organisms—that have evolved to become uniquely essential in mycobacteria (**Figure 5.1**). The Clp protease is required for viability in mycobacteria, due in part to its ability to degrade WhiB1, an essential cell cycle regulator (Raju *et al.* 2012a, Raju *et al.* 2012b, Raju *et al.* 2014). Additionally, the proteasome—an unusual machine for a prokaryote—is essential for *Mtb* virulence, as its substrates play significant roles in the cell's response to nitric oxide stress, as

	Clp	FtsH	Proteasome	HtrA
Location	Cytoplasm	Cytoplasm	Cytoplasm	Periplasm
Substrates	WhiB1, ssrA-tagged substrates	?	Log, HspR, pupylated substrates	Ami3
Essentiality	Yes	For virulence	For virulence and survival of nitric oxide stress	Yes
Drug candidates?	Yes	No	Yes	Yes

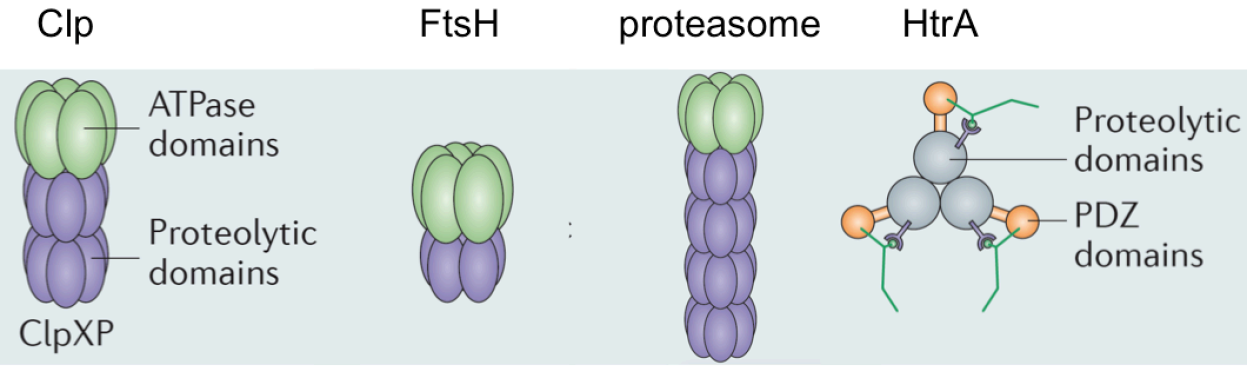

Figure 5.1: The drug candidacy of conserved mycobacterial proteases. Mycobacteria encode several conserved proteases, all of which are viable drug candidates due to their complex structure and importance to cellular viability or virulence. Although several studies have investigated the function of Clp and the proteasome, mycobacterial FtsH and HtrA remain mostly unstudied. The work contained in this dissertation seeks to address these gaps in knowledge. FtsH is likely a nonessential protease; its stress responsive roles in *Mtb* remain to be uncovered.

well as zinc and copper homeostasis during infection (Samanovic and Darwin 2016; Alhuwaider and Dougan 2017).

The high degree of conservation between mycobacterial protease homologs and their cognates in other species may facilitate the synthesis or discovery of novel drugs. Compounds active against homologs of HtrA, the proteasome, and Clp have already been identified; notably, preliminary studies have even isolated a handful of drugs that are bactericidal against *Mtb* by modulating Clp activity (Raju *et al.* 2012a). To effectively bring these drugs into the clinic and develop new ones to follow in their wake, a better understanding of these conserved proteases' mechanisms of action and importance to cellular physiology is needed.

While several groups (including other members of the Rubin Lab) are conducting ongoing work in Clp and the proteasome, HtrA and FtsH have been virtually untouched in recent years. What's more, most of the studies of proteases and their contributions to cellular homeostasis revolve around agents active in the cytoplasm (**Figure 5.1**), leaving substrates relegated to the inner membrane and beyond mostly unexplored through the lens of proteolysis.

Thus, HtrA and FtsH may not only shed light on mycobacterial drug discovery, but also functionally define a poorly understood cellular compartment in this genus of pathogenic bacteria. The body of work presented in this dissertation thus seeks to increase our understanding of these two potentially crucial proteases in mycobacteria, as well as the players that contribute to mycobacterial physiology beyond the cytoplasm, including the players that contribute to cellular growth and division.

In **Chapter 2**, we present the first functional characterization of mycobacterial HtrA. Our data confirm its essentiality in *Mycobacterium smegmatis*, previously only predicted by several Tn-

seq datasets (Rubin Lab, unpublished data). Additionally, we identify an essential binding partner for HtrA: LppZ, a putative lipoprotein also anchored in the inner membrane. The resulting complex of HtrA-LppZ appears to play a crucial role in maintaining cell wall homeostasis, blocking the potentially toxic activity of Ami3, a putative N-acetylmuramoyl-L-alanine amidase. Ami3 is transcribed at fairly low levels (**Figure A1.8**), but is stabilized through mannosylation by Pmt, a prolific O-mannosyltransferase responsible for the vast majority of extracytoplasmic O-mannosylation in *Mtb* and *Msm* (VanderVen *et al.* 2005; Liu *et al.* 2013) (**Figures 2.5, A1.4**). When overexpressed, Ami3 accumulates to the point of cellular toxicity, likely due to its peptidoglycan-cleaving activity, lysing cells that exhibit compromised cell wall integrity (**Figure 2.3**). At physiological levels, however, Ami3 is kept in check by HtrA-LppZ (**Figure 2.4**). As such, loss-of-function mutations in either *ami3* or *pmt* relieve the essentiality of both *htrA* and *lppZ* (**Figure 2.2**). These data indicate that HtrA-LppZ is a complex whose essentiality is mediated entirely by its ability to negatively regulate Ami3 (**Figure 2.7**).

At first pass, this seems like an exceptionally complex way to regulate a nonessential enzyme. However, we hypothesize that Ami3 levels fluctuate over the course of the cell cycle, cleaving pre-existing bonds in peptidoglycan to allow for the incorporation of new cell wall material; to cap Ami3 activity before the point of cellular lysis, HtrA-LppZ clears this enzyme from the periplasm to restore homeostasis as the cell progresses towards division (**Figure 5.2**).

While it is not unusual to see proteolysis play a role in the regulation of cell wall enzymes, to have such a function mediate the essentiality of a protease is unusual. Similar systems have been described in *E. coli* and *P. aeruginosa,* regulating cell wall hydrolases. In *E. coli,* the peptidoglycan hydrolase MepS is degraded by a protease-lipoprotein complex consisting of Prc and NlpI, wherein NlpI acts as an adaptor, bringing MepS and the Prc protease together and facilitating degradation (Singh *et al.* 2015).

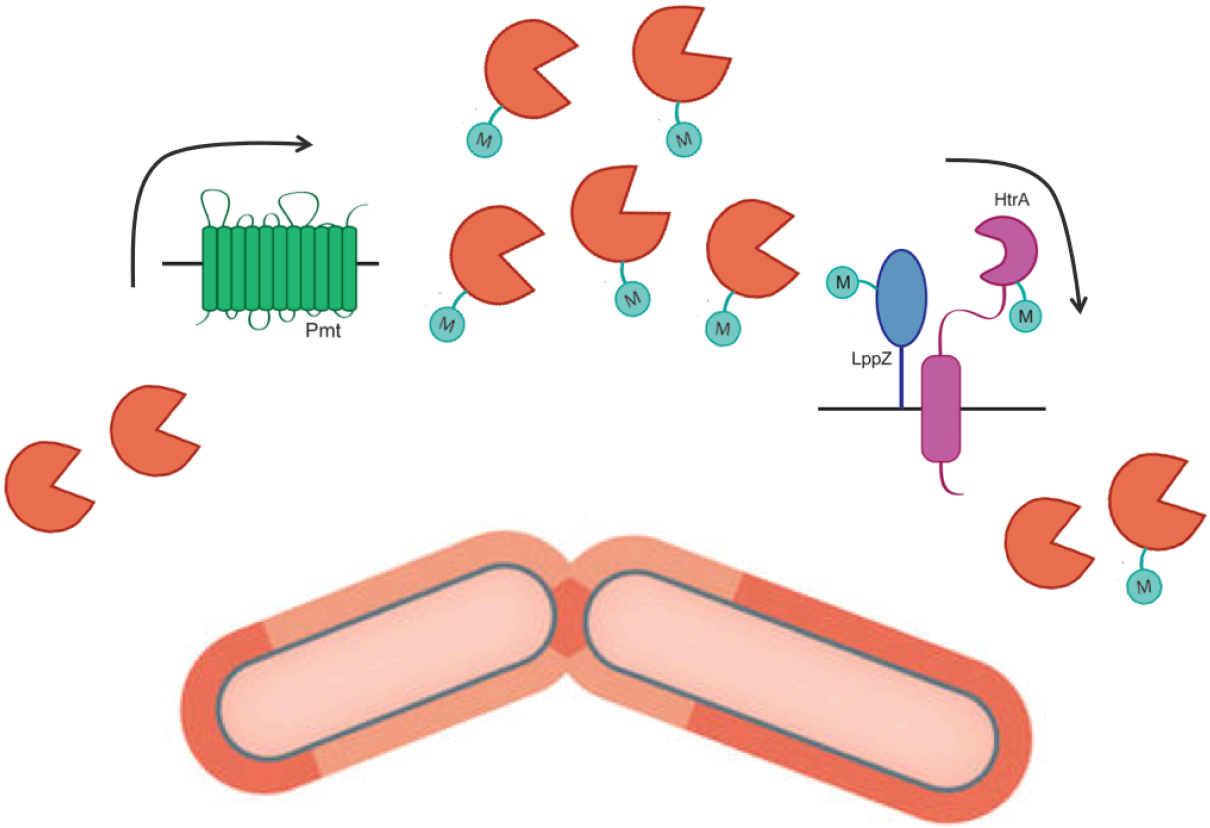

Figure 5.2: A proposed model for the cycle of cell wall construction and destruction fueled by the HtrA-LppZ pathway. As mycobacterial cells grow and divide, pre-existing bonds in the peptidoglycan infrastructure must be broken to make room for new cell wall material. Amidases such as Ami3 are likely to play a prominent role in this cycle of destruction; however, their activity must be under tight spatiotemporal regulation to ensure that they are efficient but not overactive. It is possible that Ami3 is stabilized at certain locales and/or at certain points along the course of the cell cycle by Pmt-mediated mannosylation. Then, to conclude its stint of activity, HtrA-LppZ degrades the stabilized enzyme to clear it from the cell wall as new bonds are built and reinforced. Further testing to show spatiotemporal cycling of Ami3 is needed to confirm this tentative model.

Similarly, in *Pseudomonas aeruginosa,* a fairly analogous system is responsible for the degradation of the peptidoglycan hydrolases MepM, PA1198, PA1199, and PA4404, a feat accomplished by a complex between the protease CtpA and the lipoprotein LbcA (Srivastava *et al.* 2018). In both these previously characterized systems in *E. coli* and *P. aeruginosa,* morphological defects and stress-sensitivity phenotypes brought on by loss of the protease and/or lipoprotein are suppressed by additional loss of the target hydrolase. However, while these serve as encouraging precedents for the newly discovered system in *M. smegmatis,* the latter is distinct due to HtrA's essentiality. Thus, though HtrA's function falls in line with what appears to be a widely conserved mechanism of cell wall homeostasis, the presence of HtrA is entirely crucial for cellular survival. This highlights the importance of cell wall integrity to mycobacterial viability, increasing the appeal of these outer layers as future drug targets.

Additionally, this work expands our knowledge of the mycobacterial periplasm, including the post-translational modifications that affect the stability of cell wall enzymes. To the best of our knowledge, our findings represent the first that demonstrate the contribution of O-mannosylation to cell wall homeostasis, and the first that highlight proteolysis in the regulation of a mycobacterial cell wall enzyme. Previous work has shown that the protease MarP activates the cell wall hydrolase RipA through cleavage (Botella *et al.* 2017); however, HtrA's effect on Ami3 abrogates, rather than stimulates, its cycle of activity. Finally, this work confirms HtrA's appeal as a drug target, due to the combination of its essentiality to cell viability and promising druggability, as established in other bacterial species.

In **Chapter 3**, we present data that adds to the growing body of literature on the mycobacterial divisome. In many ways, mycobacteria share the broad classes of division machinery that appear to govern the cell cycles of most bacteria. However, as pole growers with unusually long division times and unusual, highly fatty cell walls, mycobacteria require unique tools to progress

through cycles of growth and division in the ever-changing extracellular milieu. Thus, we undertook a characterization of the mycobacterial divisome, identifying homologs of FtsL and FtsB, partners of the already-identified FtsQ in *Mycobacterium smegmatis.* In *E. coli,* these proteins cue the initiation of septation, acting as probable scaffolds for binding partners with enzymatic activity (Tsang and Bernhardt 2015). Depletion of any of these essential divisome factors in *Msm* results in long, branched cells that are ultimately unviable, though localization of early septal factors such as FtsZ and FtsK remains intact. Our data shows that each of these factors, as well as FtsK, reach the site of septation after FtsZ (**Figure 3.3, Table 3.1**). FtsB and FtsL also appear to require FtsQ localization to properly localize, though these results await confirmation given that our co-localization data with FtsZ put these factors earlier in the septation cascade (**Figure 3.2**). However, FtsQ localization preceding FtsB and FtsL localization is in keeping with previous work in *E. coli* and thus may represent the most logical order of succession (Buddelmeijer *et al.* 2002; Goehring and Beckwith 2005; Goehring *et al.* 2006; Wadenpohl and Bramkamp 2010).

Through an FtsQ-based pulldown (**Table 3.2**), we also identified a novel septal factor which we named SepIVA. Like many other septal factors, SepIVA is required for cell viability, and depletion of this factor results in long, branched cells (**Figure 3.5**). Additionally, SepIVA localizes to mid-cell late in the cell cycle, eventually relocating to the intracellular membrane domain (IMD), a putative site for organizing enzymes involved in the biosynthesis of cell surface precursors (Hayashi *et al.* 2016). Thus, SepIVA may play multiple roles, the independence of which has yet to be determined. Furthermore, based on homology, SepIVA may play similar scaffolding roles to Wag31, recruiting and/or activating cell wall enzymes without performing these functions itself (Jani *et al.* 2010; Meniche *et al.* 2014; Xu *et al.* 2014).

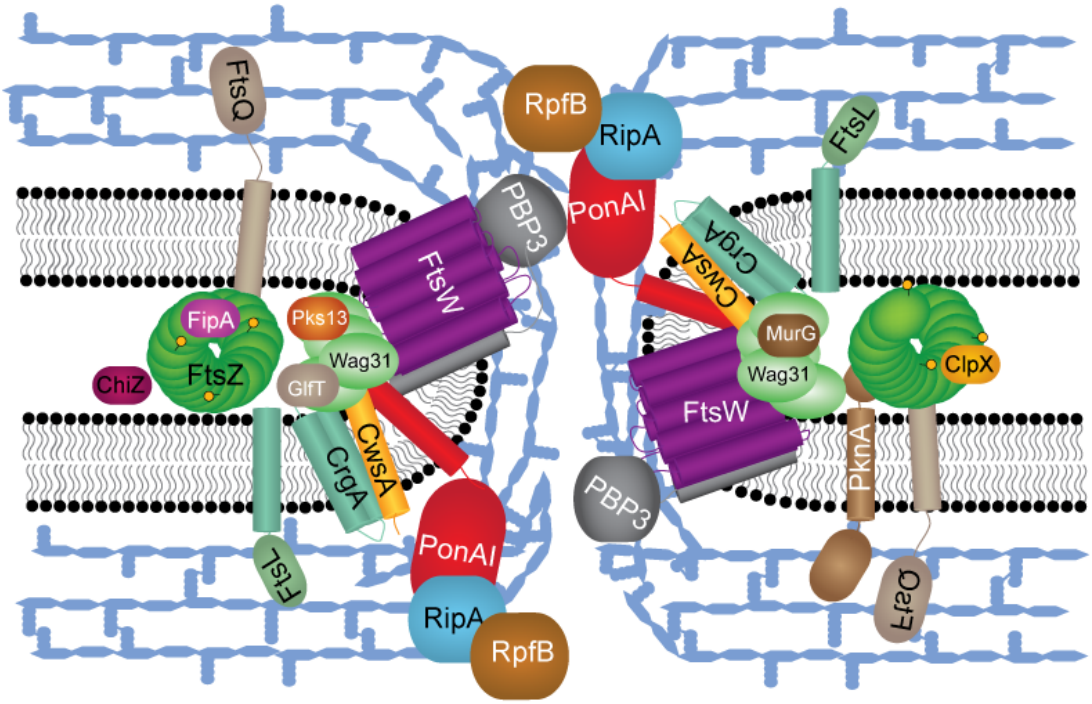

Figure 5.3: A (still incomplete) model of the mycobacterial divisome. Decades of research on the *E. coli* divisome has built a rough foundation for studies of septation in mycobacteria. In *E. coli,* polymerization of FtsZ initiates cell division. FtsEX then acts on FtsA, which becomes monomeric and recruits downstream divisome proteins FtsK, FtsQLB, and FtsWI. The arrival of FtsN triggers the activation of septal PG synthesis. In mycobacteria, the picture is less clear, and blends in themes from other Gram-positive bacteria such *Bacillus subtilis*. Homologs of several known factors have already been identified in mycobacteria, though others, including an FtsN homolog, still elude characterization (*Figure by Cara Boutte, University of Texas, Arlington*).

These findings both place *Msm* within the matrix of well-understood rod-shaped bacteria that divide through common mechanisms, and distinguish *Msm* from laterally growing species (**Figure 5.3**). While many bacterial species bear similar motifs in the various enzymes and scaffolding proteins that contribute to septation, unique features have evolved in each lineage. Additionally, by leveraging the interactions that govern cell division, such as those observed between FtsQ and SepIVA, novel factors can be identified in ways that might otherwise be missed through simple homology-based bioinformatics searches.

In **Chapter 4**, we present preliminary findings on FtsH, showing for the first time that this gene is indeed nonessential in *Mtb* and *Msm,* and that loss of *ftsH* appears to have negligible effects on viability under normal growth conditions. Previous genetic screens have presented conflicting reports on the essentiality of *ftsH;* however, differences between growth conditions, lab-specific strains, and saturation of mutagenesis could account for some of these discrepancies. Prior work characterizing mycobacterial FtsH has reported unsuccessful attempts to generate *ftsH* knockouts in both *Mtb* H37Rv as well as *Msm* SN2; in 2009, Kiran and colleagues utilized an RNA-based knockdown approach to study the effects of FtsH depletion on *Mtb* (Anilkumar *et al.* 2004; Srinivasan *et al.* 2006; Kiran *et al.* 2009). However, in our hands, *ftsH* is dispensable in both *Mtb* and *Msm,* with knockouts exhibiting relatively normal growth kinetics *in vitro.*

While FtsH is essential in certain organisms such as *E. coli,* where this protease has been co-opted to maintain membrane homeostasis, it is nonessential in most bacteria. However, FtsH may still play an important role in the virulence of *Mtb.* Preliminary experiments in *Msm* indicate that FtsH may play a role in mediating the response to certain environmental stressors such as oxidative stress and possibly high temperature (**Figure 4.1**), both of which are purported to mimic the extremes experienced by *Mtb* in the host. Notably, robust growth in the presence of oxidative stress or high temperature appeared dependent on proteolytic activity, as a Δ*ftsH*

mutant complemented with a variant of FtsH unable to bind zinc (FtsH(H425Y)) did not exhibit wild-type growth, while complementation with wild-type FtsH fully restored viability (**Figure 4.1**).

Additionally, the high degree of conservation between mycobacterial FtsH and its homologs in other species indicates that this gene may still be undergoing positive selection in this genus, and is serving a yet-undescribed function that contributes to the wellbeing of the cell. For instance, *Mtb* FtsH has been shown to functionally complement an ∆*ftsH* knockout in *E. coli,* an organism in which *ftsH* is typically indispensable, and is capable of degrading known *E. coli* substrates (Srinivasan *et al.* 2006).

However, due to the significant differences in physiology between *E. coli* and mycobacteria, the most relevant substrates of FtsH in *Mtb* are unlikely to have much overlap with *E. coli,* particularly if FtsH plays significant roles in virulence. It remains possible, however, that broad similarities exist. For instance, in *E. coli,* FtsH has been shown to degrade alternative sigma factors that allow cells to mount defenses in the face of environmental stressors (Langklotz *et al.* 2012, Sauer and Baker 2011). Given that mycobacteria encode at least 13 different sigma factors, only one of which is essential for viability (Manganelli 2014), it is entirely possible that one or more alternative sigma factors is susceptible to FtsH-mediated degradation. Additionally, FtsH may directly modulate the stability of specific virulence factors such as MgtC, a phenomenon that has been observed in *Salmonella* species (Alix *et al.* 2008).

Our initial foray into probing the substrates of FtsH was performed in *Msm* (**Table 4.1**); however, given our preliminary results, we suspect the more tractable line of inquiry will be identifying substrates in *Mtb.* These first experiments may then serve as proof of concept, showing that FtsH can be successfully epitope tagged and immunoprecipitated with potential interactors. Notably, our search did not reveal any of the previously discussed candidates; however, this

could be due to the conditions under which we performed the immunoprecipitation (normal growth conditions, which may preclude the degradation of alternative sigma factors). Importantly, we conducted the immunoprecipitation in a non-pathogenic species that does not encode virulence factors such as MgtC. Future experiments will address these remaining questions. For the time being, our work represents the first evidence that FtsH, though nonessential, remains a promising candidate for future drug targeting, as this protease may play a role in surviving environmental stressors.

Chapter 5, Section 5.2: Future directions

As with any body of scientific work, the more findings surface, the more questions they bring. Though the chapters of this dissertation represent works in various stages of completion, further lines of inquiry stem from each of them.

Beyond the work presented in **Chapter 2**, further characterization of the HtrA(-LppZ) system is warranted. Most pressing is the need for biochemical data to validate the genetic findings presented in this chapter. Although we were unable to successfully purify all the components needed to attempt an *in vitro* reconstruction of HtrA-LppZ-mediated degradation of Pmt-mannosylated Ami3, even a partial recapitulation of this system could be informative in future work. For instance, it appears that Ami3 does not need to be mannosylated to be degraded by HtrA-LppZ (**Figure A1.4E**). Additionally, the role of LppZ in this system requires further clarification. Although LppZ does not appear to be a substrate of HtrA, its role as an adaptor could take many forms, either ensnaring and guiding Ami3 towards HtrA's proteolytic chamber, or altering the conformation or oligomerization of the protease itself. Purification of Ami3 itself would also be useful, as such a sample could be assayed for peptidoglycan-cleaving activity *in vitro,* supporting the idea that overexpression leads to lethality due to loss of cell wall integrity. Zeroing in on the specific bonds that Ami3 targets would be particularly illuminating. Furthermore, it remains to be verified if Ami3's putative activity is dependent on mannosylation, though our current data indicates that this is unlikely to be the case, as Ami3 overexpression in a Δ*pmt* strain still compromises growth and viability (**Figure 2.6**). In any case, as mannosylation appears to contribute to at least stabilization of this enzyme, future work should clarify under what conditions mannosylation occurs, and if there is spatiotemporal regulation of this modification.

In the absence of biochemical data, further localization data would lend support to our current model. While fluorescent-protein-tagged Ami3 appears to localize to logical points of growth and division (i.e., the poles and the septum) (**Figure A1.7**), co-localization with septal proteins, as well as with Pmt, HtrA, and/or LppZ, would substantiate our current findings. Additionally, time-lapse microscopy of these factors would help untangle the points along the cell cycle at which Ami3 accumulates, presumably under the stabilizing influence of Pmt mannosylation, or recedes to homeostatic levels, perhaps due to degradation by HtrA-LppZ.

On a broader scale, new questions have arisen that warrant further investigation. For instance, the role of *mprB* in this system is still unclear. While preliminary data shows that MprB appears to positively affect the transcription of Ami3, the effect is modest (**Figure A1.8**) and these results do not preclude another way for MprB to play a role in this complex network of genes. While the MprB regulon has been characterized, genes that expressed at very low levels such as *ami3* are often missed by RNA-seq-based screens. Notably, because MprB may affect transcription of both *sigE* and *pepD* (He *et al.* 2006; White *et al.* 2010), multiple pathways may be engaged or affected by loss of this gene. Furthermore, because the initial suppressor mutations identified were in-frame SNPs, a strict loss of *mprB* may not be necessary to confer suppression of *htrA* essentiality. These SNPs occur in what appears to be a periplasmic domain of MprB, and may thus affect its ability to sense extracytoplasmic stress, or its phosphorylation status. However, these ideas are purely speculative.

Furthermore, while the essentiality of HtrA can be fully suppressed by loss of this amidase-centric network, this protease may have additional functions that are not essential for cellular viability, but still play important roles in growth and, when it comes to pathogenic mycobacteria, virulence. HtrA is highly conserved within the *Mycobacterium* genus, and retains a great deal of homology with its paralogs in other species. What's more, PepA and PepD, nonessential HtrA

homologs, co-occur with HtrA in the periplasm. Whether these proteases play overlapping roles remains to be seen. With respect to our current findings, it remains unclear why loss of HtrA leads to shorter cells (**Figure 2.2D**), though this effect appears to be independent of modulation of Ami3. A reduction in cell length could indicate either a failure to elongate, premature septation, or both.

Additionally, our initial immunoprecipitation of HtrA yielded LppZ as the most prominent interactor; however, this method may be a viable way to search for additional substrates of HtrA proteolysis or chaperone activity, or other adaptors. These experiments could be repeated under different stress conditions, for instance, as more HtrA appears to be required in environments that increase the strain on the outer layers of the cell. Thus, it is highly likely that HtrA has other substrates that affect the cell cycle or the mycobacterial stress response.

The work presented in **Chapter 3** forms a strong foundation for future studies of the mycobacterial divisome. However, many of the players that work at this interface still remain mysterious. Our work presents a viable strategy for identifying novel septal factors: By capitalizing on their interactions with known proteins, new components of the divisome will continue to be identified. In the meantime, the specific dynamics of the FtsQLB system require further elucidation. For instance, we were unable to show interactions between these proteins in unbiased pulldowns; however, this is perhaps due to the extremely low abundance of these proteins in the cell. Targeted co-immunoprecipitations may resolve this in the future.

Additionally, future work on SepIVA will open many doors in its own right. This novel factor bears a great deal of resemblance to other DivIVA homologs, particularly mycobacterial Wag31; based on homology, we hypothesize that it is a scaffold with negligible enzymatic activity, instead initiating dialogs between factors that eventually come together to execute proper

septation in growing cells. Its essentiality indicates that, like Wag31, these roles in coordination are integral to the proper execution of septation.

Importantly, many of these experiments warrant repeating in *Mtb.* Given the high degree of homology between these two species, and the importance of proper cell division to both species, our findings are likely to translate from *Msm* to its pathogenic relatives. However, additional results may arise from studies in *Mtb,* due in part to the speculated importance of alterations in the regulation of cell division for *Mtb* latency and survival of stress. For instance, *Mtb* cells in stationary phase or undergoing carbon-nitrogen starvation exhibit vastly reduced cell length (Cara Boutte, unpublished data).

The vast majority of future work on SepIVA and FtsQLB in mycobacteria will be conducted in the newly established lab of Dr. Cara Boutte, who is senior author on the manuscript featured in Chapter 3, at the University of Texas, Arlington.

The findings presented in **Chapter 4** are preliminary; as such, future work in the Rubin Lab will continue to unveil the functions of FtsH in mycobacteria. However, now that mutants have been generated in *Msm* and *Mtb,* several experiments can easily be conducted with these tools. Most pressingly, the stress experiments conducted in *Msm* should be repeated in *Mtb,* testing the Δ*ftsH* strain's susceptibility to various *in vitro* environmental stressors. Additionally, to test previous Tn-seq-based predictions about *ftsH* essentiality for virulence, the viability of the *Mtb* knockout strain should be assessed in macrophages and in mice, and/or be subjected to a competitive index with a wild-type or complemented strain. The results of these experiments will guide fruther research. Currently, we predict that *ftsH* will indeed be essential for virulence, likely due to a role in the regulation of the mycobacterial stress response—perhaps by degradation of an alternative sigma factor.

Additionally, although our preliminary immunoprecipitations of the protease strap FtsH(H425Y) in *Msm* have not yet yielded particularly obvious candidates, these experiments warrant repeating under conditions of stress. As FtsH may be involved in the stress response, its most pertinent and important substrates may not be isolated under normal growth conditions. However, careful experimental design will be required to grow a sufficient number of cells to an appropriate OD to perform a successful immunoprecipitation.

Furthermore, simple repition of the immunoprecipitation in *Mtb* may yield entirely different results; for instance, if MgtC is indeed a substrate, it will only appear in an *Mtb*-based experiment, as this gene has no homolog in the nonpathogenic *Msm.* Additionally, knowledge of substrates in other species could inform directed co-immunopreciptations in both *Mtb* and *Msm;* particularly appealing would be the identification of an interaction with SigH, FtsZ, or, as already discussed, MgtC. However, a novel substrate is perhaps even likelier, given the specific growth requirements of mycobacteria: As a highly-conserved, membrane bound protease, FtsH is uniquely positioned to interact with a wide variety of proteins, and is poised to exert influence on several pathways ranging from cell division to the conveyance of extracellular messages into the cytoplasm.

Notably, it remains possible that the three projects discussed in this dissertation may be connected in some way. There is not yet evidence for such genetic or biochemical interactions, but given the convergence of these three topics on cell division and stress responses, overlaps may be worth considering. For instance, given that Ami3 is so unstable, it is very possible that it is susceptible to degradation by multiple proteases. The active sites of HtrA and FtsH exist in separate cellular compartments, but because Ami3 likely undergoes translation at or near the inner membrane, it likely encounters a locale over which FtsH has influence. Furthermore, given

that *htrA* depletion strains so closely resemble previously characterized mutants in cell wall homeostasis, HtrA may engage cell wall factors beyond Ami3, including components of the divisome. Such interactions may even explain the nonessential role HtrA plays in governing cell length and/or septation (**Figure 2.2D**).

Interestingly, overexpression of catalytically inactive variants of Ami3 exhibit branching and increased length (**Figure 2.3**)—a phenotype that recognizably resembles depletions of divisome factors such as FtsZ, FtsI, and FtsQLB (**Figure 3.1, 3.3**). Of course, many genetic manipulations can result in the same morphological defect; however, the similarities between these strains may inform future investigations of Ami3. Depletions of divisome factors prevent cells from properly dividing, resulting in elongation and branching. Overexpression of wild-type Ami3 results in polar bulges, presumably due to loss of cell wall integrity; however, overexpression of catalytically inactive variants of Ami3 mimic the compromised divisome phenotype. This may indicate that Ami3 plays an important role in resolving the septum, as has been described for other N-acetylmuramoyl-L-alanine amidases in both *E. coli* and mycobacteria (van Heijenoort, 2011; Senzani *et al.* 2017), perhaps through an interaction with another septal factor that is reliant on Ami3 catalytic activity. For instance, if Ami3 binds and sequesters another enzyme, but is unable to execute its own enzymatic activity, it could lock the cell into a compromised state that precludes proper division. This dominant negative effect is only observed upon overexpression, however, and not at physiological levels; however, this may be reconciled with the idea that Ami3 itself is nonessential, and has homologs that include Ami1 and Ami4. Alternatively, catalytically inactive Ami3 could be directly binding peptidoglycan and, without completing hydrolysis, blocking other enzymes from acting upon substrates that would otherwise be liberated by Ami3 activity. Future work is required to distinguish between these possibilities.

Finally, the regulatory role of bacterial lipoproteins has gained increasing attention in the past several years. While best studied in Gram-negative bacteria such as *E. coli,* lipoproteins are found across diverse species, playing roles in transducing environmental stress signals to the cytoplasm, drug efflux, the maintenance of cell wall and outer membrane integrity, and, oftentimes, virulence (Okuda and Tokuda 2011; Nguyen and Götz 2016; Laloux and Collet 2017). In fact, lipoprotein processing has been implicated in the pathogenicity of *Mtb* (Sander *et al.* 2004). As these diverse proteins exist at the interface between bacterial cells and their environment, they are both structures and sentinels that guard their hosts against onslaughts from drugs and extreme conditions, often through interactions with other proteins. For instance, with regard to the cell wall, lipoproteins such as LpoA and LpoB have been shown to activate PBPs in *E. coli*, acting as essential cofactors in the polymerization of peptidoglycan (Paradis-Bleau *et al.* 2010). Additionally, the *E. coli* lipoproteins RcsF and NlpE transduce envelope stress signals between the outer envelope and the cytoplasm, activating the Rcs and Cpx systems, respectively (Laloux and Collet 2017). Due to the complexity and intricacy of the outer layers of the mycobacterial cell, the possibilities are endless; indeed, mycobacteria encode about 100 lipoproteins, with this family of genes comprising at least 2.5% of the mycobacterial proteome (Sutcliffe and Harrington 2004).

Past findings in *E. coli* and *P. aeruginosa* have already set precedence for lipoprotein adaptors of proteases (Singh *et al.* 2015; Srivastava *et al.* 2018). Intriguingly, lipoproteins appeared in the unbiased immunoprecipitations of both FtsQ (**Table 3.2**) and FtsH (**Table 4.1**), leaving open the possibility that such adaptors may play roles in these networks as well. While much of the work in mycobacterial lipoproteins has focused on their roles in virulence and immunogenicity (Becker and Sander 2016), future work will certainly expand perspectives on the importance of these proteins to cell structure, growth, and protein homeostasis.

Chapter 5, Section 5.3: References

1. Alhuwaider AAH and Dougan DA. AAA+ Machines of Protein Destruction in Mycobacteria. Front Mol Biosci 4:49 (2017). doi: 10.3389/fmolb.2017.00049.

2. Alix E and Blanc-Potard AB. Peptide-assisted degradation of the Salmonella MgtC virulence factor. EMBO J 27: 546-557 (2008). doi: 10.1038/sj.emboj.7601983.

3. Becker K and Sander P. (2016). Mycobacterium tuberculosis lipoproteins in virulence and immunity - fighting with a double-edged sword. FEBS Lett 590(21):3800-3819. doi: 10.1002/1873-3468.12273.

4. Botella H, Vaubourgeix J, Lee MH, Song N, Xu W, Makinoshima H, Glickman MS, Ehrt S. (2017). Mycobacterium tuberculosis protease MarP activates a peptidoglycan hydrolase during acid stress. EMBO J 36(4):536-48, doi:10.15252/embj.201695028.

5. Buddelmeijer N, Judson N, Boyd D, Mekalanos JJ, Beckwith J. (2002). YgbQ, a cell division protein in Escherichia coli and Vibrio cholerae, localizes in codependent fashion with FtsL to the division site. Proceedings of the National Academy of Sciences 99:6316-6321.

6. Centers for Disease Control and Prevention. Tuberculosis: Data and Statistics (2018).

7. Goehring NW and Beckwith J. (2005). Diverse Paths to Midcell: Assembly of the Bacterial Cell Division Machinery. Current Biology 15:R514-R526.

8. Goehring NW, Gonzalez MD, Beckwith J. (2006). Premature targeting of cell division proteins to midcell reveals hierarchies of protein interactions involved in divisome assembly. Mol Microbiol 61:33-45.

9. Hayashi JM, Luo C-Y, Mayfield JA, Hsu T, Fukuda T, Walfield AL, Giffen SR, Leszyk JD, Baer CE, Bennion OT, Madduri A, Shaffer SA, Aldridge BB, Sassetti CM, Sandler SJ, Kinoshita T, Moody DB, Morita YS. (2016). Spatially distinct and metabolically active membrane domain in mycobacteria. Proceedings of the National Academy of Sciences 113:5400-5405.

10. He H, Hovey R, Kane J, Singh V, and Zahrt TC. (2006). MprAB is a stress-responsive two-component system that directly regulates expression of sigma factors SigB and SigE in *Mycobacterium tuberculosis*. *J Bacteriol* 188(6): 2134-2143.

11. van Heijenoort J. (2011). Peptidoglycan hydrolases of Escherichia coli. Microbiol Mol Biol Rev 2011 Dec;75(4):636-63. doi: 10.1128/MMBR.00022-11.

12. Jani C, Eoh H, Lee JJ, Hamasha K, Sahana MB, Han J-S, Nyayapathy S, Lee J-Y, Suh J-W, Lee SH, Rehse SJ, Crick DC, Kang C-M. (2010). Regulation of Polar Peptidoglycan Biosynthesis by Wag31 Phosphorylation in Mycobacteria. BMC Microbiology 10:327.

13. Laloux G and Collet JF. (2017). Major Tom to Ground Control: How Lipoproteins Communicate Extracytoplasmic Stress to the Decision Center of the Cell. J Bacteriol 199(21). pii: e00216-17. doi: 10.1128/JB.00216-17.

14. Langklotz S et al. Structure and function of the bacterial AAA protease FtsH. Biochim Biophys Acta 1823: 40-48 (2012).

15. Liu CF, Tonini L, Malaga W, Beau M, Stella A, Bouyssié D, Jackson MC, Nigou J, Puzo G, Guilhot C et al. (2013). Bacterial protein-O-mannosylating enzyme is crucial for virulence of Mycobacterium tuberculosis. PNAS 110(16):6560-5, doi:10.1073/pnas.1219704110.

16. Manganelli R. Sigma Factors: Key Molecules in Mycobacterium tuberculosis Physiology and Virulence. (2014). Microbiol Spectr 2(1):MGM2-0007-2013. doi: 10.1128/microbiolspec.MGM2-0007-2013.

17. Meniche X, Otten R, Siegrist MS, Baer CE, Murphy KC, Bertozzi CR, Sassetti CM. (2014). Subpolar addition of new cell wall is directed by DivIVA in mycobacteria. Proc Natl Acad Sci USA 111:E3243-51.

18. Nguyen MT and Götz F. (2016). Lipoproteins of Gram-Positive Bacteria: Key Players in the Immune Response and Virulence. Microbiol Mol Biol Rev 80(3):891-903. doi: 10.1128/MMBR.00028-16.

19. Okuda S and Tokuda H. (2011). Lipoprotein sorting in bacteria. Annu Rev Microbiol 65:239-59. doi: 10.1146/annurev-micro-090110-102859.

20. Paradis-Bleau C, Markovski M, Uehara T, Lupoli TJ, Walker S, Kahne DE, Bernhardt TG. (2010). Lipoprotein cofactors located in the outer membrane activate bacterial cell wall polymerases. Cell 143(7):1110-20, doi:10.1016/j.cell.2010.11.037.

21. Raju RM, Goldberg AL, and Rubin EJ. (2012). Bacterial proteolytic complexes as therapeutic targets. Nat Rev Drug Discov 11:777-89, doi:10.1038/nrd3846.

22. Raju RM, Jedrychowski MP, Wei JR, Pinkham JT, Park AS, O'Brien K, Rehren G, Schnappinger D, Gygi SP, and Rubin EJ. (2014). Post-Translation Regulation via Clp Protease Is Critical for Survival of Mycobacterium tuberculosis. PLoS Pathog 10(3):e1003994, doi:10.1371/journal.ppat.1003994.

23. Raju RM, Unnikrishnan M, Rubin DH, Krishnamoorthy V, Kandror O, Akopian TN, Goldberg AL, and Rubin EJ. (2012). Mycobacterium tuberculosis ClpP1 and ClpP2 Function Together in Protein Degradation and Are Required for Viability in vitro and During Infection. PLoS Pathog 8(2):e1002511, doi:10.1371/journal.ppat.1002511.

24. Samanovic MI and Darwin KH. Game of 'Somes: Protein Destruction for Mycobacterium tuberculosis Pathogenesis. Trends Microbiol 24(1):26-34 (2016). doi: 10.1016/j.tim.2015.10.001.

25. Sander P, Rezwan M, Walker B, Rampini SK, Kroppenstedt RM, Ehlers S, Keller C, Keeble JR, Hagemeier M, Colston MJ, Springer B, and Böttger EC. (2004). Lipoprotein processing is required for virulence of Mycobacterium tuberculosis. Mol Microbiol 52(6):1543-52.

26. Sauer RT and Baker TA. AAA+ Proteases: ATP-Fueled Machines of Protein Destruction. Annu Rev Biochem 80: 587-612 (2011).

27. Senzani S, Li D, Bhaskar A, Ealand C, Chang J, Rimal B, Liu C, Joon Kim S, Dhar N, and Kana B. (2017). An Amidase_3 domain-containing N-acetylmuramyl-L-alanine amidase is required for mycobacterial cell division. Sci Rep 7(1):1140, doi:10.1038/s41598-017-01184-7.

28. Singh SK, Parveen S, SaiSree L, and Reddy M. (2015). Regulated proteolysis of a cross-link-specific peptidoglycan hydrolase contributes to bacterial morphogenesis. PNAS 112(35):10956-61, doi:10.1073/pnas.1507760112.

29. Srivastava D, Seo J, Rimal B, Kim SJ, Zhen S, and Darwin AJ. A Proteolytic Complex Targets Multiple Cell Wall Hydrolases in Pseudomonas aeruginosa. MBio 9(4). pii: e00972-18 (2018). doi: 10.1128/mBio.00972-18.

30. Sutcliffe IC and Harrington DJ. (2004). Lipoproteins of Mycobacterium tuberculosis: an abundant and functionally diverse class of cell envelope components. FEMS Microbiol Rev 28(5):645-59.

31. Tsang M-J and Bernhardt TG. (2015). A role for the FtsQLB complex in cytokinetic ring activation revealed by an ftsLallele that accelerates division. Mol Microbiol 95:925-944.

32. VanderVen BC, Harder JD, Crick DC, and Belisle JT. (2005). Export-mediated assembly of mycobacterial glycoproteins parallels eukaryotic pathways. Science 309(5736):941-3.

33. Wadenpohl I and Bramkamp M. (2010). DivIC Stabilizes FtsL against RasP Cleavage. J Bacteriol 192:5260-5263.

34. White, MJ et al. PepD Participates in the Mycobacterial Stress Response Mediated through MprAB and SigE. J Bacteriol 192(6): 1498-1510 (2010).

35. World Health Organization. Fact Sheets: Tuberculosis (2018).

36. World Health Organization. Multidrug-resistant Tuberculosis (MDR-TB) (2017).

37. Xu W-X, Zhang L, Mai J-T, Peng R-C, Yang E-Z, Peng C, Wang H-H. (2014). The Wag31 protein interacts with AccA3 and coordinates cell wall lipid permeability and lipophilic drug resistance in Mycobacterium smegmatis. Biochemical and Biophysical Research Communications 448:255-260.

Appendices

Appendix 1: Supplementary Material for Chapter 2

Supplemental Methods for Chapter 2

Calcein staining and flow cytometry: Mid-log-phase cultures were stained with 0.5 µg/mL calcein for 1 hour at 37°C. These cells were then analyzed by flow cytometry (MACSQuant VYB excitation: 488 nm; emission filter: 525/50).

Total cell length, bulge length, maximum cell width, and mean fluorescence intensity (MFI) were measured manually where indicated.

A.

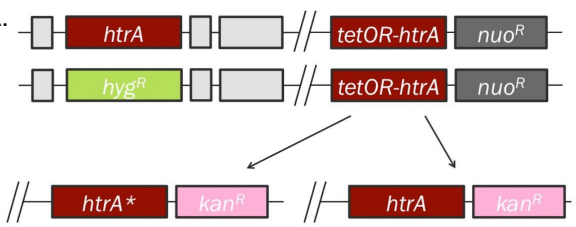

	Swap	Double integrantion
gfp	0	100
*htrA*Δcyto	8	92
*htrA*ΔPDZ	5	95
*htrA*ΔcytoΔPDZ	6	94

B.

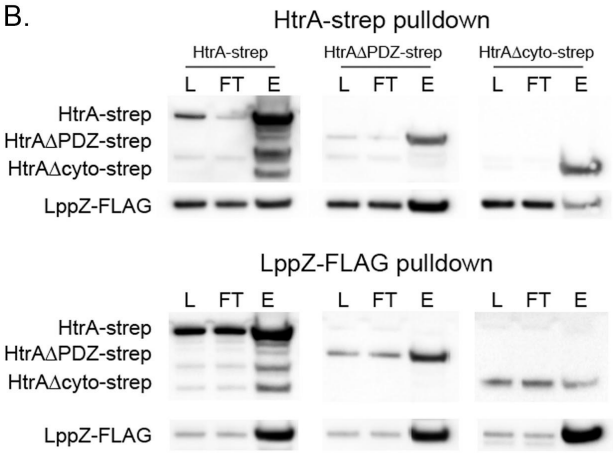

C.

Strain	L5 integration allele	Genomic polymorphism
KW236	HtrAΔcyto	*ami3*: +g in AA154
KW294	HtrAΔcyto	*pmt*: +c in AA27
KW296	HtrAΔcyto	*ami3*: +g in AA93
KW527	HtrAΔPDZ	*mprB*: L81C+I82S
KW529	HtrAΔcytoΔPDZ	*mprB*: L81C+I82S, *ami3*: -c in AA192
KW531	HtrAΔcytoΔPDZ	*pmt*: +c in AA27
KW1S	HtrAΔcytoΔPDZ	*ami3*: +c in AA192
KW2S	HtrAΔPDZ	*ami3*: +cg in AA114
KW3S	HtrAΔPDZ	*ami3*: -c in AA192

D.

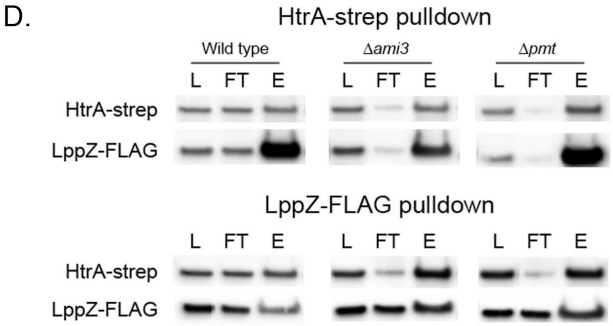

Figure A1.1, related to Figure 2.2: HtrA suppressor screen and HtrA-LppZ interactions. A. The cytoplasmic and PDZ domains of HtrA are essential for viability. Top: a schematic of the L5 essentiality swap. Placing a second copy of *htrA,* along with a nourseothricin resistance cassette, at the L5 phage integration site allows replacement of endogenous *htrA* with a hygromycin resistance cassette. The L5-integrated copy of *htrA* can be swapped for another copy of *htrA* attached to another antibiotic resistance marker, but not for truncations of *htrA* missing the cytoplasmic and/or PDZ domains (*htrA**). Bottom: quantification of *htrA* swaps. A total of 100 transformants were tested for antibiotic resistance. **B. HtrA and LppZ still interact even when the PDZ or cytoplasmic domains of HtrA are removed.** Different alleles of HtrA-Strep and LppZ-FLAG were individually immunoprecipitated using anti-Strep and anti-FLAG magnetic beads, respectively, and the following fractions were analyzed by Western blot: L = lysate, FT = flow through, E = elution. **C. Successful HtrA truncation swaps were whole genome sequenced for extragenic suppressors.** All strains sequenced carried mutations in *ami3, pmt*, and/or *mprB.* **D. HtrA and LppZ interact even in the absence of Ami3 or Pmt.** In the indicated genetic backgrounds, HtrA-Strep and LppZ-FLAG were individually immunoprecipitated using anti-Strep and anti-FLAG magnetic beads, respectively, and the following fractions were analyzed by Western blot: L = lysate, FT = flow through, E = elution.

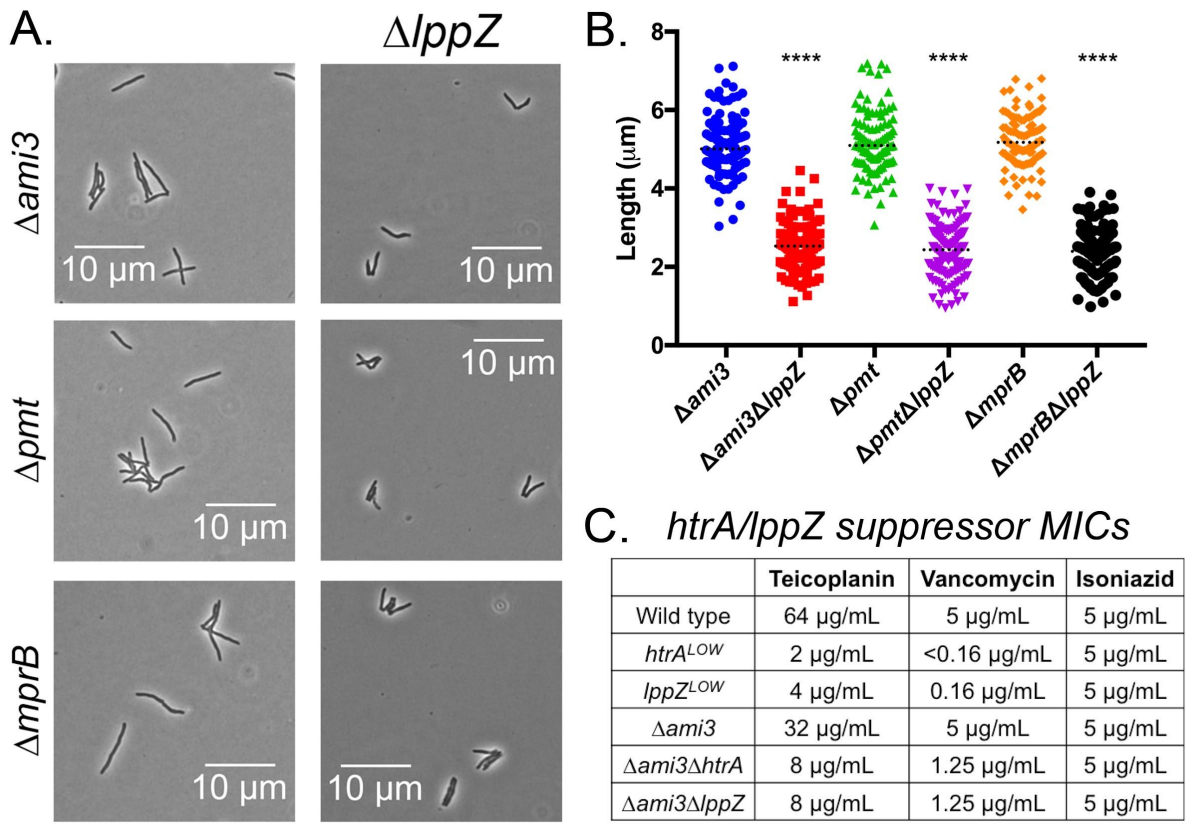

C. *htrA/lppZ suppressor MICs*

	Teicoplanin	Vancomycin	Isoniazid
Wild type	64 μg/mL	5 μg/mL	5 μg/mL
htrA^{LOW}	2 μg/mL	<0.16 μg/mL	5 μg/mL
lppZ^{LOW}	4 μg/mL	0.16 μg/mL	5 μg/mL
Δ*ami3*	32 μg/mL	5 μg/mL	5 μg/mL
Δ*ami3*Δ*htrA*	8 μg/mL	1.25 μg/mL	5 μg/mL
Δ*ami3*Δ*lppZ*	8 μg/mL	1.25 μg/mL	5 μg/mL

Figure A1.2, related to Figure 2.2: Suppressors of *htrA* essentiality also suppress *lppZ* essentiality and produce morphologically similar cells. A and B. Morphology of *lppZ* suppressor strains. Single suppressor knockouts and *lppZ* double knockouts were grown to log phase and analyzed for total cell length. At least 100 cells were quantified in each condition. Dotted black lines indicate median values. **** = p-value <0.0001. **C. Loss of *htrA* or *lppZ* in a suppressor background partially rescues antibiotic susceptibility.** The indicated strains were grown in teicoplanin, vancomycin, and isoniazid.

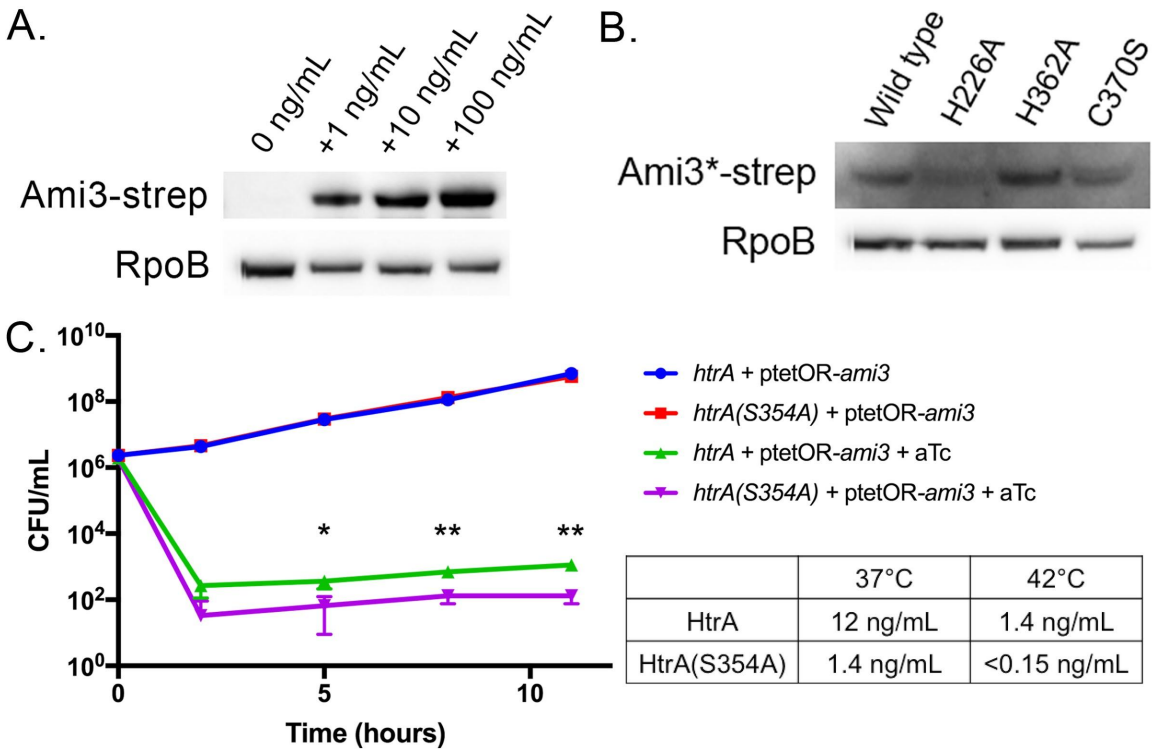

	37°C	42°C
HtrA	12 ng/mL	1.4 ng/mL
HtrA(S354A)	1.4 ng/mL	<0.15 ng/mL

Figure A1.3, related to Figure 2.3 and Figure 2.4: Variable toxicity of Ami3. A. Different amounts of aTc induce different amounts of Ami3. A strain carrying an aTc-inducible copy of *ami3* was grown in the indicated concentrations of aTc for two hours. Cell lysate was analyzed by Western blotting using anti-Strep and anti-RpoB as a loading control. **B. Catalytic mutants of Ami3 accumulate to varying degrees.** Whole cell lysate of the indicated strains was analyzed by Western blotting using anti-Strep and anti-RpoB as a loading control. Ami3* indicates the respective Ami3 allele. **C. Killing dynamics of Ami3 overexpression in different HtrA genetic backgrounds.** Left: Strains expressing either wild-type *htrA* or *htrA(S354A)* and *ami3* under an aTc-inducible episomal construct were grown in the presence or absence of 100 ng/mL aTc. Aliquots were taken at the indicated time points for CFU analysis. *p<0.05, **p<0.01. Error bars represent standard deviation of the mean. Right: the aTc MIC of strains expressing either wild-type *htrA* or *htrA(S354A)* and *ami3* under an aTc-inducible episomal construct was measured at two different temperatures.

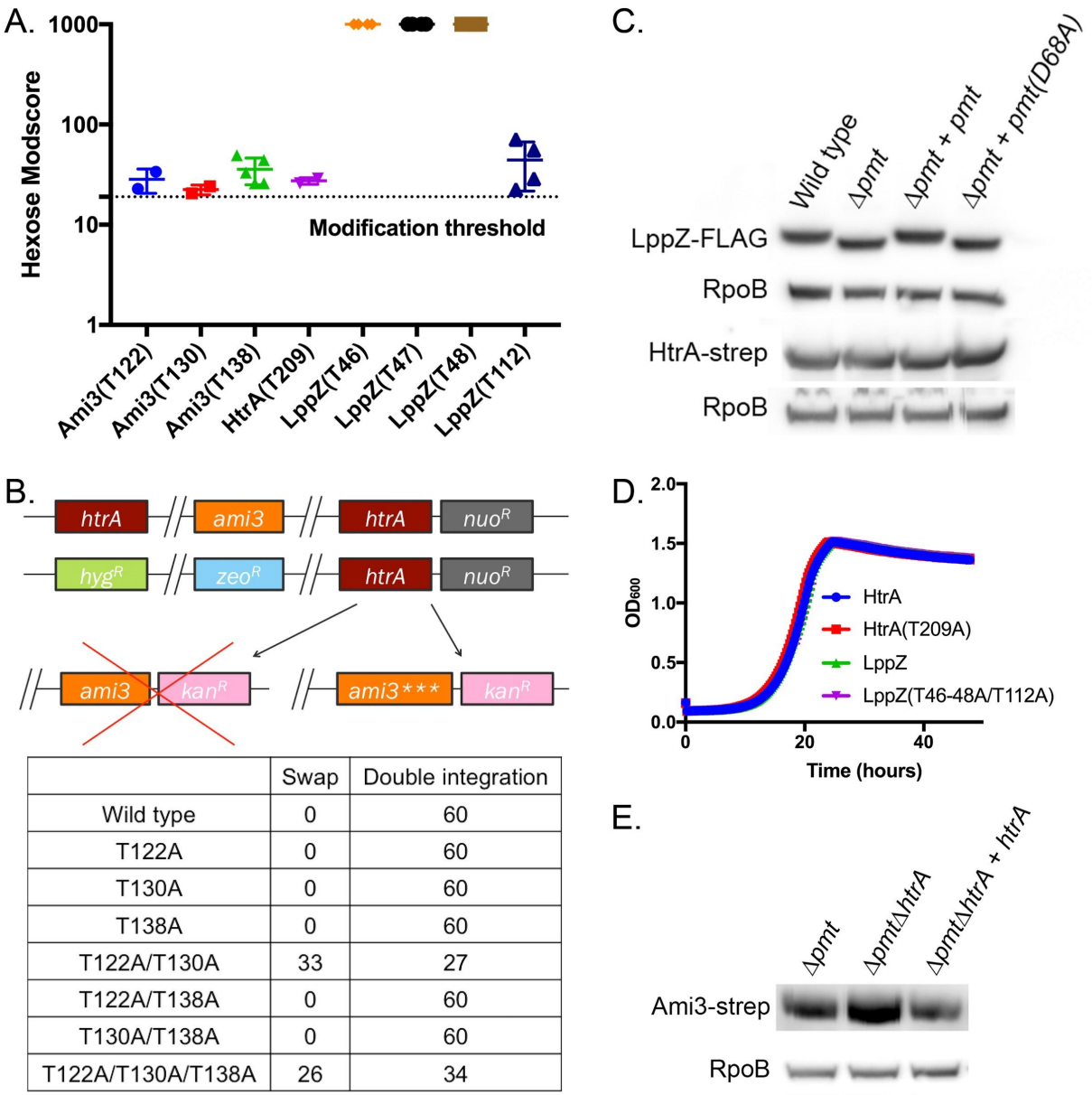

	Swap	Double integration
Wild type	0	60
T122A	0	60
T130A	0	60
T138A	0	60
T122A/T130A	33	27
T122A/T138A	0	60
T130A/T138A	0	60
T122A/T130A/T138A	26	34

Figure A1.4, related to Figure 2.5: Ami3, HtrA, and LppZ are mannosylated. A. Hexose modification scores for Ami3, HtrA, and LppZ. Ami3-Strep, HtrA-Strep, and LppZ-FLAG were immunoprecipitated and analyzed by mass spectrometry for hexose modifications. Scores over 19 are considered confident assignments. Scores of 1000 are unequivocable. Error bars represent standard deviation of the mean. **B. Toxicity of Ami3 mannosylation mutants.** Top: the endogenous copies of *ami3* and *htrA* were replaced with zeocin and hygromycin resistance cassettes, respectively, and a copy of *htrA* was integrated at the L5 site. *ami3* or mannosylation mutant alleles of *ami3* (*ami3****) were transformed into this background. Full swaps that acquire kanamycin resistance at the expense of noursethricin resistance render strains devoid of *htrA* and must thus carry a suppressor mutation. Bottom: quantification of *ami3* and *ami3**** swaps. A total of 60 transformants were tested for antibiotic resistance. **C. LppZ, but not HtrA, mannosylation affects molecular weight.** Cell lysate from the indicated strains was run on an

Figure A1.4 (Continued): SDS-PAGE gel and blotted for HtrA-Strep, LppZ-FLAG, and RpoB. **D. LppZ and HtrA mannosylation are not required for their essential function.** Strains expressing only HtrA(T209A) and LppZ(T46A/T47A/T48A/T112A), variants of HtrA and LppZ, respectively, that lack all mannosylation sites, were grown at 37°C in rich media. Error bars represent standard deviation of the mean. **E. Ami3 stability is still dependent on HtrA in the absence of Pmt.** Whole cell lysate of the indicated strains was analyzed by Western blotting using anti-Strep and anti-RpoB as a loading control.

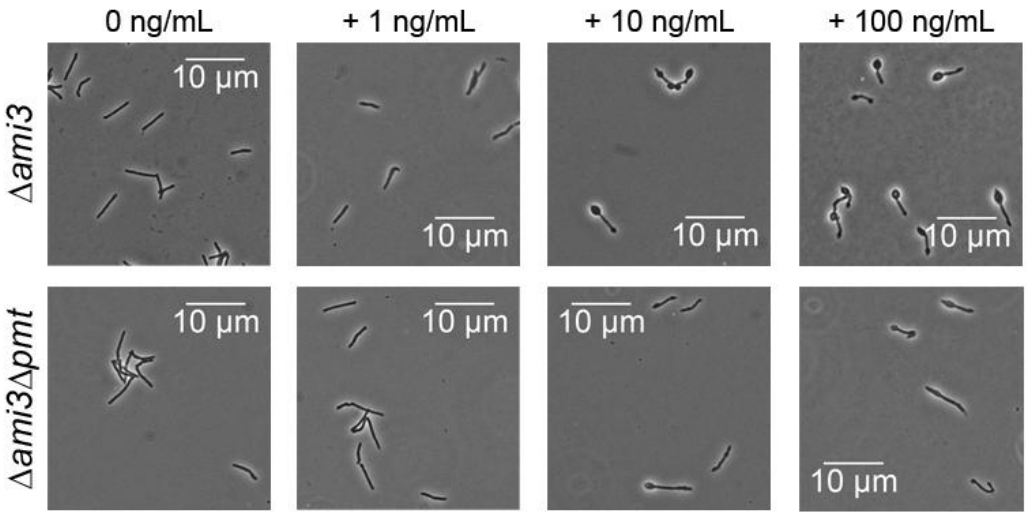

Figure A1.5, related to Figure 2.6: Loss of *pmt* relieves morphological defects in Ami3 overexpressions in a dose-dependent manner. Strains expressing *ami3* in a wild-type or Δ*pmt* background under an aTc-inducible promoter were grown in the indicated concentrations of aTc.

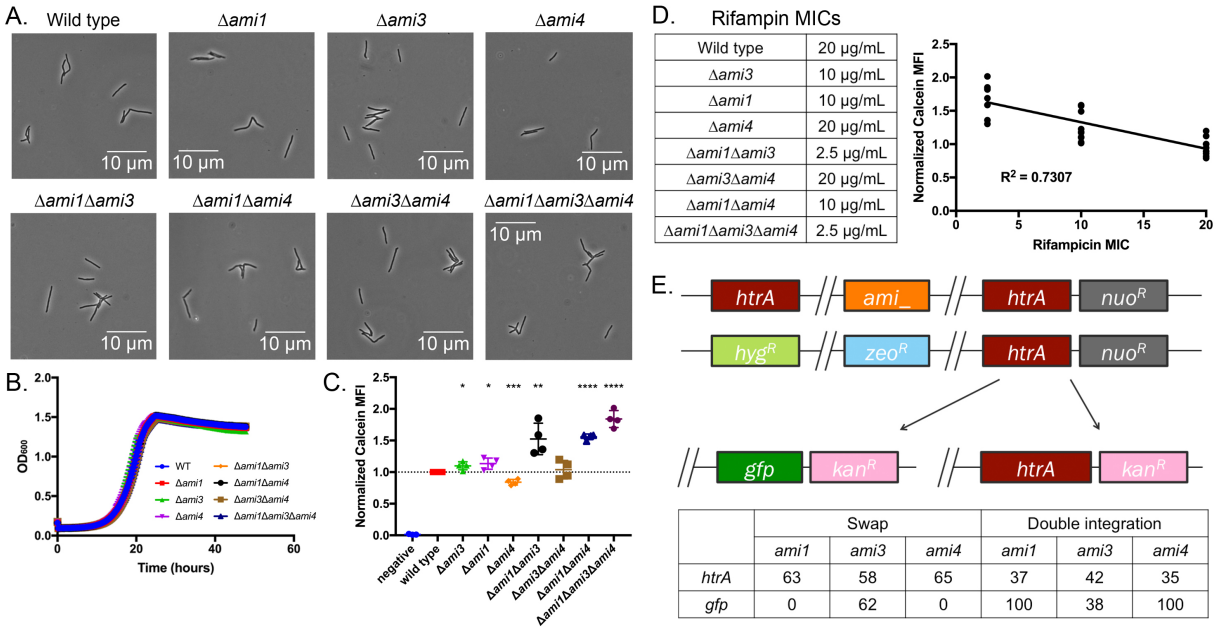

	Swap			Double integration		
	ami1	*ami3*	*ami4*	*ami1*	*ami3*	*ami4*
htrA	63	58	65	37	42	35
gfp	0	62	0	100	38	100

Figure A1.6, related to Figure 2.2: Ami1, Ami3, and Ami4 contribute to cell wall impermeability. A and B. Single and combinatorial knockouts of *ami1, ami3,* and *ami4* grow normally. The indicated strains were grown to log phase and observed by microscopy, or grown at 37°C. Error bars represent standard deviation of the mean. **C and D. Combinatorial amidase knockouts exhibit increased permeability to calcein and rifampin.** The indicated strains were grown in the presence of calcein or rifampin; calcein permeability and rifampin MIC are negatively correlated. Calcein mean fluorescence intensity (MFI) was measured by flow cytometry and normalized to wild type. *p<0.05, **p<0.01, ***p<0.001, ****p<0.0001. Error bars represent standard deviation of the mean. **E. Knocking out *ami3,* but not *ami1* or *ami4*, suppresses *htrA* essentiality.** Top: the endogenous copies of the indicated amidase allele and *htrA* were replaced with zeocin and hygromycin resistance cassettes, respectively, and a copy of *htrA* was integrated at the L5 site. *htrA* or *gfp* were transformed into this background. Full swaps that acquire kanamycin resistance at the expense of noursethricin resistance render strains devoid of *htrA* and must thus carry a suppressor mutation. Bottom: quantification of amidase suppressor swaps. A total of 100 transformants were tested for antibiotic resistance.

Table A1.1 Strains used in Chapter 2

Strain List		
Strain #	**Strain Name**	**Genotype**
	Wild type	mc2 155
KW109	$HtrA^{LOW}$	mc2 155 Δ*htrA*::hygR L5::pKW97 tetOFF4-*htrA*-strep
KW111	$HtrA^{HIGH}$	mc2 155 Δ*htrA*::hygR L5::pKW98 tetOFF5-*htrA*-strep
KW236	HtrAΔcyto-strep (suppressor)	mc2 155 Δ*htrA*::hygR L5::pKW214 *htrA*Δcyto-strep *ami3*: +g in AA154
KW294	HtrAΔcyto-strep (suppressor)	mc2 155 Δ*htrA*::hygR L5::pKW214 *htrA*Δcyto-strep *pmt*: +c in AA27
KW296	HtrAΔcyto-strep (suppressor)	mc2 155 Δ*htrA*::hygR L5::pKW214 *htrA*Δcyto-strep *ami3*: +g in AA93
KW298	HtrA-strep	mc2 155 Δ*htrA*::hygR L5::pKW278 *htrA*-strep
KW527	HtrAΔPDZ-strep (suppressor)	mc2 155 Δ*htrA*::hygR L5::pKW243 *htrA*ΔPDZ-strep *ami3*: +g in AA154
KW529	HtrAΔcytoΔPDZ-strep (suppressor)	mc2 155 Δ*htrA*::hygR L5::pKW518 *htrA*ΔcytoΔPDZ-strep *mprB*: L81C+I82S *ami3*: -c in AA192
KW531	HtrAΔcytoΔPDZ-strep (suppressor)	mc2 155 Δ*htrA*::hygR L5::pKW518 *htrA*ΔcytoΔPDZ-strep *pmt*: +c in AA27
KW694	Δ*ami3*	mc2 155 Δ*ami3*::zeoR
KW735	Ami3-strep	mc2 155 Δ*ami3* L5::pKW1156 *ami3*-strep
KW746	Δ*ami3*Δ*htrA*	mc2 155 Δ*ami3*::zeoR Δ*htrA*::hygR
KW778	Δ*ami3*Δ*htrA*+*htrA*	mc2 155 Δ*ami3*::zeoR Δ*htrA*::hygR L5::pKW278 *htrA*-strep
KW801	Δ*pmt*	mc2 155 Δ*pmt*::zeoR
KW843	Δ*pmt*Δ*htrA*	mc2 155 Δ*pmt*::zeoR Δ*htrA*::hygR
KW846	Δ*mprB*	mc2 155 Δ*mprB*::zeoR
KW873	Δ*pmt*Δ*htrA*+*htrA*	mc2 155 Δ*pmt*::zeoR Δ*htrA*::hygR L5::pKW278 *htrA*-strep
KW905	Δ*mprB*Δ*htrA*	mc2 155 Δ*mprB*::zeoR Δ*htrA*::hygR
KW918	Δ*mprB*Δ*htrA*+*htrA*	mc2 155 Δ*mprB*::zeoR Δ*htrA*::hygR L5::pKW278 *htrA*-strep
KW1104	*ami3-htrA* L5 swap background strain	mc2 155 Δ*ami3*::zeoR Δ*htrA*::hygR L5::pKW98 tetOFF5-*htrA*-strep
KW1106	*pmt-htrA* L5 swap background strain	mc2 155 Δ*pmt*::zeoR Δ*htrA*::hygR L5::pKW98 tetOFF5-*htrA*-strep
KW1241	$HtrA^{LOW}$, LppZ-FLAG	mc2 155 Δ*htrA*::hygR L5::pKW278*htrA*-strep Tw::pKW1218 *lppZ*-FLAG
KW1243	P_{htrA}-*htrA*, LppZ-FLAG	mc2 155 Δ*htrA*::hygR L5::pKW97 tetOFF4-*htrA*-strep Tw::pKW1218 *lppZ*-FLAG

Table A1.1 (Continued)

KW1245	P_{htrA}-*htrA(S354A)*, LppZ-FLAG	mc2 155 Δ*htrA*::hygR L5::pKW1034 *htrA(S354A)*-strep Tw::pKW1218 *lppZ*-FLAG
KW1256	$LppZ^{LOW}$	mc2 155 Δ*lppZ*::zeoR L5::pKW1251 tetOFF1-*lppZ*-strep
KW1274	Ami3-strep	mc2 155 Δ*ami3*::zeoR L5::pKW1156 *ami3*-strep
KW1288	LppZ-FLAG	mc2 155 Δ*lppZ*::zeoR L5::pKW1145 *lppZ*-FLAG
KW1325	Δ*pmt*Δ*lppZ*	mc2 155 Δ*pmt* Δ*lppZ*::zeoR
KW1327	*pmt-lppZ* L5 swap background strain	mc2 155 Δ*ami3* Δ*lppZ*::zeoR L5::pKW1253 tetOFF5-*lppZ*-strep
KW1339	Δ*pmt*, LppZ-FLAG	mc2 155 Δ*pmt* Δ*lppZ*::zeoR L5::pKW1145 *lppZ*-FLAG
KW1346	HtrA-strep, LppZ-FLAG	mc2 155 Δ*htrA*::hygR Δ*lppZ*::zeoR L5::pKW1145 *lppZ*-FLAG Tw::pKW1285 *htrA*-strep
KW1350	Δ*ami3*Δ*lppZ*	mc2 155 Δ*ami3* Δ*lppZ*::zeoR
KW1352	Δ*mprB*Δ*lppZ*	mc2 155 Δ*mprB* Δ*lppZ*::zeoR
KW1412	Ami3(C370S)-strep	mc2 155 Δ*ami3*::zeoR L5::pKW1404 *ami3(C370S)*-strep
KW1437	Δ*pmt* Ami3-strep	mc2 155 Δ*ami3* Δ*pmt*::zeoR L5::pKW1156 *ami3*-strep
KW1438	Δ*pmt*Δ*htrA*, Ami3-strep	mc2 155 Δ*ami3* Δ*pmt*::zeoR Δ*htrA*::hygR L5::pKW1156 *ami3*-strep
KW1457	Ami3(H226A)-strep	mc2 155 Δ*ami3*::zeoR L5::pKW1431 *ami3(H226A)*-strep
KW1458	Ami3(H362A)-strep	mc2 155 Δ*ami3*::zeoR L5::pKW1432 *ami3(H362A)*-strep
KW1509	Δ*ami3*, HtrA-strep, LppZ-FLAG	mc2 155 Δ*ami3* Δ*htrA*::hygR Δ*lppZ*::zeoR L5::pKW1145 *lppZ*-FLAG Tw::pKW1285 *htrA*-strep
KW1511	Δ*pmt*, HtrA-strep, LppZ-FLAG	mc2 155 Δ*pmt* Δ*htrA*::hygR Δ*lppZ*::zeoR L5::pKW1145 *lppZ*-FLAG Tw::pKW1285 *htrA*-strep
KW1679	Δ*pmt*Δ*htrA*+*htrA*, Ami3-strep	mc2 155 Δ*ami3* Δ*pmt*::zeoR Δ*htrA*::hygR L5::pKW1156 *ami3*-strep Tw::pKW1359 *htrA*
KW1691	ptetOR-*ami3*	mc2 155 Δ*ami3* pKW1645 tetOR-*ami3*-strep
KW1693	Δ*pmt* ptetOR-*ami3*	mc2 155 Δ*ami3* Δ*pmt*::zeoR pKW1645 tetOR-*ami3*-strep
KW1695	Δ*pmt*+*pmt*, Ami3-strep	mc2 155 Δ*ami3* Δ*pmt*::zeoR L5::pKW1156 *ami3*-strep Tw::pKW1683 *pmt*
KW1697	Δ*pmt*+*pmt(D68A)*, Ami3-strep	mc2 155 Δ*ami3* Δ*pmt*::zeoR L5::pKW1156 *ami3*-strep Tw::pKW1686 *pmt(D68A)*
KW1701	tetOR-*htrA,* Ami3-strep	mc2 155 Δ*ami3* Δ*htrA*::hygR L5::pKW1602 tetOR-*htrA* Tw::pKW1684 *ami3*-strep
KW1703	Δ*pmt*, tetOR-*htrA,* Ami3-strep	mc2 155 Δ*ami3* Δ*pmt* Δ*htrA*::hygR L5::pKW1602 tetOR-*htrA* Tw::pKW1684 *ami3*-strep
KW1713	Δ*ami1*	mc2 155 Δ*ami1*::zeoR
KW1715	*ami4-htrA* L5 swap background strain	mc2 155 Δ*ami4*::zeoR Δ*htrA*::hygR L5::pKW97 tetOFF4-*htrA*-strep

Table A1.1 (Continued)

KW1717	*ami1-htrA* L5 swap background strain	mc2 155 Δ*ami1*::zeoR Δ*htrA*::hygR L5::pKW97 tetOFF4-*htrA*-strep
KW1723	Ami3(T122A/T130A/T138A)-strep	mc2 155 Δ*ami3* L5::pKW1783 *ami3(T122A/T130A/T138A)*-strep
KW1725	Δ*pmt,* Ami3(T122A/T130A/T138A)-strep	mc2 155 Δ*ami3* Δ*pmt*::zeoR L5::pKW1783 *ami3(T122A/T130A/T138A)*-strep
KW1727	Δ*pmt+pmt,* Ami3(T122A/T130A/T138A)-strep	mc2 155 Δ*ami3* Δ*pmt*::zeoR L5::pKW1783 *ami3(T122A/T130A/T138A)*-strep Tw::pKW1683 *pmt*
KW1729	Δ*pmt+pmt(D68A),* Ami3(T122A/T130A/T138A)-strep	mc2 155 Δ*ami3* Δ*pmt*::zeoR L5::pKW1783 *ami3(T122A/T130A/T138A)*-strep Tw::pKW1686 *pmt(D68A)*
KW1733	HtrAΔPDZ-strep, LppZ-FLAG	mc2 155 L5::pKW1145 *lppZ*-FLAG, Tw::pKW1708 *htrA*ΔPDZ-strep
KW1741	Δ*ami3*Δ*htrA, htrA*-strep, ptetOR-*ami3*-FLAG	mc2 155 Δ*ami3*::zeoR Δ*htrA*::hygR Tw::pKW1285 *htrA*-strep pKW1784-*ami3*-FLAG
KW1755	tetOR-*lppZ,* Ami3-strep	mc2 155 Δ*ami3* Δ*lppZ*::zeoR L5::pKW1156 *ami3*-strep Gi::pKW1608 tetOR-*lppZ*
KW1772	ptetOR-*ami3(H226A)*	mc2 155 Δ*ami3* pKW1767 tetOR-*ami3(H226A)*-strep
KW1773	ptetOR-*ami3(H362A)*	mc2 155 Δ*ami3* pKW1768 tetOR-*ami3(H362A)*-strep
KW1774	ptetOR-*ami3(C370S)*	mc2 155 Δ*ami3* pKW1769 tetOR-*ami3(C370S)*-strep
KW1775	tetOR-*htrA(S354A),* Ami3-strep	mc2 155 Δ*ami3* Δ*htrA*::hygR L5::pKW1771 tetOR-*htrA(S354A)* Tw::pKW1684 *ami3*-strep
KW1795	ptetOR-*ami3(T122A/T130A/T138A)*	mc2 155 Δ*ami3* pKW1785 tetOR-*ami3(T122A/T130A/T138A)*-strep
KW1796	Δ*pmt* ptetOR-*ami3(T122A/T130A/T138A)*	mc2 155 Δ*ami3* Δ*pmt*::zeoR pKW1785 tetOR-*ami3(T122A/T130A/T138A)*-strep
KW1797	ptetOR-*ami3*	mc2 155 Δ*ami3* pKW1784 tetOR-*ami3*-FLAG
KW1806	LppZ(T46-48A/T112A)-FLAG	mc2 155 Δ*lppZ*::zeoR L5::pKW1789 *lppZ(T46-48A/T112A)*-FLAG
KW1813	Δ*ami1*Δ*ami3*	mc2 155 Δ*ami1*::zeoR Δ*ami3*
KW1815	Δ*ami3*Δ*htrA, htrA(S354A)*-strep, ptetOR-*ami3*-FLAG	mc2 155 Δ*ami3*::zeoR Δ*htrA*::hygR Tw::pKW1423 *htrA(S354A)*-strep pKW1784-*ami3*-FLAG
KW1827	Δ*ami3*Δ*ami4*	mc2 155 Δ*ami3* Δ*ami4*
KW1834	HtrAΔcyto-strep, LppZ-FLAG	mc2 155 L5::pKW214 *htrA*Δcyto-strep, Tw::pKW1220 *lppZ*-FLAG
KW1837	Δ*ami1*Δ*ami3*Δ*ami4*	mc2 155 Δ*ami1*::zeoR Δ*ami3* Δ*ami4*
KW1861	HtrA(T209A)-strep	mc2 155 Δ*htrA*::hygR L5::pKW1856 *htrA(T209A)*-strep
KW1865	tetOR-*htrA(S354A),* tetO-*htrA(S354A),* Ami3-strep	mc2 155 Δ*ami3* Δ*htrA*::hygR L5::pKW1859 tetO-*htrA(S354A)* Tw::pKW1684 *ami3*-strep Gi::pKW1835 tetOR-*htrA(S354A)*
KW1869	*ami3-lppZ* L5 swap background strain	mc2 155 Δ*ami3* Δ*lppZ*::zeoR L5::pKW1605 tetOR-*lppZ*

Table A1.1 (Continued)

KW1879	Δ*ami4*	mc2 155 Δ*ami4*
KW1886	Δ*pmt* ptetOR-*ami3(H362A)*	mc2 155 Δ*ami3* Δ*pmt*::zeoR pKW1768 tetOR-*ami3(H362A)*-strep
KW1891	Δ*ami1*Δ*ami4*	mc2 155 Δ*ami1*::zeoR Δ*ami4*
KW1895	Δ*pmt*+*pmt*, HtrA-strep	mc2 155 Δ*pmt::zeoR* ΔhtrA::hygR L5::pKW278 *htrA*-strep Tw::pKW1683 *pmt*
KW1897	Δ*pmt*+*pmt(D68A)*, HtrA-strep	mc2 155 Δ*pmt::zeoR* ΔhtrA::hygR L5::pKW278 *htrA*-strep Tw::pKW1686 *pmt(D68A)*
KW1899	Δ*pmt*+*pmt*, LppZ-FLAG	mc2 155 Δ*pmt* Δ*lppZ*::zeoR L5::pKW1145 *lppZ*-FLAG Tw::pKW1683 *pmt*
KW1901	Δ*pmt*+*pmt(D68A)*, LppZ-FLAG	mc2 155 Δ*pmt* Δ*lppZ*::zeoR L5::pKW1145 *lppZ*-FLAG Tw::pKW1686 *pmt(D68A)*
KW1S	HtrAΔcytoΔPDZ-strep (suppressor)	mc2 155 Δ*htrA*::hygR L5::pKW518 *htrA*ΔcytoΔPDZ-strep *ami3*: +c in AA192
KW2S	HtrAΔPDZ-strep (suppressor)	mc2 155 Δ*htrA*::hygR L5::pKW243 *htrA*ΔPDZ-strep *ami3*: +cg in AA114
KW3S	HtrAΔPDZ-strep (suppressor)	mc2 155 Δ*htrA*::hygR L5::pKW243 *htrA*ΔPDZ-strep *ami3*: -c in AA192

Table A1.2 Plasmids used in Chapter 2

Plasmid Name	Used in Strains	Parent Vector Reference
pKK216-tetO-*gfp*	Swapped into KW1104, KW1106, KW1327, KW1869; failed to swap into KW1715, KW1717	(Kieser et al., 2015)
pKW97 tetOFF4-*htrA*-strep	KW109, KW1241	(Park et al. 2011)
pKW98 tetOFF5-*htrA*-strep	KW111	(Park et al. 2011)
pKK216-*htrA*Δcyto-strep	KW1834	(Kieser et al., 2015)
pKK216-*htrA*ΔPDZ-strep	KW527, KW2S, KW3S	(Kieser et al., 2015)
pKK216-*htrA*-strep	KW298, KW778, KW873, KW918, KW1895, KW1897, KW1243	(Kieser et al., 2015)
pKK216-*htrA*ΔcytoΔPDZ-strep	KW529, KW531, KW1S	(Kieser et al., 2015)
pKK216-*htrA(S354A)*-strep	KW1245	(Kieser et al., 2015)
pKK216-*lppZ*-FLAG	KW1288, KW1339, KW1346, KW1509, KW1511, KW1733, KW1899, KW1901	(Kieser et al., 2015)
pKK216-*pmt*-strep	Failed to swap into KW1106 (except for one spontaneous suppressor) and KW1327	(Kieser et al., 2015)
pKK216-*ami3*-strep	KW735, KW1274, KW1437, KW1438, KW1679, KW1695, KW1697, KW1755; failed to swap into KW1104, KW1869	(Kieser et al., 2015)
pDE43-MCtZ-*lppZ*-FLAG	KW1241, KW1243, KW1245	(Pham et al. 2007)
pTwN-*lppZ*-FLAG	KW1834	(Pham et al. 2007)
pKW1251 tetOFF1-*lppZ*-strep	KW1256	(Park et al. 2011)
pKW1253 tetOFF5-*lppZ*-strep	KW1327	(Kieser et al., 2015)
pTwN-*htrA*-strep	KW1346, KW1509, KW1511, KW1741	(Pham et al. 2007)
pKK216-*pmt(D68A)*-strep	Swapped into KW1106 and KW1327	(Kieser et al., 2015)
pTwN-*htrA*	KW1679	(Pham et al. 2007)
pKK216-*ami3(C370S)*-strep	KW1412; swapped into KW1104, KW1869	(Kieser et al., 2015)
pTwN-*htrA(S354A)*-strep	KW1815	(Pham et al. 2007)
pKK216-*ami3(H226A)*-strep	KW1457; swapped into KW1104, KW1869	(Kieser et al., 2015)
pKK216-*ami3(H362A)*-strep	KW1458; swapped into KW1104, KW1869	(Kieser et al., 2015)
pMC1s-tetOR-*htrA*	KW1701	(Ehrt et al., 2005)
pMC1s-tetOR-*lppZ*	KW1869	(Ehrt et al., 2005)
pGilesN-tetOR-*lppZ*	KW1755	(Huff et al., 2010)

Table A1.2 (Continued)

petetOR-*ami3*-strep	KW1691, KW1693	(Guo et al., 2007)
pTwN-*pmt*	KW1695, KW1727, KW1895, KW1899	(Pham et al. 2007)
pDE43-MCtZ-*ami3*-strep	KW1701, KW1775, KW1865	(Pham et al. 2007)
pTwN-*pmt(D68A)*	KW1697, KW1729, KW1897, KW1901	(Pham et al. 2007)
pKK216-*ami3(T138A)*-strep	Failed to swap into KW1104	(Kieser et al., 2015)
pTwN-*htrA*ΔPDZ-strep	KW1733	(Pham et al. 2007)
petetOR-*ami3(H226A)*-strep	KW1772	(Guo et al., 2007)
petetOR-*ami3(H362A)*-strep	KW1773, KW1886	(Guo et al., 2007)
petetOR-*ami3(C370S)*-strep	KW1774	(Guo et al., 2007)
pMC1s-tetOR-*htrA(S354A)*	KW1775	(Ehrt et al., 2005)
pKK216-*ami3(T122A/T138A)*-strep	Failed to swap into KW1104	(Kieser et al., 2015)
pKK216-*ami3(T130A/T138A)*-strep	Failed to swap into KW1104	(Kieser et al., 2015)
pKK216-*ami3(T122A/T130A/T138A)*-strep	KW1723, KW1725, KW1727, KW1729; swapped into KW1104	(Kieser et al., 2015)
petetOR-*ami3*-FLAG	KW1741, KW1797, KW1815	(Guo et al., 2007)
petetOR-*ami3(T122A/T130A/T138A)*-strep	KW1795, KW1796	(Guo et al., 2007)
pKK216-*lppZ(T46-48A/T112A)*-FLAG	KW1806	(Kieser et al., 2015)
pKK216-*ami3(T122A)*-strep	Failed to swap into KW1104	(Kieser et al., 2015)
pKK216-*ami3(T130A)*-strep	Failed to swap into KW1104	(Kieser et al., 2015)
pKK216-*ami3(T122A/T130A)*-strep	Swapped into KW1104	(Kieser et al., 2015)
petetOR-*ami3(H362A)*-FLAG	KW1824	(Guo et al., 2007)
pGilesN-tetOR-*htrA(S354A)*	KW1865	(Huff et al., 2010)
pKK216-*htrA(T209A)*-strep	KW1861	(Kieser et al., 2015)
pKK216-tetO-*htrA(S354A)*	KW1865	(Kieser et al., 2015)

Table A1.3 Primers used in Chapter 2

Cloning Primer List		
Strain #	**Feature(s)**	**primers**
N/A	Null vector for L5 swap, pKK216-*gfp*	ATATATCATATGGAATTCGGTACCGTGTCGAAGGGCGAG ATATATAAGCTTCTACTTGTACAGCTCGTCCATG
KW109, KW111, KW1104, KW1106, KW1715, KW1717, KW1241	pKW97 tetOFF4-*htrA*-strep, pKW98 tetOFF5-*htrA*-strep	CTTTCTTGTACAAAGTGGCTCTCCATCGATGTGACCAACCAGGAACAGTCC CTTTTTTATTTTATCCATGGATCCAGCTGCAGAATTCTCACTTCTCGAACTGGG GGTGGCTCCAGTCCTGGGCTTTTTGGTCGTCG
KW109, KW111, KW298, KW746, KW778, KW843, KW873, KW905, KW918, KW1104, KW1106, KW1245, KW1346, KW1509, KW1511, KW1679, KW1701, KW1703, KW1715, KW1717, KW1741, KW1775,KW1815, KW1861, KW1865, KW1895, KW1897	Δ*htrA*::hygR	TGGATGTCGATCACAGCTTC CCACGTCGGGGAGTGACTGTTCCTGGTTGGTCA CAACCAGGAACAGTCACTCCCCGACGTGGCCGA GGCGAACATCGTTAGGCTCCTGGGGCGGTGTC ACCGCCCCAGGAGCCTAACGATGTTCGCCAA TCATGCAACTGTTCGGTGAG
KW236, KW294, KW296, KW529, KW531, KW1S, KW1834	*htrA*Δcyto-strep, *htrA*ΔcytoΔPDZ-strep	GCACGATCCGCATGCTTAATTAAGAAGGAGATATACATATGTGTGGATCGCGC TGCTGACGCTGGCCCTGGTC GACCTCTAGGGTCCCCAATTAATTAGCTAAGCTTACTTCTCGAACTGGGGGTG GCTCCAGTCCTGGGCTTTTTGGTCGTCGCCGATG

Table A1.3 (Continued)

KW298, KW1346, KW1509, KW1511, KW1895, KW1897, KW1243	pKK216-*htrA*-strep, pTwN-*htrA*-strep	GGCCTTTTTGCGTTTAATACTGCATGCACTCTAGATTCGCCTCTCAGAGCGACG CACCTG GACCTCTAGGGTCCCCAATTAATTAGCTAAGCTTACTTCTCGAACTGGGGGTG GCTCCAGTCCTGGGCTTTTTGGTCGTCGCCGATG
KW527, KW529, KW531, KW1S, KW2S, KW3S, KW1733	*htrA*ΔPDZ-strep, *htrA*ΔcytoΔPDZ-strep	GGCCTTTTTGCGTTTAATACTGCATGCACTCTAGATTCGCCTCTCAGAGCGACG CACCTG CTAGATATCCATGGATCCAGCTGCAGAATTCGTTACAGATCCTCTTCTGAGATG AGTTTTTGTTCGACCTCCTTGACCTCGTTGACCGGG
KW694, KW735, KW746, KW778, KW1104, KW1274, KW1327, KW1350, KW1412, KW1437, KW1457, KW1458, KW1509, KW1691, KW1693, KW1695, KW1697, KW1701, KW1703, KW1723, KW1725, KW1727, KW1729, KW1755, KW1772, KW1773, KW1774, KW1775, KW1795, KW1796, KW1797, KW1813, KW1824, KW1827, KW1837, KW1851, KW1852, KW1865, KW1869	Δ*ami3*::zeoR	GTAAAACGACGGCCAGTGAATTACTTAAGAGGCCACGCCCTCGACC GGCCTCTCGAAGAGATCTCTTAAGGGACTGATGTTACGTATGCGTCTG CAGACGCATACGTAACATCAGTCCCTTAAGAGATCTCTTCGAGAGGCC GGCTTTTCGGGCTTTTCGGCGCTCGAATTAAGTACTTCTAGACTCGAG CTCGAGTCTAGAAGTACTTAATTCGAGCGCCGAAAAGCCCGAAAAGCC CATGATTACGCCAAGCTTGCATGCCTGCAGTCAGCTCGCCCGGTTACG

Table A1.3 (Continued)

KW735, KW1274, KW1437, KW1438, KW1679, KW1695, KW1697, KW1755	pKK216-*ami3*-strep	CTTTTTGCGTTTAATACTGCATGCACTCTAGAGGCGCCCAGGCGGC CTCTAGGGTCCCCAATTAATTAGCTAAGCTTCACTTCTCGAACTGGGGGTGGC TCCAGTCGGCGATCGGCGTGAAGC
KW801, KW843, KW873, KW1106, KW1325, KW1339, KW1437, KW1438, KW1511, KW1679, KW1693, KW1695, KW1697, KW1703, KW1725, KW1727, KW1729, KW1796, KW1813, KW1886, KW1895, KW1897, KW1899, KW1901	Δ*pmt*::zeoR	GACGAGCCGATAGCCCGG GGCCTCTCGAAGAGATCTCTTAAGGGCGACCCCAGGTTCAAG CTTGAACCTGGGGTCGCCCTTAAGAGATCTCTTCGAGAGGCC CGCCGGAACAAACAGAAGCTAGCTCGAATTAAGTACTTCTAGACTCGAG CTCGAGTCTAGAAGTACTTAATTCGAGCTAGCTTCTGTTTGTTCCGGCG CGGACGTCTTTTGCCACATACAC
KW846, KW905, KW918, KW1352, KW1852	Δ*mprB*::zeoR	GCAGGCAGCTTCGCAGC GGCCTCTCGAAGAGATCTCTTAAGCTACGGAGGCGTTTCCCG CGGGAAACGCCTCCGTAGCTTAAGAGATCTCTTCGAGAGGCC CGCTGTTGCCTGCCTCACGCTCGAATTAAGTACTTCTAGACTCGAG CTCGAGTCTAGAAGTACTTAATTCGAGCGTGAGGCAGGCAACAGCG CACGAGCGTCGCGACG
KW1042, KW1775, KW1865, KW1245, KW1815	*htrA(S354A)*	CTCGGCGTTCATGTTGATCAGCGGACCACCGGCGTTGCCGTGATTGATCGAG GCGTCGGTCTG CAGACCGACGCCTCGATCAATCACGGCAACGCCGGTGGTCCGCTGATCAACA TGAACGCCGAG

Table A1.3 (Continued)

KW1241, KW1243, KW1245, KW1288, KW1339, KW1346, KW1509, KW1511, KW1733, KW1834, KW1899, KW1901	pKK216-*lppZ*-FLAG, pTwN-lppZ-FLAG, pDE43-MCtZ-lppZ-FLAG	CTTTTTGCGTTTAATACTGCATGCACTCTAGACCACGGGTCCTGCGAGG CTAGGGTCCCCAATTAATTAGCTAAGCTTCACTTGTCGTCGTCGTCCTTGTAGT CGGTCTTGTCGGCATCGCC
KW1256, KW1327	pKW1251-tetOFF1-*lppZ*-strep, pKW1253 tetOFF5-*lppZ*-strep	CAGCTTTCTTGTACAAAGTGGCTCTCCATCGATATGAAATCGCGCCGGCG CTTTTTTATTTTATCCATGGATCCAGCTGCAGAATTCTCACTTCTCGAACTGGG GGTGGCTCCAGTCGGTCTTGTCGGCATCGCC
KW1256, KW1288, KW1325, KW1327, KW1339, KW1346, KW1350, KW1352, KW1755, KW1806, KW1869, KW1899, KW1901	Δ*lppZ*::zeoR	GCCTCGTCTCCCGGCG GGCCTCTCGAAGAGATCTCTTAAGCTGTCTCATCCGCCGGC GCCGGCGGATGAGACAGCTTAAGAGATCTCTTCGAGAGGCC CTGCGAAAAGGGTTGTGGCGCTCGAATTAAGTACTTCTAGACTCGAG CTCGAGTCTAGAAGTACTTAATTCGAGCGCCACAACCCTTTTCGCAG GTACTCGCGCGGAGCG
KW1412, KW1774	*ami3(C370S)*	CCGCGTTGCCCGGGGAGTCGGTGTTGCCGACG CGTCGGCAACACCGACTCCCCGGGCAACGCGG
KW1457, KW1772	*ami3(H226A)*	GCTGCCCGCCGTGTGGGCCACGATGCCGGCCCGG CCGGGCCGGCATCGTGGCCCACACGGCGGGCAGC
KW1458, KW1773	*ami3(H362A)*	GTTGCCGACGTCGCGGGCGGTGAAGATCGCGGGCAGC GCTGCCCGCGATCTTCACCGCCCGCGACGTCGGCAAC
KW1679	pTwN-*htrA*	GGCCTTTTTGCGTTTAATACTGCATGCACTCTAGATTCGCCTCTCAGAGCGACG CACCTG GGGGACCTCTAGGGTCCCCAATTAATTAGCTAAGCTTACTGGGCTTTTTGGTC GTCGCCGATG
KW1691, KW1693	petetOR-*ami3*-strep	GAGCACGATCCGCATGCTTAATTAAGAAGGAGATATACATCGTGCAGTCACGT CGTCCCG GTCCCCAATTAATTAGCTAAAGCTTGATATCTCAGGCGATCGGCGTGAAG
KW1695, KW1727, KW1895, KW1899	pTwN-*pmt*	GGCCTTTTTGCGTTTAATACTGCATGCACTCTAGAAGCTCAGCACCCGCCC CTCTAGGGTCCCCAATTAATTAGCTAAGCTTCTAGCGCCAGCTCGGC
KW1697, KW1729, KW1897, KW1901	*pmt(D68A)*	GGCGCGTAGTGCTTCTCGGCGAAGATCGGCGTGCCG CGGCACGCCGATCTTCGCCGAGAAGCACTACGCGCC

Table A1.3 (Continued)

KW1701, KW1703	pMC1s-tetOR-htrA	CGCATGCTTAATTAAGAAGGAGATATATCGATGTGACCAACCAGGAACAGTCC CTAGATATCCATGGATCCAGCTGCAGAATTCTTACTGGGCTTTTTGGTCGTCG
KW1701, KW1703, KW1775, KW1865	pDE43-MCtZ-*ami3*-strep	TCAATTGATTTAAATACTAGTGTTCTGCATGCACTCTAGAAATATTGGA GTCGTCGCCACCAATCCCCACGATCGTACGCTAGTTAACTACG
KW1713, KW1717, KW1813, KW1837, KW1891	Δ*ami1*::zeoR	CGGCAGACCGAAGCCG GGCCTCTCGAAGAGATCTCTTAAGTCACGACCGCGGCGC GCGCCGCGGTCGTGACTTAAGAGATCTCTTCGAGAGGCC CGAGGGCTAGCCGAGGGGCTCGAATTAAGTACTTCTAGACTCGAG CTCGAGTCTAGAAGTACTTAATTCGAGCCCCTCGGCTAGCCCTCG GACCGCAGATGGGCGG
KW1715, KW1827, KW1837, KW1879, KW1891	Δ*ami4*::zeoR	CACGAGGATCATCAGGATGCGTC GGCCTCTCGAAGAGATCTCTTAAGCTTGAAGTCACCGTGTCCACG CGTGGACACGGTGACTTCAAGCTTAAGAGATCTCTTCGAGAGGCC CCTTGAGTCCGGGCGTACGCTCGAATTAAGTACTTCTAGACTCGAG CTCGAGTCTAGAAGTACTTAATTCGAGCGTACGCCCGGACTCAAGG CGGGGCGGCCGACGATTG
KW1723, KW1725, KW1727, KW1729, KW1795, KW1796	*ami3(T122A), ami3(T130A), ami3(T138A), ami3(T122A/T130A), ami3(T122A/T138A), ami3(T130A/T138A), ami3(T122A/T130A/T138A)*	GCGATCTGCACGGTGTTGGCGCGTCCGACGAACACCG CGGTGTTCGTCGGACGCGCCAACACCGTGCAGATCGC GCGTTCTCGGGCCGGGCGATCGCGATCTGCACGGTG CACCGTGCAGATCGCGATCGCCCGGCCCGAGAACGC CTTGGGGGCCGGGGCGGCCGGCGCGGCGTTCTCGG CCGAGAACGCCGCGCCGGCCGCCCCGGCCCCCAAG
KW1741, KW1797, KW1815	petetOR-*ami3*-FLAG	GAGCACGATCCGCATGCTTAATTAAGAAGGAGATATACATCGTGCAGTCACGT CGTCCCG GGGTCCCCAATTAATTAGCTAAAGCTTGATATCTCACTTGTCGTCGTCGTCCTT GTAGTCGGCGATCGGCGTGAAGC
KW1806	*lppZ(T46-48A/T112A)*	GGGGCGGCGGCGGAGCCGCGGCGGGGCCGGGCCGCAG CTGCGGCCCGGCCCCGCCGCGGCTCCGCCGCCGCCCC GATCGACGGGGATCACGGCCTTGATCTTCGGCTCGGCAC GTGCCGAGCCGAAGATCAAGGCCGTGATCCCCGTCGATC
KW1861	*htrA(T209A)*	CTTGCTCTTGGCCTCGATCGCGACGACGGAATCGGCCACC GGTGGCCGATTCCGTCGTCGCGATCGAGGCCAAGAGCAAG
KW1865	pGilesN-tetOR-*htrA(S354A)*	GTTGATCGTCAAAAAGTGCTCATCATTGGAAAACGGATGGCCTTTTTGCGTTTA ATAC GACAATAACCCTGATAAATGCTTCAATAATGCCGCTGATTAGCTAAGCAGAAG
KW1865	pKK216-tetO-*htrA(S354A)*	GATCCGCATGCTTAATTAAGAAGGAGATATACATATGTGACCAACCAGGAACA GTCCGGG GGGGACCTCTAGGGTCCCCAATTAATTAGCTAAGCTTACTGGGCTTTTTGGTC GTCGCCGATG
KW1869	pMC1s-tetOR-*lppZ*	CGCATGCTTAATTAAGAAGGAGATATATCGATGAAATCGCGCCGGCG CTTTAAATCTAGATATCCATGGATCCAGCTGCAGAATTCAGGTCTTGTCGGCAT CG

Additonal preliminary findings on HtrA suppressors

Ami3

Our initial goal was to purify Ami3 and test its ability to cleave peptidoglycan *in vitro* to confirm its activity as an N-acetylmuramoyl-L-alanine amidase. However, our attempts to purify Ami3 were unsuccessful. Thus, to help build evidence that Ami3 is indeed an active amidase, we tagged its C-terminus with mRFP and localized the protein through fluorescence microscopy of cells overexpressing the construct under an aTc-inducible episomal plasmid (**Figure A1.7**). In all cells, Ami3-mRFP localized to either the poles or the septum, and appeared to be particularly prominent within bulges presumably caused by compromised cellular integrity. These locales are in keeping with Ami3's putative roles in cellular growth and division as an N-acetylmuramoyl-L-alanine amidase. Further experiments will confirm septal localization and co-localize Ami3 with HtrA and/or LppZ.

MprB

Although we identified mutations in *mprB* as additional suppressors of *htrA* essentiality, we left this avenue mostly unexplored in our recent manuscript for several reasons: First, *mprB* was the weakest suppressor of *ami3, pmt,* and *mprB.* Second, *mprB* is a putative sensor histidine kinase that, paired with its response regulator *mprA,* is predicted to affect the transcription of a bevy of genes in *Msm* (Zahrt et al. 2001, Zahrt et al. 2003), making it unlikely that we would be able to address the breadth of *mprB's* influence on the *htrA* interactome within the scope of a single paper. Third, *mprB* has previously been shown to potentially affect the transcription of *pepD,* a nonessential *htrA* homolog (White *et al.* 2010), and possibly *htrA* itself due to its location downstream of *sigE* (He et al. 2006), complicating our ability to study its influence on individual factors in the system.

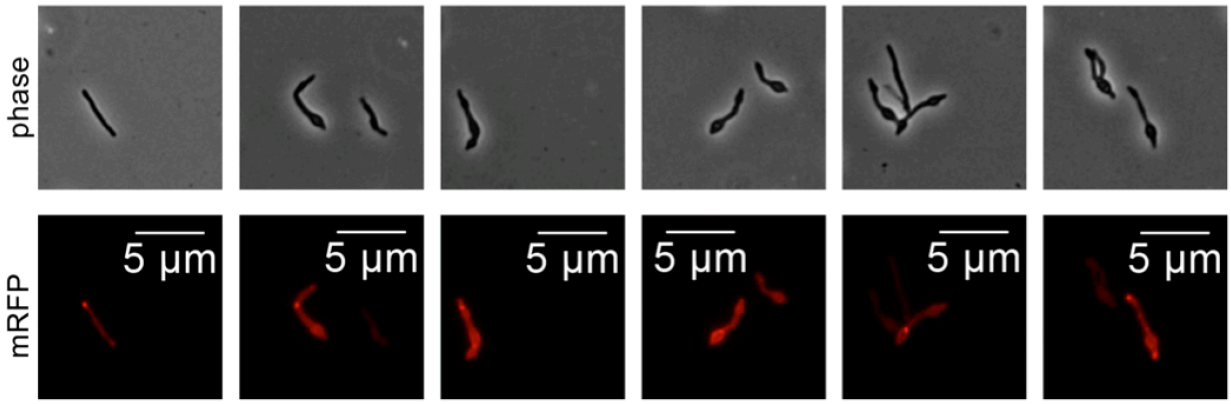

Figure A1.7: Ami3 localizes to points of cellular growth and division. Micrographs of strains expressing Ami3-mRFP under an aTc-inducibe promoter on an episomal construct.

Keeping these caveats in mind, we hypothesized that the role of *mprB* in this pathway might have a similar regulatory function. Previous characterizations of the MprAB regulon did not reveal *ami3* (He et al. 2006). However, *ami3* has been shown to be expressed at only very low levels, and thus may have evaded detection by RNA-seq-based methods. Using qPCR, we found that *ami3* transcript levels were upregulated about two-fold in wild-type cells compared to Δ*mprB* cells (**Figure A1.8A**). These differences disappeared when we expressed *ami3* under a constitutive UV15 promoter (**Figure A1.8B**). Thus, MprB appears to exert a modest amount of positive transcriptional regulation on *ami3*. However, the nature of this regulation and the conditions under which MprB upregulates *ami3* expression are not yet clear. Further studies are required to clarify this relationship.

Materials and Methods

Microscopy

Still images were taken of cells immobilized on agar pads on a Nikon Ti inverted widefield epifluorescence microscope with a Photometrics coolSNAP CCD monochrome camera and a Plan Apo 100X objective with a numerical aperture of 1.4. Images were processed using NIS Elements version 4.3 and ImageJ. Red fluorescent images were taken with a 528-553 excitation filter and a 590-650 emission filter. aTc-inducible strains were induced by the addition of 100 ng/mL anhydrotetracycline (aTc).

mRNA quantification

For each sample, cultures were grown to log phase, harvested by centrifugation, resuspended in TRIzol (Thermo Fisher), and disrupted by bead beating. Total RNA was isolated by isopropanol precipitation, residual contaminating genomic DNA was digested with TURBO DNase (Ambion), and samples were cleaned with RNA clean-up columns (Zymo Research). cDNA was prepared with random hexamers as per manufacturer instructions (Life Technologies

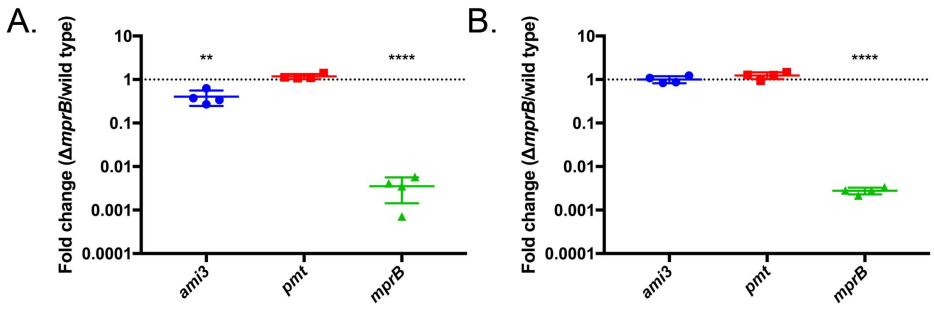

Figure A1.8: MprB positively affects the transcription of *ami3*. A. Under its native promoter, *ami3* is transcribed 2-fold less in an *mprB* knockout compared to wild type. Transcript levels were measured using quantitative real-time PCR. **B. Under a UV15 constitutive promoter, there is no difference in *ami3* transcripts between Δ*mprB* and wild type.** **p<0.01, ****p<0.0001. Error bars represent standard deviation around the mean.

Superscript IV). RNA was then removed by incubation with RNase H (New England Biolabs). cDNA levels were then quantified by quantitative real-time PCR (qRT–PCR) on a Viia7 light cycler (Applied Biosystems) using iTaq Universal SYBR Green Supermix (BioRad). All qPCR primer pairs were verified to be >95% efficient and cDNA masses tested were experimentally validated to be within the linear dynamic range of the assay. Signals were normalized to the housekeeping sigA transcript and quantified by the ΔΔCt method. All qPCR experiments were performed at least twice using technical triplicates of biological triplicates.

References

1. He H, Hovey R, Kane J, Singh V, and Zahrt TC. (2006). MprAB is a stress-responsive two-component system that directly regulates expression of sigma factors SigB and SigE in *Mycobacterium tuberculosis*. *J Bacteriol* 188(6): 2134-2143.

2. White, MJ et al. PepD Participates in the Mycobacterial Stress Response Mediated through MprAB and SigE. J Bacteriol 192(6): 1498-1510 (2010).

3. Zahrt TC and Deretic V. (2001). *Mycobacterium tuberculosis* signal transduction system required for persistent infections. *Proc Natl Acad Sci* 98(22): 12706-12711.

4. Zahrt TC, Wozniak C, Jones D, and Trevett A. (2003). Functional analysis of the *Mycobacterium tuberculosis* MprAB two-component signal transduction system. *Infect Immun* 71(12): 6962-70.

Appendix 2: Supplementary material for Chapter 3

Table A2.1 Strains used in Chapter 3

Strain list		
Strain #	nickname	genotype
CB168	Ptet::FtsL	mc2155 Δ*ftsL*::zeoR L5::pL5tetOR-*ftsL* / petetR
CB971	GFPmut3-ftsL, FtsZ-mcherry2B	mc2155 Δ*ftsL*::zeoR L5::pKK216-GFPmut3-*ftsL* tw::pMCtH-p21-ftsZ-mcherry2B
CB972	GFPmut3-FtsB, FtsZ-mcherry2B	mc2155 ΔMSMEG_5414 Δ Rv1025 homolog::zeoR L5::pKK216-GFPmut3-FtsB-1025-strep Tweety::pMCtZ-p21-FtsZ-mCherry2B
CB170	Ptet::PBP3	mc2155 ΔPBP3::zeoR L5::pL5ptetOR::PBP3 / petetR
CB858	GFPmut3-FtsQ, FtsZ-mcherry2B	mc2155 ΔftsQ::zeoR L5::KK216-mGFPmut3-ftsQstrep tweety:: pMCtH-p21-ftsZ(wk)-mCherry2B
CB749	FtsQ-strep	mc2155 ΔftsQ::zeoR L5::KK216-ftsQ-strep
CB414		mc2155 Δ*ftsL*::zeoR L5::CT16-*ftsL*
KB65		mc2155 Δ*ftsL*::ZeoR L5::pKK216-myc-ftsLΔ340-380
KB66		mc2155 Δ*ftsL*::ZeoR L5::pKK216-myc-ftsLΔ260-380
KB67		mc2155 ΔftsL::ZeoR L5::pKK216-myc-ftsLΔ200-380
CB913	MSMEG_5223-GFPmut3	mc2155 L5::pCB909
CB989	GFPmut3-MSMEG_1353	mc2155 L5::pCB910-MSMEG_1353
CB990	GFPmut3-SepIVA	mc2155 L5::pCB910-SepVIA
CB991	GFPmut3-MSMEG_3027	mc2155 L5::pCB910-MSMEG_3027
CB919	GFPmut3-MSMEG_4287	mc2155 L5::pCB910-MSMEG_4287
CB1001	GFPmut3-MSMEG_6394	mc2155 L5::pCB910-MSMEG_6394
CB1156	MSMEG_0736-mRFP	mc2155 L5::pKK215-MSMEG_0736-mRFP-strep
CB1157	MSMEG_6942-mRFP	mc2155 L5::KK216-MSMEG_6942-mRFP-strep
CB1163	GFPmut3-SepIVA ftsZ-mcherry	mc2155 L5::CB910-SepIVA tw::pMCtH-p21-ftsZ-mcherry2B
CB1165	SepIVA-DAS, P(medium)-sspB	mc2155 sepIVA::FLAG-das-pKM482 gi::pGMCgS-TetOFF-9 sspB
CB1166	SepIVA-DAS, P(strong)-sspB	mc2155 sepIVA::FLAG-das-pKM482 gi::pGMCgS-TetOFF-18 sspB
KW558	tetOFF4-ftsB	mc2 155 ΔMSMEG_5414::zeoR L5::pKW97 tetOFF4-f*tsB*-strep
KW585	tetOFF4-ftsQ	mc2 155 ΔftsQ::zeoR L5::pKW97 tetOFF4-*ftsQ*-strep
KW994	pami-ftsZ, GFPmut3-*ftsB*	mc2155 ΔftsZ::pami-ftsZ L5::pKK216 GFPmut3-*ftsB*-strep

Table A2.1 (Continued)

KW995	pami-ftsZ, GFPmut3-*ftsL*	mc2155 ΔftsZ::pami-ftsZ L5::pKK216 GFPmut3-*ftsL*
KW996	pami-ftsZ, GFPmut3-*ftsQ*	mc2155 ΔftsZ::pami-ftsZ L5::pKK216 GFPmut3-*ftsQ*-strep
KW998	pami-ftsZ, *ftsK*-GFPmut3	mc2155 ΔftsZ::pami-ftsZ L5::pKK216 *ftsK*-GFPmut3
KW1303	tetOFF4-ftsB, ftsZ-mcherry, ftsK-GFPmut3	mc2 155 ΔMSMEG_5414::zeoR L5::pKW97 tetOFF4-ftsB-strep Tweety::pMCtH-p21-ftsZ-mCherry2B Giles::pKK216 *ftsK*-GFPmut3
KW1305	tetOFF4-ftsB, ftsZ-mcherry, GFPmut3-ftsL	mc2 155 ΔMSMEG_5414::zeoR L5::pKW97 tetOFF4-ftsB-strep Tweety::pMCtH-p21-ftsZ-mCherry2B Giles::pKK216 GFPmut3-ftsL
KW1307	tetOFF4-ftsB, ftsZ-mcherry, GFPmut3-ftsQ	mc2 155 ΔMSMEG_5414::zeoR L5::pKW97 tetOFF4-ftsB-strep Tweety::pMCtH-p21-ftsZ-mCherry2B Giles::pKK216 GFPmut3-ftsQ
KW1309	Ptet::ftsL, ftsZ-mcherry, GFPmut3-ftsB	mc2 155 ΔMSMEG_4234::zeoR L5::pL5tetOR-ftsL Tweety::pMCtH-p21-ftsZ-mCherry2B Giles::pKK216 GFPmut3-ftsB
KW1311	Ptet::ftsL, ftsZ-mcherry, ftsK-GFPmut3	mc2 155 ΔMSMEG_4234::zeoR L5::pL5tetOR-ftsL Tweety::pMCtH-p21-ftsZ-mCherry2B Giles::pKK216 ftsK-GFPmut3
KW1313	Ptet::ftsL, ftsZ-mcherry, GFPmut3-ftsQ	mc2 155 ΔMSMEG_4234::zeoR L5::pL5tetOR-ftsL Tweety::pMCtH-p21-ftsZ-mCherry2B Giles::pKK216 GFPmut3-ftsQ
KW1315	tetOFF4-ftsQ, ftsZ-mcherry, GFPmut3-ftsB	mc2 155 ΔftsQ::zeoR L5::pKW97 tetOFF4-ftsQ Tweety::pMCtH-p21-ftsZ-mCherry2B Giles::pKK216 GFPmut3-ftsB
KW1317	tetOFF4-ftsQ, ftsZ-mcherry, ftsK-GFPmut3	mc2 155 ΔftsQ::zeoR L5::pKW97 tetOFF4-ftsQ Tweety::pMCtH-p21-ftsZ-mCherry2B Giles::pKK216 *ftsK*-GFPmut3
KW1319	tetOFF4-ftsQ, ftsZ-mcherry, GFPmut3-ftsL	mc2 155 ΔftsQ::zeoR L5::pKW97 tetOFF4-ftsQ Tweety::pMCtH-p21-ftsZ-mCherry2B Giles::pKK216 GFPmut3-ftsL
KW1738	SepIVA-DAS, P(strong)-sspB, ftsZ-mCherry	mc2155 MSMEG_2416::FLAG-das-P38-orbit gi::pGMCgS-TetOFF-18 sspB Tweety::pMCtZ-p21-ftsZ-mCherry2B

Table A2.2 Plasmids used in Chapter 3

Plasmid list			
in strain #	plasmid name	used in strains	Reference for parent vector
CB146	pL5tetOR-ftsL	CB168, KW1309, KW1311, KW1313	(Ehrt, 2005)
CB837	pKK216-GFPmut3-ftsQ-strep	CB84, KW996, KW1307, KW1313	(Kieser et al., 2015)
CB438	pMCtH-p21-ftsZ-mcherry2B	CB971, CB858, CB1163, KW1303, KW1305, KW1307, KW1309, KW1311, KW1313, KW1315, KW1317, KW1319, KW1738	(Meniche et al, 2014)
CB682	pKK216-ftsQ-strep	CB749	(Kieser et al., 2015)
KB47	pKK216-myc-MSMEG_4234Δ340-380	KB65	(Kieser et al., 2015)
KB49	pKK216-myc-MSMEG_4234Δ260-380	KB66	(Kieser et al., 2015)
KB50	pKK216-myc-MSMEG_4234Δ220-380	KB67	(Kieser et al., 2015)
KB51	pKK216-myc-MSMEG_4234Δ200-380	couldn't make	(Kieser et al., 2015)
CB909	pCB909	CB913	(Kieser et al., 2015)
CB910	pCB910		(Kieser et al., 2015)
CB968	pCB910-MSMEG_1353	CB989	(Kieser et al., 2015)
CB987	pCB910-SepIVA	CB990, CB1163	(Kieser et al., 2015)
CB988	pCB910-MSMEG_3027	CB991	(Kieser et al., 2015)
CB917	pCB910-MSMEG_4287	CB919	(Kieser et al., 2015)

Table A2.2 (Continued)

CB1063	pCB910-MSMEG_6394	CB1001	(Kieser et al., 2015)
CB1148	pKK216-MSMEG_0736-mRFP-strep	CB1156	(Kieser et al., 2015)
CB1149	pKK216-MSMEG_6942-mRFP-strep	CB1157	(Kieser et al., 2015)
CB942	pKM482	CB1165, CB1166, KW1738	Kenan Murphy, manuscript in revision
CB1034	pGMCgS-TetOFF-9-sspB	CB1165	(Kim, Schnappinger, 2011)
CB1036	pGMCgS-TetOFF-18 sspB	CB1166, KW1738	(Kim, Schnappinger, 2011)
CB147	pL5tetOR-PBP3	CB170	(Ehrt, 2005)
KB14	pKK216-GFPmut3-ftsL	CB971, KW995, KW1305, KW1319	(Kieser et al., 2015)
KW914	pKK216-ftsK-GFPmut3	KW998, KW1303, KW1311, KW1317	(Kieser et al., 2015)
KW55	pKK216-GFPmut3-ftsB-strep	CB972, KW525, KW994, KW1309, KW1315	(Kieser et al., 2015)
KW533	pKW97 tetOFF4-ftsB-strep	KW1303, KW1305, KW1307	Park et al. 2011 - http://journals.plos.org/plospathogens/article?id=10.1371/journal.ppat.1002264
KW582	pKW97 tetOFF4-ftsQ-strep	KW1315, KW1317, KW1319	Park et al. 2011 - http://journals.plos.org/plospathogens/article?id=10.1371/journal.ppat.1002264

Table A2.3 Primers used in Chapter 3

Primer list		
Strain #	Feature	primers
CB168	ΔftsL::zeoR	AGAGGATATCcgaatcctgcgcgactacg taacgctggtcgtgcTCAtcctggtcgcttcgcctt ggt aag cgt cag ccg TGAgcacgaccagcgtta cgccccgccggctcatcagtcctgctcctc gaggagcaggactgatgagccggcggggcg AGAGGATATCtcatctgaggtcgacgag
CB168/ CB146	pL5tetOR-ftsL	ATATTTAATTAAtgggggaaggggcagct ATATGAATTCtcatgcgaccggggcga
CB858/ KW585	ΔftsQ::zeoR	cgggtgttcgacgactatgcgcacca ACATTATACGAAGTTATgatcttcagcggggtcaccgt gtgaccccgctgaagatcATAACTTCGTATAATGTATG agtttcagcgctttttcctgATAACTTCGTATAGCATACA TGTATGCTATACGAAGTTATcaggaaaaagcgctgaaact cagcagctcctcgatgtcgtccttgg
CB170	ΔPBP3::zeoR	TATAGATATCgtcgtcgaacctcgtgag ATTATACGAAGTTATttcttgcgcggttgt a caa ccg cgc aag aaA TAA CTTCGTATAAT gaacggaacatcgagATAACTTCGTATAGC GCTATACGAAGTTATctcgatgttccgttcg TAGAGATATCcgaggtcggacgacgag
CB170	pL5tetOR-PBP3	ATATTTAATTAAGAAGGAGATAT atg agc cgg cgg ggc GAGAGAATTCtcaggtggcctgcaa
CB846/ CB837	KK216-GFPmut3-ftsQ-strep	TTAATTAAGAAGGAGATATACATATGAGTAAAGGAGAAGAACTTTTCACTGGAGTT accgtggggacccgtcccggtCATTTTGTATAGTTCATCCATGCCATGTGTAA GCATGGATGAACTATACAAAATGaccgggacgggtccccac TTCTCGAACTGGGGGTGGCTCCAGTCtttgaccgtcggcaggtcc CCAATTAATTAGCTAAAGCTTctaCTTCTCGAACTGGGGGTGGC

Table A2.3 (Continued)

CB971, CB858, CB1163	pMCtH-p21-ftsZ-mcherry2B	ccTGAGGCGCGCCagaagtagaATCGatgaccccaccgcataacta GGGGACAAGTTTGTACAAAAAAGCAGGCTccTGAGGCGCGCCaa GGGGACCACTTTGTACAAGAAAGCTGGGTGCCTAGGCTTAAGgtgccgcatgaagggc GGGGACAGCTTTCTTGTACAAAGTGGccGATAGCACTGAGAGC GGGGACAACTTTGTATAATAAAGTTGActaACTGGATCCGCTAGATCC
CB749	pKK216-ftsQ-strep	TAAGAAGGAGATATACATATGaccgggacgggtccccac TTCTCGAACTGGGGGTGGCTCCAGTCtttgaccgtcggcaggtcc CCAATTAATTAGCTAAAGCTTctaCTTCTCGAACTGGGGGTGGC
KB65	pKK216-myc-MSMEG_4234Δ340-380	GCGGCGCATatgGAGCAGAAGCTGATCAGCGAGGAAGACCTGaaggcgaagcgaccagg CGCCGCAAGCTTtcacggggcgggtgccggaac
KB66	pKK216-myc-MSMEG_4234Δ260-380	GCGGCGCATatgGAGCAGAAGCTGATCAGCGAGGAAGACCTGaaggcgaagcgaccagg CGCCGCAAGCTTtcacggagcggcctggatacccg
KB67	pKK216-myc-MSMEG_4234Δ220-380	GCGGCGCATatgGAGCAGAAGCTGATCAGCGAGGAAGACCTGaaggcgaagcgaccagg CGCCGCAAGCTTtcacgggggcagcggcgcg
KB64	pKK216-myc-MSMEG_4234Δ200-380	GCGGCGCATatgGAGCAGAAGCTGATCAGCGAGGAAGACCTGaaggcgaagcgaccagg CGCCGCAAGCTTtcagaccaccacccagttgcccg
CB913	pCB909	gggccgtcactcgcgggacGGTACCAGTAAAGGAGAAGAACTTTTCAC GGTCCCCAATTAATTAGCTAAAGCTTtcaTTTGTATAGTTCATCCATGCCATGT AATGAGCACGATCCGCATGCTTAATTAAGAAGGAGGATATCatgccgtggtggggtgccgt CAGTGAAAAGTTCTTCTCCTTTACTGGTACCgtcccgcgagtgacggccccgc
	pCB910	TTAATTAAGAAGGAGATATACATATGAGTAAAGGAGAAGAACTTTT gtggggacccgtcccggtCATTTTGTATAGTTCATCCATGC GATTACACATGGCATGGATGAACTATACAAAGGTACCgtgccgtggtggggtg CATGGTCCTTCTTGAGTTTGTAACAGCTGCTGGGATTACACATGGCATGGATG AGGGTCCCCAATTAATTAGCTAAAGCTTtcagtcccgcgagtgacggcc

Table A2.3 (Continued)

CB989	pCB910-MSMEG_1353	CATGGATGAACTATACAAAGGTACCagcactacgccggcgaaaacca GTCCCCAATTAATTAGCTAAAGCTTtcaggccttgtccccgctgg
CB990	pCB910-SepIVA	CATGGATGAACTATACAAAGGTACCtaccgagtttttgaagcgctcga GTCCCCAATTAATTAGCTAAAGCTTtcagcgggtcacgtagtcgtgt
CB991	pCB910-MSMEG_3027	CATGGATGAACTATACAAAGGTACCgctgaggactggggtgccgaac GTCCCCAATTAATTAGCTAAAGCTTctacctggcactgtcgaggacac
CB919	pCB910-MSMEG_4287	GGCATGGATGAACTATACAAAGGTACCatggcgaagacgcgcaacacc AGGGTCCCCAATTAATTAGCTAAAGCTTtcagcgacgacgcgccgtacg
CB1001	pCB910-MSMEG_6394	GGCATGGATGAACTATACAAAGGTACCatggcaaagaacgctcggcgtaag AGGGTCCCCAATTAATTAGCTAAAGCTTtcaaccgtgtttcggatggggc
CB1156	pKK216-MSMEG_0736-mRFP-strep	ATGCTTAATTAAGAAGGAGATATACATatggtcccgctctggttcacg ttgatgaCGTCCTCGGAGGAGGCCATGGTACCgcgctggaagtggctggcctcac
CB1157	pKK216-MSMEG_6942-mRFP-strep	ATGCTTAATTAAGAAGGAGATATACATatgtttaacttcttcagcttgga ttgatgaCGTCCTCGGAGGAGGCCATGGTACCtcgtttccgcttcttggggcg
CB1165, CB1166	sepIVA::FLAG-das-pKM482	taccgcaatcctacggcgacgccatattcgcgccgcggcacgtcgccgtcaccgcaggttgagcagatgcGGTTTGT ACCGTACACCACTGAGACCGCGGTGGTTGACCAGACAAACCgcgggtcacgtagtcgtgtgtc cccgcggtggtccgcaactggtgacgtccgcggccgaccgaccgcagg
KB14	pKK216-GFPmut3-ftsL	GCGGCGCATatgAGTAAAGGAGAAGAACTTTTCACTG cggtcctggtcgcttcgccttcgagccgccTTTGTATAGTTCATCCATGCCATGTG CACATGGCATGGATGAACTATACAAAggcggctcgaaggcgaagcgaccaggaccg CGCCGCAAGCTTtcatgcgaccggggcgac
KW914	pKK216-ftsK-GFPmut3	CCGCATGCTTAATTAAGAAGGAGATATACATATGTTGCTCATACAACGATCACTGG CTCCAGTGAAAAGTTCTTCTCCTTTACTGAACTCCTCGCCGTCCTCG CGAGGACGGCGAGGAGTTCAGTAAAGGAGAAGAACTTTTCACTGGAG CTAGGGTCCCCAATTAATTAGCTAAGCTTCATTTGTATAGTTCATCCATGCCATGTGT AATC

Table A2.3 (Continued)

KW55	pKK216-GFPmut3-ftsB-strep	GCATGCTTAATTAAGAAGGAGATATACAATGAGTAAAGGAGAAGAACTTTTCAC CTCGGATCGGGCCGCTTCGGGTCGGGTTTGTATAGTTCATCCATGCCATGTG CACATGGCATGGATGAACTATACAAACCCGACCCGAAGCGGCCCGATCCGAG GGGTCCCCAATTAATTAGCTAATCACTTCTCGAACTGGGGGTGGCTCCAGTCACCAC CGGGAGCGGGTGGGATC
KW533	pKW97-tetOFF4-ftsB-strep	GCTTTCTTGTACAAAGTGGCTCTCCATCGATATGCCCGACCCGAAGCGGCCCGATC CTTTTTTATTTTATCCATGGATCCAGCTGCAGAATTCTCACTTCTCGAACTGGGGGTG GCTCCAGTCACCACCGGGAGCGGGTGGGATC
KW582	pKW97-tetOFF4-ftsQ-strep	CCACCCAGCTTTCTTGTACAAAGTGGCTCTCCATCGATGTGACCGGGACGGGTCCC CAC CTTTTTTATTTTATCCATGGATCCAGCTGCAGAATTCTACTTCTCGAACTGGGGGTGG CTCCAGTCTTTGACCGTCGGCAGGTCCGGG